NATIONAL TECHNICAL UNIVERSITY OF ATHENS

SCHOOL OF CIVIL ENGINEERING

DEPARTMENT OF WATER RESOURCES AND ENVIRONMENTAL ENGINEERING

Προσομοίωση και ανάλυση τρωτότητας αστικών δικτύων διανομής νερού σε επιθέσεις οργανικού φορτίου

Simulation and vulnerability assessment of water distribution networks under organic attacks

PELEKANOS NIKOLAOS

Athens, March 9, 2020

Supervisor: Prof. Makropoulos Christos

NATIONAL TECHNICAL UNIVERSITY OF ATHENS

SCHOOL OF CIVIL ENGINEERING

DEPARTMENT OF WATER RESOURCES AND ENVIRONMENTAL ENGINEERING

Προσομοίωση και ανάλυση τρωτότητας αστικών δικτύων διανομής νερού σε επιθέσεις οργανικού φορτίου

Simulation and vulnerability assessment of water distribution networks under organic attacks

PELEKANOS NIKOLAOS

Athens, March 9, 2020

Supervisor: Prof. Makropoulos Christos

“Science must begin with myths,

and with the criticism of myths.”

--Karl Popper

Ευχαριστίες | Acknowledgements

Ολοκληρώνοντας την παρούσα εργασία, κλείνει και ο κύκλος της πενταετούς φοίτησης μου στη σχολή Πολιτικών Μηχανικών Ε.Μ.Π. Ένας κύκλος σημαντικός όχι μόνο για την εκπαίδευση πάνω στο ευρύ αυτό αντικείμενο, αλλά πάνω απ' όλα για τις αμέτρητες εμπειρίες και τα μαθήματα ζωής που μου προσέφερε σε κάθε κομμάτι του.

Θέλω αρχικά να ευχαριστήσω τον καθηγητή μου κ. Μακρόπουλο Χρήστο για την εμπιστοσύνη που μου έδειξε να αναλάβω ένα απαιτητικό αλλά και τόσο ενδιάφερον θέμα και για τις καίριες συμβουλές του κατά΄τη διάρκεια της χρονιάς. Σίγουρα θα μου μείνει αξέχαστη η διάλεξη του στο $9^{ο}$ εξάμηνο για τους γενετικούς αλγορίθμους και οι αναφορές που έκανε στη φιλοσοφία της επιστήμης.

Έπειτα οφείλω ένα τεράστιο ευχαριστώ στον Διονύση Νικολόπουλο, ο οποίος στάθηκε πραγματικά σε κάθε βήμα της διπλωματικής εργασίας δίπλα μου, και αφιέρωσε πολλές ώρες βοηθώντας με έμπρακτα με ιδέες και σκέψεις πάνω στο αντικείμενο. Η συμβολή του ήταν καθοριστική καθ' όλη τη διάρκεια και η συνεισφορά του ανεκτίμητη για το πέρας της εργασίας. Τον ευχαριστώ επίσης για την άψογη συνεργασία που είχαμε και επικοινωνία μας όλο αυτό το διάστημα.

Ακόμη, ένα ακόμα μεγάλο ευχαριστώ στον Γιώργο Μωραΐτη για τις «υπερωρίες» που έμεινε μαζί μου μέχρι να βρούμε τα υπολογιστικά σφάλματα, για τα εύστοχα σχόλια του πάνω στο αντικείμενο της εργασίας και για την εγκαρδιότητα του, που πάντα τον χαρακτηρίζει.

Τέλος, το μεγαλύτερο ευχαριστώ το οφείλω στους δικούς μου ανθρώπους, την οικογένεια μου για την αμέριστη υποστήριξη τους, τους φίλους μου για τις μοναδικές στιγμές που ζήσαμε όλα αυτά τα χρόνια και τη Μάνια που ήταν πάντα εκεί όταν χρειαζόταν.

Νίκος Πελεκάνος

Αθήνα, Μάρτιος 2020

ABSTRACT: This work contributes a modeling framework to characterize the effect of deliberate organic contamination events on water distribution systems (WDSs). A bacterial regrowth model and a first parallel chlorine decay model were combined to describe the kinetics of organic carbon, flowing and attached bacteria, and chlorine during a deliberate contaminant injection consisting of organic (TOC) and bacterial (Heterotrophic Plate Count) load. Realistic network water quality conditions were achieved by a 30-day network operating simulation, mainly aiming in the formation of biofilm to pipe surface. The attack was modeled using EPANET-MSX through EPANET-MATLAB Toolkit, as a steady 30-minute injection delivering 7000 g to a single node of the water distribution system. The same injection was repeated in each node at all nodes of the pipe network. The impact of the attack in each case was quantified by vulnerability indexes measuring the potential exposure of either TOC or bacteria to consumers. Those vulnerability indexes were then used to construct empirical probability mass function (PMF) and cumulative density function (CDF) diagrams in order to interpret the results of total network response due to a contamination event. Two maps were constructed to depict the ability of each node to expose downstream consumers at risk, as well as, the likelihood of every single one of them to be affected by a contaminant injection. In part II of the investigation, a sensitivity analysis was carried out to determine the network's sensitivity to three dynamic network variables (mass injection, injection duration and organic carbon concertation in water).The three mentioned variables appeared to have a significant impact on bacterial regrowth levels, in contrast to exposure of total population, that was slightly affected.

Key words: *Simulation, Water distributions systems, Contamination events, Vulnerability, Sensitivity analysis, Heterotrophic plate count bacteria, Bacterial regrowth*

Εκτεταμένη Περίληψη / Extended Summary in Greek

Εισαγωγή

Τα δίκτυα διανομής νερού είναι ζωτικής σημασίας δεδομένου ότι έχουν σχεδιαστεί για την παροχή ασφαλούς και αξιόπιστου νερού σε κάθε κοινότητα για οικιακές, εμπορικές και βιομηχανικές χρήσεις. Η επεξεργασία και η μεταφορά του πόσιμου ύδατος από τους ταμιευτήρες έως τον καταναλωτή αποτελεί μία συστημική προσέγγιση με πολλούς φραγμούς (Lindley και Buchberger, 2002). Κατά τη διάρκεια προηγούμενων δεκαετιών, αυτά τα εμπόδια συνήθως περιλάμβαναν μόνο την προστασία των μονάδων επεξεργασίας νερού καθώς και την εξασφάλιση της ασφαλούς λειτουργίας του δικτύου υδρευσης, παρέχοντας επαρκές απολυμαντικό υπόλειμμα σε όλα τα μέρη του δικτύου και ακόμα εξασφαλίζοντας την υπό πίεση διανομή νερού μέσω του συστήματος. Πλέον, έχει αναγνωριστεί πως οι συνέπειες μιας μόλυνσης στο δίκτυο ύδρευσης νερού, είτε από σκόπιμη ενέργεια, είτε ακούσια, μπορεί να είναι εξαιρετικά σοβαρές, καθώς δεν υπάρχουν αρκετά εμπόδια (τεχνολογικά ή σχεδιασμού) για την πρόληψη μιας τέτοιας καταστροφής. Σήμερα είναι πλέον αποδεκτό από μεγάλο μέρος της επιστημονικής και πολιτικής κοινότητας πως η ύπαρξη κατάλληλων υποδομών ύδρευσης, καθώς και η κατάστρωση συγκεκριμένων στρατηγικών για τον περιορισμό και αντιμετώπιση ενδεχόμενων απειλών μόλυνσης του δικτύου, ιδιαίτερα από μια τρομοκρατική ενέργεια είναι καθοριστικής σημασίας (Clark και Buchberger, 2004· Danneels και Finley, 2009· Gleick, 2006· Maiolo και Pantusa, 2018).

Τα συστήματα διανομής νερού αποτελούνται από σύνθετα δίκτυα αγωγών, δεξαμενών, αντλιών και βαλβίδων, που συνήθως εκτείνονται σε εκτάτεμενη χωρική κάλυψη. Το γεγονός αυτό, έχει ως αποτέλεσμα την πιθανή εύρεση πολυάριθμων σημείων πρόσβασης, τα οποία είναι ιδιαίτερα ευάλωτα σε μια απειλή μόλυνσης. Υπάρχουν διάφορες αιτίες που μπορούν να οδηγήσουν σε περιστατικά σκόπιμης υποβάθμισης ενός δικτύου διανομής νερού. Οι πιο συχνές απειλές που έχουν καταγραφεί είναι η φυσική επίθεση στις υποδομές με στόχο τη δολιοφθορά τους, η διαταραχή του κυβερνοχώρου (cyber-attack) στο σύστημα ελέγχου και απόκτησης δεδομένων του δικτύου (SCADA) και όπως προηγούμενως αναφέρθηκε η πιθανότητα βιοχημικής μόλυνσης (Nilsson et al., 2005). Όσον αφορά τη τελευταία περίπτωση, οι πιθανότητες μιας ανάλογης επίθεσης αυξάνονται αισθητά, δεδομένου ότι οι συγκεκριμένες ενέργειες μπορούν να πραγματοποιηθούν χρησιμοποιώντας σχετικά απλό εξοπλισμό, παρακάμπτοντας έτσι, την πίεση του δικτύου (Schwartz et al., 2014). Τέλος, πέρα από εσκεμμένες ενέργειες υποβάθμισης ενός δικτύου διανομής, ένας ρύπος μπορεί να εισέλθει στο δίκτυο, από ανθρώπινη αμέλεια ή υποβαθμισμένες υποδομές (π.χ. ελαττωματικές διασυνδέσεις, αρνητικές πιέσεις σε ραγισμένους σωλήνες), και ακόμα από έλλειψη συντήρησης ή βιολογικά ασταθές νερό (π.χ. ευτροφισμός).

Οι μέθοδοι διάθεσης αισθητήρων κατά μήκος ενός συστήματος διανομής μπορούν να εφαρμοστούν, ώστε να επιτρέπουν την ανίχνευση τυχόν ρύπου σε πραγματικό χρόνο και σε κρίσιμα σημεία του δικτύου. Παρ’ όλα αυτά, η συγκεκριμένη μέθοδος εξακολουθεί να θεωρείται μη ρεαλιστική λόγω του υψηλού κόστους ανάπτυξης και διάθεσης των αισθητήρων, καθώς και της ακόμα αναξιόπιστης τεχνολογίας όσον αφορά την ικανότητα ανίχνευσης κάθε είδους ρύπου, η οποία μελετάται από μεγάλη μερίδα της επιστημονικής κοινότητας. Ως εκ τούτου, πρέπει να δοθεί μεγάλη έμφαση στην κατανόηση των αδυναμιών ενός συστήματος και της απόκρισης τους σε περιπτώσεις εσκεμμένου ή μη, γεγονότος μόλυνσης προκειμένου να δοθεί προτεραιότητα στο σχεδιασμό για την προφύλαξη τους αλλά και τον προγραμματισμο για την αντιμετώπιση καταστάσεων έκτακτης ανάγκης. Οι τεχνικές αναλύσεις και οι προγραμματιστικές δυναμικές προσομοιώσεις συμβάλλουν στον εντοπισμό των πλεόν ευαίσθητων σημείων μόλυνσης, τις δυνητικές συνέπειες, αλλά και τον αντίκτυπο από ένα μολυσματικό γεγονός. Σε αυτή την κατεύθυνση, η μελέτη αυτή περιγράφει μια μέθοδο για την αξιολόγηση της απόκρισης και τρωτότητας των δικτύων διανομής νερού σε εσκεμμένες περιπτώσεις εισροής ρύπου από οργανικό φορτίο.

Μεθοδολογία

Ο στόχος της παρούσας εργασίας είναι η παροχή μιας αποτελεσματικής μεθόδου εκτίμησης των επιπτώσεων και πιθανών συνεπειών μιας μόλυνσης από οργανικό φορτίο σε δίκτυα διανομής νερού, που προέρχεται από εσκεμμένη ενέργεια. Τα συστήματα διανομής νερού είναι σύνθετα δικτυα αποτελούμενα από αγωγούς, τα οποία λειτουργούν ως βιοαντιδραστήρες, όπου αλληλεπδρά συνεχώς ένας μεγάλος αριθμός από διαφορετικά χημικά, βιολογικά και φυσικά είδη. Όταν αυτή η ισορροπία διασπαστεί ξαφνικά λόγω εξωτερικών συνθηκών (π.χ. απότομη αύξηση του οργανικού φορτίου), η ποίοτητα του νερού θα επηρεαστεί σοβαρά και είναι πιθανό να προκαλέσει σοβάρες συνέπειες στους καταναλωτές.

Ο πρώτος στόχος της μελέτης αφορά την ανάπτυξη ενός μοντέλου ποιότητας νερού, που περιγράφει τις δυναμικές κινήσεις των κυρίαρχων βιολογικών και χημικών ειδών που επηρεάζονται από μια ξαφνική αύξηση του οργανικού άνθρακα. Για να επιτευχθεί αυτό, υιοθετείται από τη βιβλιογραφία (Zhang et al., 2004) ένα μοντέλο ανάπτυξης βακτηρίων, το οποίο περιλαμβάνει τους ρυθμούς ανάπλασης των ελεύθερων βακτηρίων στο νερό, των προσκολλημένων βακτηρίων στα τοιχώματα των αγωγών (biofilm) και του βιοδιασπώμενου διαλυμένου οργανικού άνθρακα (BDOC), δηλαδή ενός κλάσματος του συνολικού οργανικού άνθρακα (TOC). Το συγκεκριμένο μοντέλο υιοθετήθηκε, γιατί ταιριάζει απόλυτα στις επιθυμητές πειραματικές προσομοιώσεις, αφού περιέχει κινητικές εξισώσεις βακτηρίων και οργανικής ύλης, οι οποίες καθορίζονται σε μεγάλο βαθμό από την παρουσία ή μη, υπολειμματικού χλωρίου. Οι αναφερθείσες εξισώσεις εφαρμόζονται χωρίς τροποποίηση στο μοντέλο με εξαίρεση την εξίσωση κίνησης του χλωρίου, η οποία είναι πρώτου βαθμού με σταθερό μειωτικό συντελεστή και αντικαταστάθηκε καθώς αποτύγχανε να ερμηνεύσει τη συμπεριφορά του χλωρίου σε οποιαδήποτε μεταβολή της ποιότητας του νερού.

Για να συμπληρωθεί το μοντέλο ανάπτυξης βακτηρίων που περιγράφηκε προηγούμενως, διεξήχθη εκτεταμένη βιβλιογραφική ανασκόπηση με στόχο την εύρεση ενός επαρκούς μοντέλου αποσύνθεσης χλωρίου, που θα επιτρέψει ρεαλιστικές προσομοιώσεις εισβολής οργανικού φορτίου στα δίκτυα διανομής νερού. Κάτα ένα σημαντικό μέρος της επιστημονικής κοινότητας είναι πλεόν αποδεκτό πως το μοντέλο αποσύνθεσης χλωρίου first parallel order παρέχει τα καλύτερα αποτελέσματα περιγραφής της πραγματικότητας σε σχέση με υπόλοιπα μοντέλα (Brown et al., 2011; Haas και Karra, 1984; Helbling et al., 2009; Vieira et al., 2004). Κατά συνέπεια το ίδιο μοντέλο χρησιμοποίθηκε στην παρούσα εργασία (Πίνακας 1).

Πίνακας 1: Αναλυτικές εξισώσεις του first parallel order μοντέλου αποσύνθεσης χλωρίου

Όνομα	Δομή	Αναλυτική σχέση	Παράμετροι
Parallel first order	$\frac{dC_{fast}}{dt} = -k_1 C_{fast}$ $\frac{dC_{slow}}{dt} = -k_2 C_{slow}$ $C_{0,fast} = zC_0$ $C_{0,slow} = (1-z)C_0$	C=$C_0 zexp(-k_1 t) + C_0(1-z)$exp $(-k_2$t)	k_1, k_2, z

Οι παράμετροι του μοντέλου που πρέπει να οριστούν είναι k_1, k_2 και z. Αυτές συμβολίζουν μια ταχεία σταθερά αποσύνθεσης, μια βραδεία σταθερά αποσύνθεσης και τη τιμή του ποσοστού της συνολικής συγκέντρωσης του χλωρίου, που θα μειώνεται με την ταχεία σταθερά, ενώ η υπόλοιπη (1-*z)* θα μειώνεται με την βραδεία. Οι συντελεστές αυτοί υπολογίστηκαν από τους Vieira και Nahas, (2005) σε εργαστηριακά πειράματα που πραγματοποιήθηκαν σε δείγματα νερού με σκοπό την περιγραφή της μείωσης του χλωρίου, όταν (1) βρίσκεται σε περίσσεια εναντι των υπολοίπων χημικών στοιχείων και (2) όταν προστίθεται οργανική ύλη (TOC).

Τα δύο μοντέλα (βακτηριακής ανάπτυξης και αποσύνθεσης χλωρίου) προσαρμόστηκαν κατάλληλα και οι εξισώσεις τους γράφτηκαν σε αρχείο EPANET-MSX ώστε να επιτευχθούν οι προσομοιώσεις των επιθέσεων. Ο ολικός οργανικός άνθρακας (TOC) δεν ορίστηκε στο αρχείο MSX ως ξεχωριστό είδος, επομένως οι κινητικές του εξισώσεις δεν περιγράφονται απευθείας. Για να ξεπεραστεί αυτό, η συγκέντρωση TOC μετράται ως συγκέντρωση BDOC, αφού το BDOC συνιστά ένα κλάσμα του TOC σε αναλογία 18%. Το ποσοστό αυτό προέκυψε από την ανασκόπηση της βιβλιογραφίας και από συνδυασμό πηγών.

Τέλος, ακόμη σημαντικότερο είναι το ερώτημα σχετικά με το πότε το προστιθέμενο TOC θεωρείται σε επαρκή ποσότητα έτσι ώστε να επηρεάσει τις παραμέτρους της αποσύνθεσης του χλωρίου. Η απάντηση αυτή δόθηκε πειραματικά συγκρίνοντας τις παράμετρους για διάφορες τιμές του TOC με τις αντίστοιχες τιμές του μοντέλου χωρίς την προσθήκη TOC. Θεωρήθηκε πως η συγκέντρωση της συνολικής οργανικής ύλης άνω των 12.9 mg/L είναι επαρκής έτσι ώστε το χλώριο να αρχίσει πιο γρήγορη συνολικά αποσύνθεση.

Η πειραματική φάση αποτελείται από δύο επί μέρους στόχους. Ο πρώτος στόχος είναι να αναπτυχθεί μια μέθοδος αξιολόγησης της τρωτότητας των δικτύων και να εξεταστεί η απόκριση του συστήματος συνυπολογίζοντας τις πιθανές συνέπειες των καταναλωτών από τις επιθέσεις ενός βιοχημικού ρύπου, αποτελούμενου από TOC και βακτήρια, που εισέρχεται σε διάφορα σημεία του δικτύου. Ο δεύτερος στόχος είναι να διερευνηθεί η ευαισθησία της απόκρισης του δικτύου σε τρεις δυναμικές μεταβλητές, εκ των οποίων οι δύο εξαρτώνται από τον εισβολέα (μάζα ρύπου, διάρκεια γεγονότος) και η τελευταία εξαρτάται από τη λειτουργία της μονάδας επεξεργασίας νερού (συγκέντρωση BDOC στο επεξεργασμένο νερό). Η τελευταία μεταβλητή με τη σειρά της, επηρεάζει την συνολική ποιότητα νερού του δικτύου αφού είναι υπεύθυνη για το σχηματισμό του biofilm.

Στη πρώτη φάση η προσομοίωση επίθεσης στο δίκτυο έγινε με τα ίδια ακριβώς χαρακτηριστικά (μάζα, διάρκεια) σε κάθε κόμβο του δικτύου έναν προς έναν. Τα αποτελέσματα για κάθε επίθεση αναλύθηκαν χρησιμοποιώντας δείκτες ευαισθησίας για την ποσοτικοποίηση των επιπτώσεων. Συνοπτικά οι δείκτες παρουσιάζονται στον παρακάτω πίνακα.

Πίνακας 2: Δείκτες ευαισθησίας για την ποσοτικοποίηση των επιπτώσεων από κάθε επίθεση

Περιγράφη δείκτη ευαισθησίας	**Μαθηματική σχέση**
Ποσοστό του πληθυσμού που εκτέθηκε στον ρύπο	$P_k = \sum_{n=1}^{N} f_n I_{k,n}$
Γινόμενο καταναλωτών επί συνολικά λεπτά (Consumer-Minutes)	$CME_k = \sum_{n=1}^{N} t_{cl2,n} \cup t_{BDOC,n} \cup t_{bact,n} \times \Pi_n$
Μέση συγκέντρωση TOC (αντίστοιχα βακτηρίων)	$A_{TOC,k} = (\sum_{n=1}^{N} C_{TOC,n,k} * \Pi_n)/\Pi_{TOC,k}$
Συνολική μάζα TOC (ανστίστοιχα βακτηρίων)	$W_{TOC,n,k} = \sum_{t_{TOC,n}} C_{TOC,n}(t) \times Q_n(t) \times \Delta t$
Συνολική διάρκεια μόλυνσης	$T_k = \bigcup_{1}^{N} t_{cl2,n} \cup t_{BDOC,n} \cup t_{bact,n}$

Δημιουργήθηκαν 7 λίστες των δεικτών ευαισθησίας με 268 στοιχεία (αριθμός κόμβων) η κάθε μια. Για κάθε δείκτη ευαισθησίας κατασκευάστηκαν τα διαγράμματα κατανομής πιθανότητας και αθροιστικής συνάρτησης κατανομής με σκοπό την σχηματική απεικόνιση της απόκρισης του δικτύου σε περίπτωση επίθεσης. Ακόμα κατασκευάστηκαν δύο χάρτες, ο χάρτης επιρροής, ο οποίος δείχνει σε τι ποσοστό του πληθυσμού (*P*) θα έχει επιρροή μια επίθεση που ξεκινάει από κάθε κόμβο και ο χάρτης ευαισθησίας, στον οποίο για κάθε σημείο αντιστοιχίζεται η πιθανότητα επιρροής του από μια επίθεση στο δίκτυο.

Αποτελέσματα και σχολιασμός

Στο Σχήμα 1 φαίνεται ο χάρτης επιρροής για το δίκτυο διανομής της Μόντενα. Τα αποτελέσματα έδειξαν πως ο πληθυσμός που ενδέχεται να επηρεαστεί από έναν οργανικό ρύπο εξαρτάται σημαντικά από την τοποθεσία εισβολής. Οι κόμβοι μεγαλύτερης επιρροής (κόκκινες και πορτοκαλί ζώνες) βρίσκονται κατά βάση κατάντη των δεξαμενών.

Σχήμα 1: Χάρτης επιρροής για το δίκτυο διανομής της Μόντενα, Ιταλία

Αντίθετα οι πράσινες ζώνες, στις οποίες ο ρύπος δεν επιδρά σε πάνω από το 5% συνολικά του πληθυσμού, βρίσκονται κατά βάση περιφερειακά, ενώ σε 17 κόμβους ο ρύπος δεν διαχέεται στο δίκτυο αλλά λόγω της υδραυλικής πίεσης μολύνει μόνο την συγκεκριμένη περιοχή (συγκεκριμένο κόμβο). Το μέγεθος του αντίκτυπου του ρύπου στους καταναλωτές είναι αντιστρόφως ανάλογο με τις ζώνες επιρρόης. Στις πράσινες ζώνες οι συγκεντρώσεις οργανικού φορτίου και βακτηρίων φτάνουν έως 350 mg/L και 1062 CFU/mL ενώ αντίθετα στις κόκκινες ζώνες τα αντίστοιχα ποσά δεν ξεπερνούν τα 3 mg/L και 133 CFU/mL αντίστοιχα.

Στο 80% των επιθέσεων παρατηρήθηκε το φαινόμενο της ανάπτυξης βακτηρίων το οποίο σχετίζεται ισχυρά από τη συνολική διάρκεια της μεταφοράς του ρύπου όπως αποδεικνύεται από το Σχήμα 2. Η ανάπτυξη βακτηρίων μπορεί να αποδοθεί στο γεγονός ότι οι υψηλές συγκεντρώσεις TOC που εισέρχονται κατά τη διάρκεια μιας εισβολής, προκαλούν άμεση αντιδράση με το χλώριο, συντελώντας στην ταχεία αποσύνθεση του. Επομένως το νερό, καθίσταται ευάλωτο στην δημιουργία των μικροοργανισμών κατά τη μεταφορά του ιδιαίτερα σε απομακρυσμένους κόμβους λόγω της μεγάλης διάρκειας μεταφοράς του.

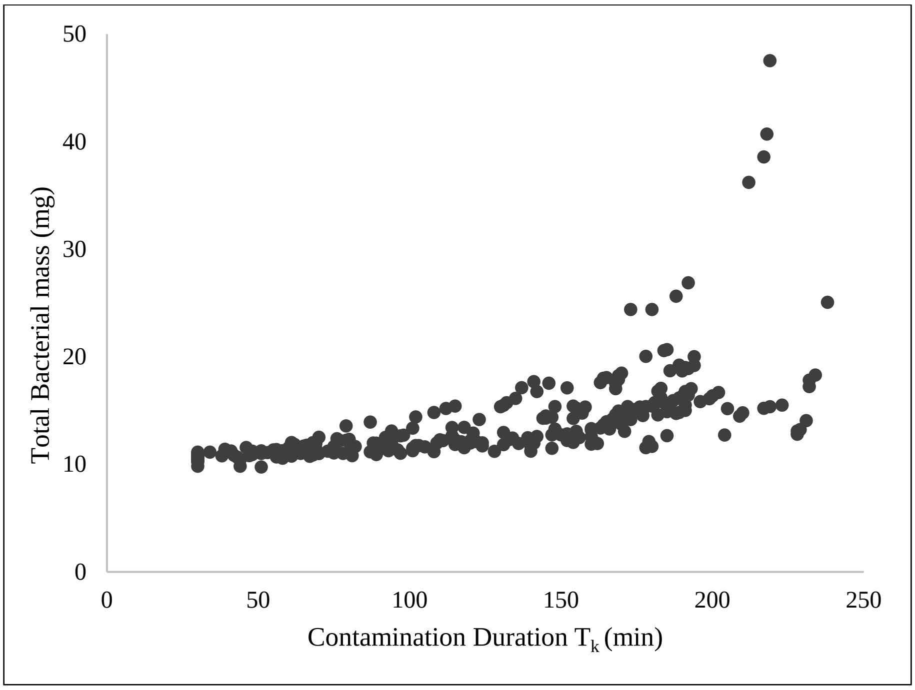

Σχήμα 2: Απεικόνιση της ολικής βακτηριακής μάζας που έφτασε στους καταναλωτές σε σχέση με τη συνολική διάρκεια της μόλυνσης για τις 268 επιθέσεις στο δίκτυο της Μόντενα

Στο Σχήμα 3 παρουσιάζεται ο χάρτης ευαισθησίας που απεικονίζει πόσο πιθανό είναι να επηρεαστεί ένας κόμβος από μια επίθεση στο δίκτυο, κάνοντας την παραδοχή πως όλοι οι κόμβοι έχουν την ιδια πιθανότητα να γίνουν σημεία εισβολής. Συνολικά σχεδόν η πλειονότητα των κόμβων (126 κόμβοι) έχουν πιθανότητα να επηρεαστούν κάτω από 4%, 39 κόμβοι έχουν πιθανότητα πάνω από 10%, ενώ μόλις 2 πάνω από 20%. Συμπερασματικά η πιθανότητα επηρεασμού του κάθε κόμβου εξαρτάται από την τοποθεσία του και από τον αριθμό των κόμβων που βρίσκεται στη διεύθυνση μεταξύ αυτού και της δεξαμενής από όπου υδρεύεται. Επομένως οι κόμβοι που υδρεύονται από περισσότερες δεξαμένες, είναι και οι πιο ευάλωτοι στο δίκτυο (π.χ. Κόμβος 266).

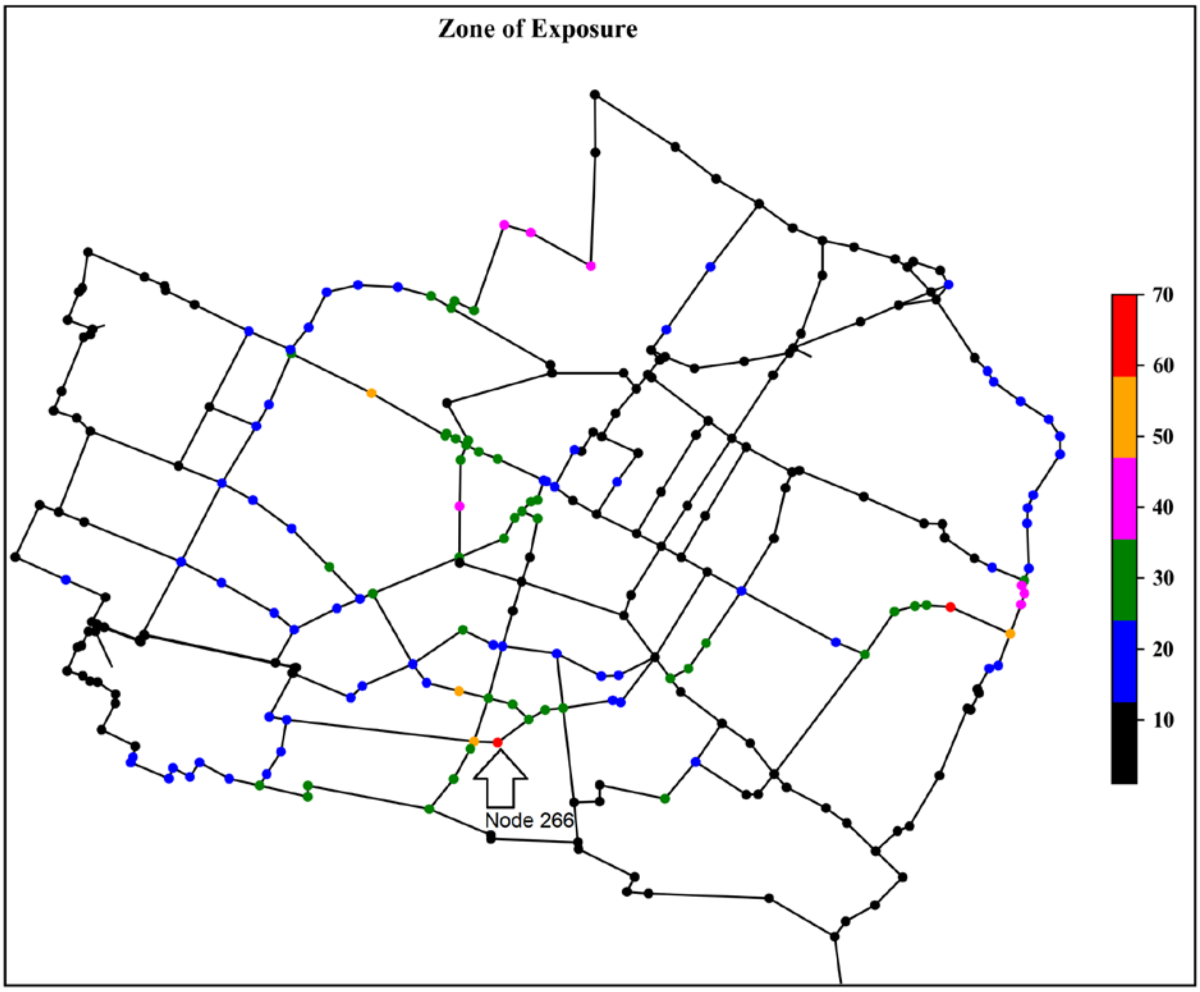

Σχήμα 3: Χάρτης ευαισθησίας για το δίκτυο διανομής της Μόντενα, Ιταλία

Συμπεράσματα

Τα συμπεράσματα που προκύπτουν από την ανάλυση τρωτότητας και απόκρισης του δικτύου διανομής νερού της Μόντενα σε εισβολή ρύπου από οργανική ύλη είναι:

- Το εύρος του δυνητικού πληθυσμού που μπορεί να εκτεθεί από ένα μόνο συμβάν μόλυνσης είναι από 106 καταναλωτές (0.01%) έως 112975 (57.8%) και εξαρτάται σε μεγάλο βαθμό από τη θέση της εισβολής.
- Από τους συνολικά 268 κόμβους, αυτοί που επηρεάζουν το μεγαλύτερο μέρος του δικτύου βρίσκονται κατάντη των υδραγωγείων (κόκκινες και πορτοκαλί ζώνες), ενώ αντίστοιχα η πλειονότητα των κόμβων ανήκει στη πράσινη ζώνη (160/268).
- Αντίθετα, οι καταναλωτές που πλήττονται από εισβολές σε πράσινους κόμβους εκτίθενται σε πολύ πιο σημαντικό ρίσκο λόγω ότι ο ρύπος δεν διαχέεται σε μεγάλο μέρος του δικτύου αλλα επιδρά στους γειτονικούς κόμβους.
- Από τις προσομοιώσεις στους 268 κόμβους διαπιστώθηκε ότι κατά την εισβολή οργανικού φορτίου, η συνολική βακτηριακή μάζα που θα φτάσει στους καταναλωτές θα αυξηθεί σημαντικά στο 70% των περιπτώσεων λόγω ανάπτυξης βακτηρίων κατά την μεταφορά του ρύπου.
- Από την ανάλυση ευαισθησίας παρατηρήθηκε πως οι μεταβλητές της προσομοίωσης που αφορούν την εισβολή (μάζα ρύπου, διάρκεια εισβολής) δε μεταβάλλουν σημαντικά τον συνολικό πληθυσμό που θα επηρεαστεί, αλλά θα επηρεάσουν ισχυρά την βακτηριακή ανάπτυξη και συνεπώς την άυξηση του ρίσκου της μόλυνσης των καταναλωτών.
- Τέλος, η καθαριότητα του δικτύου (με βάση τη συγκέντρωση των βακτηρίων (biofilm) στους αγωγούς και κατά συνέπεια τη συγκέντρωση του BDOC στο νερό) αποδείχθηκε λιγότερο σημαντική ως προς το συνολικό αντίκτυπο των επιθέσεων οργανικού φορτίου στους καταναλωτές.

Table of Contents

1 Introduction 27

1.1 Problem statement 27

1.2 Research overview 28

1.3 Work structure 30

2 Contamination threats in water distributions systems 32

2.1 Awareness of water infrastructure vulnerability 32

2.2 Bacterial regrowth in water distribution systems 33

2.2.1 Attached bacteria - Biofilm 34

2.2.2 Heterotrophic plate count 35

2.3 Mitigation measures 36

2.3.1 Chlorine residual 37

2.3.2 Monitoring methods in water distribution systems 39

3 Computational tools 41

3.1 EPANET 2 41

3.1.1 Epanet-MSX 42

3.1.2 Epanet Programmer's toolkit 44

3.2 EPANET- MATLAB Toolkit 44

4 Development of water quality model 48

4.1 Model overview 48

4.2 Bacterial regrowth model 48

4.3 Chlorine residual model 52

4.3.1 Influence of water quality on chlorine decay 53

4.4 Model adaptation to Epanet-MSX 58

5 Case study 64

5.1 Methodology overview 64

5.2 Network topology 64

5.3 Contaminant event simulations 67

5.4 Initial conditions 70

5.4.1 Investigation of minimum chlorine dose 71

5.4.2 Development of biofilm on pipe wall 73
5.5 Investigation of network response to contamination events 76
5.5.1 Attack scenario 77
5.5.2 Vulnerability assessment 78
5.5.3 Construction of demonstration tools 81
5.5.4 Sensitivity analysis 82
6 Results and Discussion 85
6.1 Vulnerability assessment 85
6.2 Sensitivity analysis 97
6.2.1 Effect of mass injection 97
6.2.2 Effect of injection duration 99
6.2.3 Effect of BDOC concentration in water 100
7 Summary and conclusions 102
Future research potential 105
BIBLIOGRAPHY 107
APPENDICES 111

List of Figures

Figure 2-1: Biofilm structure sketch | Source: semanticscholar.org....................................34

Figure 2-2: Fitting of experimental results from a chlorine decay test | Source: Vieira and Nahas, (2005)..39

Figure 2-3: Schematic of a generic urban water supply system vulnerable to pollution events | Source: Hou et. al, (2012)..39

Figure 3-1: EPANET-MSX input file template..43

Figure 3-2: MATLAB user interface (version R2018a)..45

Figure 3-3: Epanet object structured by epanet MATLAB toolkit in MATLAB interface.....46

Figure 4-1: Conceptual diagram of bacterial regrowth within a pipeline. Solid arrows represent transformation processes while dashed arrows represent reactions with chlorine. | Source: Uber, (2011)..49

Figure 4-2: Decay constants as a function of the inverse of initial chlorine concentration, $1/C_0$ |Source: Vieira et al., (2004)...54

Figure 4-3: Influence of TOC on chlorine decay constants | Source: Vieira et al., (2004) 55

Figure 4-4: Influence of initial chlorine concentration on the fraction z (no addition of organic matter – temperature conditions: 14.6 C) | Data: Vieira et al., (2004)..................................56

Figure 4-5: Influence of organic content on the fraction z (temperature conditions: 14.6 C, Initial chlorine concentration: 2.0 mg/L) | Data: Vieira et al., (2004)....................................56

Figure 4-6: Examples of chlorine decay curves for conditions described in Table 4-3 57

Figure 5-1: Network of Modena study site..65

Figure 5-2: Distribution of number of consumers at each network node of total 268, estimated from the water demand at these nodes..66

Figure 5-3: Chlorine residual and BDOC concentration in nodes 50 (top) and 104 (down) during an attack simulation...70

Figure 5-4: Flowchart of minimum chlorine dose program, used to investigate the sufficient chlorine concentration exiting the sources in order to ensure chlorine residual greater than 0.3 mg/l throughout the network...72

Figure 5-5: Timeseries of chlorine, free bacteria, attached bacteria (biofilm) and BDOC in three different nodes. 76

Figure 6-1: Zone of Influence map for Modena water distribution network 86

Figure 6-2: Contaminant trace of Node 52 injection 87

Figure 6-3: Correlation of total Bacterial mass reached consumers' taps with total contamination duration 89

Figure 6-4: Zone of Exposure for Modena water distribution Network. Colourmap indicates the frequency in which a node was exposed to contamination from total 268 node injections 90

Figure 6-5: Empirical relative frequency distribution and Weibull theoretical PDF of Percentage Population at risk to exposures for base-case intrusions in Modena network....... 92

Figure 6-6: Percentage Population Exposure CDF for base-case intrusions in Modena network 92

Figure 6-7: Empirical relative frequency distribution and Weibull theoretical PDF of Consumer-Minutes Exposure (CME) for base case intrusions in Modena network 93

Figure 6-8: Consumer-Minutes Exposure CDF for base-case intrusions in Modena network 93

Figure 6-9: Empirical relative frequency distribution and Weibull theoretical PDF of TOC concentration per Person for base case intrusions in Modena network 94

Figure 6-10: TOC concentration per Person CDF for base-case intrusions in Modena network 94

Figure 6-11: Empirical relative frequency distribution and Weibull theoretical PDF of Bacterial mass per Person for base case intrusions in Modena network.. 95

Figure 6-12: Bacterial concentration per Person CDF for base-case intrusions in Modena network 95

Figure 6-13: Empirical relative frequency distribution of Contamination durations for base case intrusions in Modena network 96

Figure 6-14: Contamination durations CDF for base-case intrusions in Modena network 96

Figure 6-15: Percentage of Population at bacterial risk to total Population exposed, relative to injected mass in Node 52 97

Figure 6-16: Percentage Tornado sensitivity chart for mass injection variable....................... 98

Figure 6-17: Percentage Tornado sensitivity chart for duration injection variable 100

Figure 6-18: Percentage Tornado sensitivity chart for BDOC concentration in water variable 101

List of Tables

Table 2-1: Literature review of bacteria population related to different pipe materials..........35

Table 2-2: Summary of bulk chlorine decay kinetic models. | Source: Brown et al., (2011)..38

Table 3-1:List of EPANET-MATLAB Toolkit Class functions...47

Table 4-1: Values of all parameters in the bacterial regrowth model. Values replaced by the author are marked with an asterisk. 52

Table 4-2: Parallel first order chlorine decay model 53

Table 4-3: Differences in parameter values among chlorine decay models. Chlorine initial concentration is assumed 0.7 mg/L...57

Table 4-4: TOC sufficient concentration lower bounds. 58

Table 4-5: Literature review of carbon fractions ratios aimed in estimating the BDOC/TOC ratio. 62

Table 5-1: Modena network main characteristics and hydraulic parameters range for base-case EPANET simulation under constant base demand for all nodes. *Roughness coefficient remains invariable in all pipes. 67

Table 5-2: Input parameters for minimum chlorine dose program...71

Table 5-3: Pipes with greater and lower concentration of attached bacteria after 30 days of simulation..74

Table 5-4: Default EPANET and EPANET-MSX Input Parameters for Base-Case Simulation 78

Table 5-5: Important variables in simulating network contamination events (Khanal et al, 2006). Bold variables are examined in the sensitivity analysis 83

Table 5-6: Input variables for Sensitivity Analysis. 84

Table 6-1: Results of base-case attack scenario for the nodes 1-5. 85

Table 6-2: Concentrations of organic carbon and bacteria per Zone of Influence 87

Table 6-3: Statistical analysis of contamination impact from all nodes' injection.................89

Table 6-4: Number of nodes related to possibility of being impacted as resulted from total 268 injections in all nodes of the Modena network 91

1 Introduction

1.1 Problem statement

Urban water distribution systems (WDSs) are of vital importance since they are designed to supply safe and reliable freshwater to every community for domestic, commercial and industrial uses. Treatment and transport of drinking water can be regarded as taking a multi-barrier approach (Lindley and Buchberger, 2002). Over the decades, these barriers included the protection of water treatments plants as well as securing the water supply network by providing sufficient disinfectant residual throughout the pipes and assuring distribution through a pressurized system. The consequences of a contamination event, occurred either intentionally or unintentionally, can be severe, as not enough barriers (technological or planning) exist to prevent such a catastrophe. Nowadays, the importance of securing water infrastructure and strategizing about such contamination threats, caused particularly by terrorist attacks, has been greatly raised (Clark and Buchberger, 2004; Danneels and Finley, 2009; Gleick, 2006; Maiolo and Pantusa, 2018).

Drinking-water distribution systems consist of complex networks of pumps, pipes and storage tanks under a broad spatial coverage. This enormous distributed special expansion of the water utilities results in finding numerous access points that are very susceptible in a contamination threat. There are various causes that can lead to contamination incidents in WDSs. Municipal pipe networks, for example, can be vulnerable to a range of terrorist threats, including physical attack, cyber-disruption and biochemical contamination (Nilsson et al., 2005). The likelihood of such occurrence is increased considering that these intrusions can be carried out using relatively simple equipment, with only constrain to overcome the network's pressure (Schwartz et al., 2014). Furthermore, unintentional events, where a contaminant may enter the network can occur by negligence, degraded infrastructure (e.g. cross-connections, negative pressures in cracked pipes), lack of maintenance and biologically unstable water (e.g. nutrients surplus) potentially leading to bacterial outbreaks.

Sensor deployment methods can be applied to enable real-time pollution detection in critical points across the pipes of a network. Nonetheless, this method is still considered unrealistic because of the high deployment costs and the unreliability of current sensor technology, which is profoundly studied by the scientific community. As a consequence, a major emphasis must be given on understanding the susceptibilities of water distribution systems as a precaution in case of a contamination event. Engineering analyses and pragmatic dynamic water simulations can help to identify most susceptible to contamination points of the network and estimate the consequences from a contamination event in order to prioritize emergency response plans. To this direction, this study describes a method to assess the vulnerability of WDSs in case of a deliberate organic contaminant intrusion.

1.2 Research overview

The overall aim of the present thesis is to provide an effective method of assessing the effects and potential consequences of organic load contamination in municipal water distribution systems, with a special focus on deliberate attacks. Water distribution systems are complex pipe networks, which function as a bioreactor, where an ample of different chemical, biological and physical species constantly interact. When this equilibrium is suddenly disrupted due to external conditions (e.g. organic load injection) the quality of water is severely affected and likely to cause serious after-effect to potential consumers.

To achieve this aim, the thesis has set the following **three objectives:**

1. The first objective of this study is to develop a water-quality model, that represents the dynamics of the predominant species affected by a sudden surging in organic carbon. To construct this, a bacterial regrowth model, including the kinetic rates of free flowing bacteria, attached bacteria (biofilm), and biodegradable dissolved organic carbon, which is a fraction of total organic carbon (TOC), is adopted from literature (Zhang et al., 2004). In addition, a more complex chlorine residual model (first parallel order decay), proposed by many studies (Brown et al., 2011; Haas and Karra, 1984; Vieira and Nahas, 2005), is incorporated in order to describe chlorine reaction to

sudden bulk organic quantity. The five (5) species' mathematical model is incorporated into EPANET-MSX, an extension of EPANET software for quality-water modeling, and through EPANET-MATLAB toolkit (Eliades et al., 2016) contaminant injections into WDSs are simulated.

2. The second objective is to achieve more realistic simulations by setting species' initial conditions for every point of the network before every injection. A simple code is programmed to estimate the required chlorine residual exiting the sources in order to avoid flowing bacterial regrowth. Eventually, the initial conditions are calculated by a 30-day simulation assuming that finished water from sources contains chlorine and a small amount of bacteria and organic carbon (BDOC), which result in different concentrations of biofilm regrowth in each pipe of the network.
3. The third objective regards the investigation of Modena's water distribution system response and is divided in two-parts. For the purposes of this study we assume a non-conservative contaminant measured in TOC and bacteria. In the first part, we run a base-case scenario of contaminant attack in each node of the network and quantify the consequences using some proposed vulnerability indexes. Extending the work of Khanal et al., (2006) a Zone of Influence and a Zone of Exposure are also constructed. In the second part, a sensitivity analysis is conducted in order to investigate the response of some dynamic variables separated in two categories, (1) those which are determined on the contamination action (injection mass, injection duration) and (2) water-quality parameters (BDOC concentration), measured at the exit of the water treatment plant, impacting the bacterial growth in the system before the intrusion.

1.3 Work structure

This study is structured into seven (7) distinct chapters, arranged in a logical sequence for the understanding of the objective.

In this **first chapter** we present a general overview over the water distribution systems' vulnerability to contamination threats, as well as a brief description of the research scope and the steps for study's implementation.

In the **second chapter** an extensive literature review about intentional and unintentional contamination threats in water distribution systems is provided. We discuss vulnerability of water infrastructure, mainly focusing on the most common causes of a potential contamination event with a special refer to bacterial regrowth, while we also refer to the state-of-art mitigation techniques.

In the **third chapter** we extensively present the computational tools used for the purpose of this study. An introduction to water distribution system modeling software EPANET 2 and its extension EPANET Multi-Species extension (MSX) is given, while emphasis is put on the EPANET-MALTAB Toolkit, a software for interfacing EPANET with MATLAB computing language, on which we based the undertake of this work.

The **fourth chapter** is a thorough analysis of the water quality model which consists of a bacterial regrowth model and the incorporation of first parallel chlorine decay mechanism. We present the water biological and chemical species involved in the model and assumed for this study, analyze their kinetic rate equations and interactions and demonstrate the process of adapting the theoretical model into an EPANET-MSX readable format to enable the dynamic simulations.

In the **fifth chapter** the experimental methodology of the vulnerability assessment is presented. At first, the case study topology is introduced and a contaminant injection is demonstrated for a better understanding of the tool. Moreover, the rationale and calculation of the initial conditions are analyzed. The chapter ends, by analytically describing the two-part investigation of our case study and the construction of the vulnerability indexes and demonstration tools used to extract the network's vulnerability assessment.

In the **sixth chapter** are discussed the results from both parts of the investigation. For the first part, are presented: The Zone of Influence and Zone of Exposure maps, and statistical graphs for each vulnerability index that gauge the likelihood of a contamination event depending on its magnitude. In the second part, the differences in the total effect of the contamination event are discussed, based on each examined variable of the sensitivity analysis.

The **seventh chapter** is a summary of the entire research focused on the methodology used, the objectives and the conclusions drawn from the experimental phase of modeling and measuring the vulnerability of the water distribution systems. Finally, suggestions for future research and enhancement of the studied model are provided.

2 Contamination threats in water distributions systems

2.1 Awareness of water infrastructure vulnerability

Water supply networks have always been an integral part of the social fabric as they ensure that consumers are provided with clean water for domestic and industrial use. The health of thousands of people daily depends directly on the quality of the water. Historically, the contamination of water supply networks, whether deliberately or inadvertently, caused untold damage to local communities. Examples of water mains contamination events have been recorded for many years and continue to this day. A significant example of the impact of an infection is the one that happened in Milwaukee in 1993, where 403.000 consumers affected, a number of whom hospitalized or died while it was estimated that total financial cost was $ 96.2 million (Eliades et al., 2014). More recently, in 2014 in West Virginia, it was estimated that 300.000 consumers had been affected, 14 of those hospitalized when a crude MCHM was accidentally spread into the drinking water distribution system (Qiu et al., 2020). Moreover, in 2019 two incidents of waterborne deceases due to bacterial infection were recorded in Norway and California, causing thousands of illnesses. These incidents are completely unrelated to deliberate actions, but rather indicate the susceptibility of the water supply systems and the magnitude of the disaster that an infestation can carry.

Terrorist acts in recent years have led to increase political and scientific awareness of the safety of water facilities. In the United States, after September 11, 2001, the water industry has really started to focus on the safety of water facilities. In 2002 the Bioterrorism Act into law was signed which requires water utilities to prepare Vulnerability Assessments and Emergence Response Plans (Clark and Buchberger, 2004). Similar methodologies and tools, amongst many studies, have been also developed not only in the US but worldwide (Association of Metropolitan Water Agencies, 2007; Centre for European Reform [CER], 2005; Instituto Superiore de Sanita, 2005).

Water systems are vulnerable to a range of intentional threats including contamination, damage or sabotage through physical destruction and cyber-attack (Maiolo and Pantusa, 2018). Physical damage is primarily related to service interruption and may also cause significant economic damage. Most vulnerable parts of water systems include their physical attributes, e.g. dams, tanks and pump stations (Maiolo and Pantusa, 2018). In WDSs, cyber-attacks potentially involve a range of actions including stealing consumer data up to invading water utility's supervisory control and data acquisition system (SCADA), aiming in causing water shortages or degrading water quality by turning pumps on or off, emptying tanks inappropriately or causing water hammer events (Hakim and Blackstone, 2014).

In the last decades, major efforts have been devoted to study the vulnerability of water systems due to deliberate contamination events caused by terrorist actions. Different aspects of the subject have been analyzed e.g. types of contaminant (Burkhardt et al., 2017; Propato and Uber, 2004; Schwartz et al., 2014), vulnerability assessment methodologies (Danneels and Finley, 2009; Janke et al., 2012; Lindley and Buchberger, 2002; Kenneth A. Nilsson et al., 2005), responding to the attacking threats and minimizing the consequences (Clark and Buchberger, 2004; Gleick, 2006; Jeong et al., 2006).

2.2 Bacterial regrowth in water distribution systems

Although public's perception is that water distribution systems' microbial ecology is limited, modern research has proved that WDSs are diverse microbial ecosystems with high bacterial and fungal abundance and a variety of microbial life including viruses and protozoa (Douterelo et al., 2014a). Water distribution systems act as a chemical and biological reactor where water-quality constantly changes. Microorganisms may be found both in the water phase and on the surface of the pipe walls in the form of biofilm. Waterborne illness and reduction of water quality are often caused to bacterial cells (King et al., 1988; Lindley and Buchberger, 2002). The bacterial regrowth in WDSs is depended on several factors such as, the type of disinfectants (chlorination, ozonation, chloramines), concentration of disinfectant, water temperature, pH, oxidant residuals, the presence of corrosion, but primarily by nutrients

(Prévost et al., 1998). A sufficient disinfectant usually acts as an inhibitory factor to bacteria growth in the bulk water. In contrary, attachment of bacteria on the pipe materials has been shown to increase disinfectant resistance (King et al., 1988; Zhang and DiGiano, 2002). Low disinfectant residual usually occurred under long water residence times can lead to sufficient bacterial. In this case, pathogenic bacteria found in the bulk water and those which are detached from the surface of the pipes are not immediately neutralized causing potentially consumers diseases.

2.2.1 Attached bacteria - Biofilm

The majority of microbial biomass in DWDs is found attached to inner surfaces of pipes forming microbial consortiums (biofilm) rather than in the bulk water (Flemming, 1998). These thin layers are protected from the environmental stress of water flow and pressure fluctuations and are firmly anchored to support microorganisms to a network of exopolymers composed of proteins and polysaccharides (Batté et al., 2003).

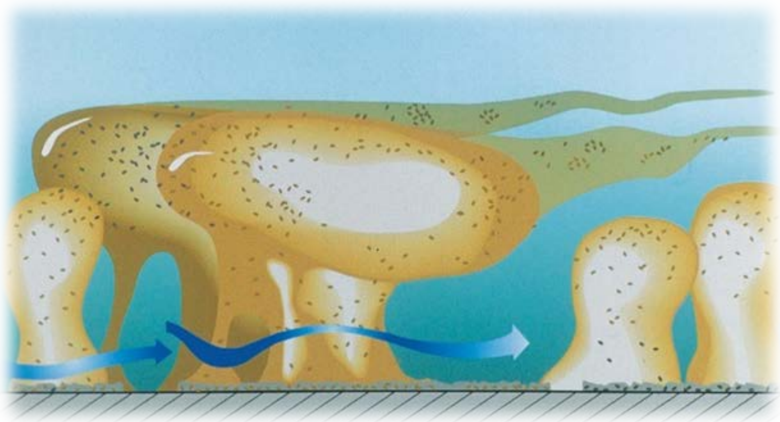

Figure 2-1: Biofilm structure sketch | Source: semanticscholar.org

Type of pipes, materials and sediment cover the bioreactor of the microbial life, thus contribute significantly in the microbial regrowth. Literature has shown that water distribution pipes with rough surface have considerably more possibilities for bacterial regrowth (Flemming, 1998; Niquette et al., 2000). Rough surface creates larger area to shelter bacteria and can accumulate elemental nutrients (e.g. phosphorous, iron, potassium) used as a bacterial substrate. The Table 2-1 shows different types of pipes with reported bacterial population according to literature review.

Table 2-1: Literature review of bacteria population related to different pipe materials

Material of pipe	**Bacteria Population** (cells/cm^2)	**Reference**
Matt steel	4.06×10^6	Pedersen, (1990)
Polyvinyl chloride (PVC)	2.8×10^6	Pedersen, (1990)
Polyethylene high-density (PE-HD)	2.5×10^6	Schwartz et al., (1998)
Copper	1.3×10^6	Schwartz et al., (1998)
Electro-polished steel	3.3×10^5	Pedersen, (1990)
Smooth stainless steel	1.7×10^5	Percival et al., (1998)

2.2.2 Heterotrophic plate count

The microbiological quality of drinking water in municipal water distribution systems is highly linked with the enumeration of heterotrophic bacteria. The characterization “heterotrophic” signifies that these microorganisms use organic nutrients for growth opposed to autotrophs like algae, that use sunlight. Heterotrophic plate count (HPC) measurements is an analytic method and a useful operational tool for monitoring general bacteriological water quality. The method assesses heterotrophic bacteria able to form colonies at specific conditions of temperature. After a defined incubation time, a general estimation of the bacteriological load can be made by counting the number of colonies growth (Douterelo et al., 2014b; Health Canada, 2013). It is highlighted that while “heterotrophic bacteria” enumerates all bacteria requiring organic nutrients for growth, HPC bacteria is a fraction only of heterotrophic bacteria that can be monitored through the specific method.

Heterotrophic plate count methods is frequently used by treatment operators to provide information concerning the microbiological and aesthetic quality of drinking water (Wolfe et al., 1985). Examples of HPC methods and their respective considerations are described in “Monitoring Heterotrophic Bacteria in Potable Water” (Reasoner, 1990). Low increases in the

HPC baseline range may arise problems: (1) non-compliance with existing regulations, (2) low quality drinking water, specifically .in taste and odor, (3) increased risk of gastrointestinal illnesses and (4) increased corrosion rates (Prévost et al., 1998) whereas higher increases in the HPC baseline could denote a serious contamination intrusion.

2.3 Mitigation measures

Water distribution systems are inherently vulnerable to both intentional and accidental contamination. The potential impact of a contaminant intrusion is highly depended upon the type and quantity of the contaminant substance, the site and duration of the intrusion, as well as the current hydraulic and quality conditions of the water system (Grayman, 2013). The maintenance of sufficient disinfectant (chlorine, chlorine dioxide or ozone) in potable water ensures that potential smaller scale organic or inorganic chemical, or microbial intrusions caused by e.g. low pressure, or pipe corrosion will react immediately, without causing harmful consequences to consumers.

In contrary, large-scale water contamination events due to serious accidents or malicious attacks, could potentially have severe health effects on a population and catastrophic economic impacts. Water authorities typically perform manual water collection and chemical analysis, routinely, in order to evaluate water quality in water distribution systems (Eliades et al., 2014). Such methods can no longer be considered efficient as they cannot provide any reliable information for a potential contaminant intrusion which will be detected after days or after customers' complaints. Consequently, the development and implementation of early warning systems (EWSs) is essential in order to mitigating the impact of a potential threat (Berry et al., 2005)

According to Seth et al., (2016), mitigation of contamination threats requires a three-part approach The first is physical security in all surface infrastructure such as storage tanks and surface water pipes. The second regards monitoring methods in order to rapidly detect an intrusion in the WDS and third, a special system control where the contaminant will be instantly isolated or neutralized (e.g. using valves, flushing network pipes or injecting decontaminant substances) and community plans in order to promptly inform to avoid using tap water.

2.3.1 Chlorine residual

Disinfection of potable water functions in order to destroy pathogenic organism and suspend microbiological incubation to prevent waterborne diseases. Chlorine is mostly used worldwide as a disinfectant as its advantages include low cost, effectiveness in controlling water quality, easy to handle, simple to dose and residual effecting (Brown et al., 2011; Vasconcelos et al., 1997) The maintenance of a residual quantity of chlorine throughout the water distribution system is of paramount importance in order to ensure the safety of drinking-water to consumers. Chlorine residual prevents the regrowth of microorganisms that enter the water distribution system from the treatment plant or during its transportation due to various causes e.g. pipe breakage, low or negative pressure intrusions or the incursion of insects in the water tanks. The chlorine dose concentration added at the treatment plant constantly and gradually lowers as it reacts in the bulk phase of the water as well as at the surface of pipes and tanks (Vasconcelos et al., 1997). Considering water high travel times in the spatial pipe networks and high residence time in the water tanks, the risk is that the water will reach the consumer without the required concentration of chlorine, leading them to potential infection. As a consequence, modeling of chlorine residual is essential in controlling disinfectant concentrations throughout the water distribution systems.

Chlorine reacts with both organic and inorganic substances in water, while controlling microbiological regrowth. The species that are most reactive with chlorine are inorganic substances such as sulfide, iron, manganese, bromide and ammonia (Brown et al., 2011). Also bulk chlorine decay rates were observed to increase significantly with higher temperature and higher total organic carbon (TOC) concentrations (Powell et al., 2000). Several rate laws for chlorine decay were systematically examined over the years (Brown et al., 2011; Haas and Karra, 1984) are presented in Table 2-2.

Table 2-2: Summary of bulk chlorine decay kinetic models. | Source: Brown et al., (2011)

Type	Equation	Adjustable parameters
First order	$C = C_0 \exp(-k_b t)$	k_b
Second order (with respect to chlorine only)	$C = \frac{C_0}{1 + C_0 k_b t}$	k_b, C_0
Second order (with respect to chlorine and another reactant	$C = \frac{U - C_0}{\frac{U}{C_0}\exp[W(U - C_{0)})t - 1]}$	U, C_0
n^{th} order	$C = [k_b''(n-1) + C_0^{-(n-1)}]^{-1/(n-1)}$	C_0, n
Limited first order	$C = C^* + (C_0 - C^*)\exp(-k_b t)$	C^*, k_b
Parallel first order	$C = C_0 z exp(-k_{bfast} t) + C_0(1-z)\exp(-k_{bslow} t)$	k_{bfast}, k_{bslow}, z

- First order decay: The classic kinetic model derived from the theory of chemical kinetics is included in most water quality analyses. The rate of reaction is proportional to the concentration of the reactant and the decay constant k_b.
- n^{th} order decay: The reaction velocity is proportional to the n^{th} power of chlorine concentration.
- Limited first order decay: This model assumes that a portion of the initial chlorine residual C^* is persistent and the remainder is subject to decay.
- Parallel first order: This model assumes that decay proceed through two mechanisms (Haas and Karra, 1984) each of first order. A component z with concentration $C_0 z$, is subject to first order decay with a rate constant of k_{bfast} and the remainder initial chlorine residual with concentration $C_o(1-z)$ with a rate constant of k_{bslow}.

Haas and Karra, (1984) reported that between all kinetic models, only parallel first order decay model fitted to the data as correlation coefficients were in excess of 0.90. A more recent study (Vieira et al., 2004) examined the same kinetic models in samples of water with added (1) chlorine, (2) chlorine and TOC and (3) chlorine and iron. Once more, the parallel first order model provided best fit with correlation (r^2) between 0.810 and 0.999. In 74% of the experiments, this model presented the most accurate results (Figure 2-2).

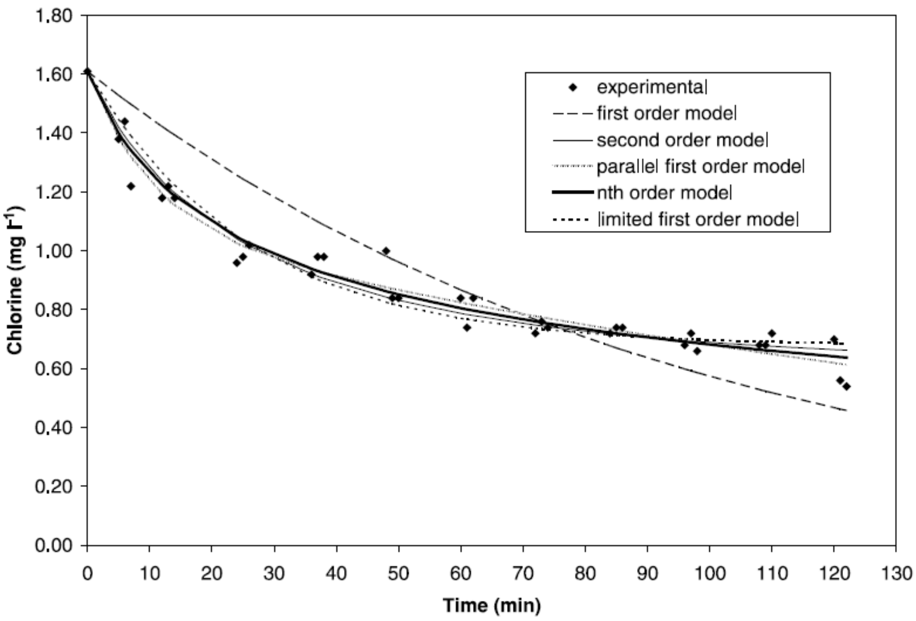

Figure 2-2: Fitting of experimental results from a chlorine decay test | Source: Vieira and Nahas, (2005)

2.3.2 Monitoring methods in water distribution systems

Sensor placement strategies for contaminant detection has been studied extensively in the frame of contamination early warning systems (EWSs) (Berry et al., 2005; Hart and Murray, 2010; Krause et al., 2008). According to Hou et al., (2013) the analysis of pollutions risks in urban water supply systems must include five (5) basic interconnected elements, which are

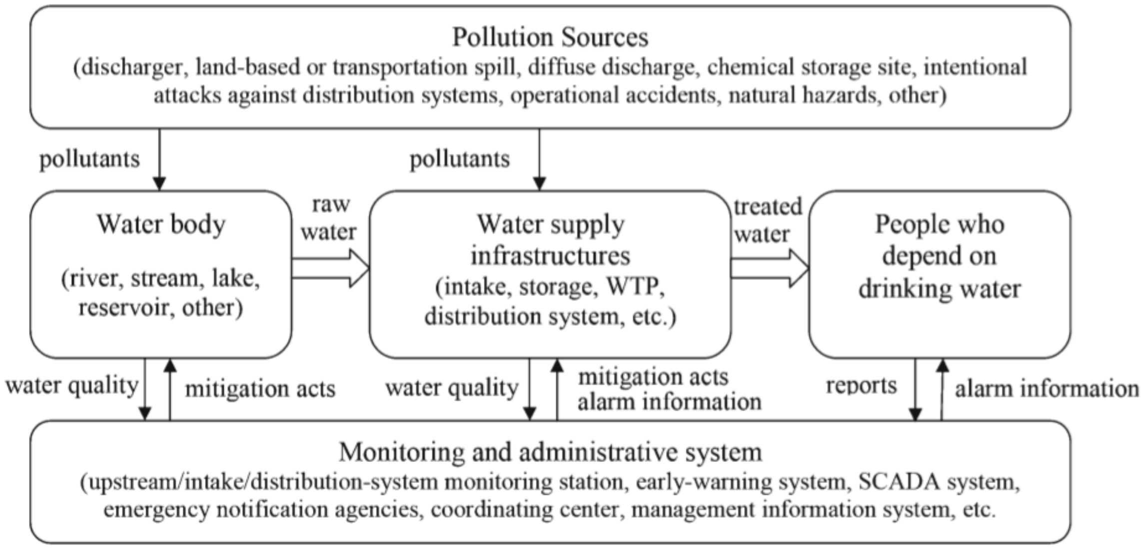

Figure 2-3: Schematic of a generic urban water supply system vulnerable to pollution events | Source: Hou et. al, (2012)

referred in Figure 2-3. An EWS combines real-time signals from online sensors indicating fluctuations in water-quality parameters (e.g. temperature, disinfectant levels, conductivity, turbidity, pH) with other detections strategies, such as public health surveillance systems, physical security monitoring, customer complaint surveillance, and routine sampling programs, in order to enable rapid decision making in case of presence of a contaminant. However, sensor placement still arises many questions concerning first, the ability to construe changes in water-quality parameters to the potential presence of a contaminant (Berry et al., 2005), and second, networks' broad spatial coverage which influences the total cost of a monitoring placement plan.

During the last decades a scientific area of simulation-optimization methods has been developed, aiming in the systematic contaminant source and release history identification problem (Di Cristo and Leopardi, 2008; Guan et al., 2006; Laird et al., 2005; Sankary and Ostfeld, 2019; Zechman and Ranjithan, 2009). However, still little is known about the advantages of each proposed algorithm method each human designer proposes. To explore this issue, the Battle of Water Sensor Networks (BWSN) was undertaken as part of 8th Annual Water Distribution Systems Analysis Symposium in Ohio. The main objective of BWSN was to compare and evaluate all outcome designs and methodologies, based on some quantitative indexes that indicate their performance. Participants were requested to place five (5) and (20) sensors for two real water distribution systems of increasing complexity and for four derivative cases (Ostfeld et al., 2008). The main conclusions drawn from this objective were that the problem of sensor placements is multiobjective, and thus, none of the proposed solutions could be characterized "best". Quantitative analysis, on the other hand, shows that sensors need not be grouped, and that positioning sensors at vertical sets (sources, reservoirs, and pumps) is not a requirement (Ostfeld et al., 2008).

3 Computational tools

3.1 EPANET 2

EPANET 2 is the most often applied software tool for simulating hydraulics and water quality in water distribution networks. It was developed by the U.S. Environmental Protection Agency to help water utilities to better understand the movement and transformations undergone by water in WDSs and is in possession of the public domain as a free demand driven software. The term “demand driven” indicates that in the model the demands will always be met, regardless the pressure in the network, as opposed to pressure driven models that use pressure as a constraint (Ricca, 2018). The network hydraulics solver employed by EPANET 2 uses the "Gradient Method" first proposed by Todini and Pilati, (1988) which is a variant of Newton-Raphson method.

EPANET 2 can perform both snapshot (steady-state) or extended-period hydraulic analyses of incompressible flow in pipe networks. It can handle various hydraulic units including reservoirs, tanks, pipes, pumps and control valves. EPANET 2 can also model water quality by simulating the behavior of chemical substances in the water distribution system with time. The water quality capabilities of EPANET 2 are expanded to allow water age and source tracing analyses to be performed (Zyl et al., 2015).

The most significant hydraulic capabilities of EPANET 2 are presented below as mentioned in the User’s Manual:

- Modeling limitless size of network systems
- Friction headloss computing using the Hazen-Williams, Darcy-Weisbach, or Chezy-Manning formulas
- Modeling constant or variable speed pumps
- Capability of pumping energy and cost computing
- Ability to explore different types of valves including shutoff, check, pressure regulating and flow control valves

- Allows storage tanks to have any shape
- Supports multiple diurnal curves at nodes, each with its own pattern of time variation

The scientific fields that EPANET 2 can be applied to are numerous as the user is able to run the model multiple times. Consequently, network optimizations, rehabilitation planning, long-term effect simulations, sensitivity and vulnerability analyses and groundwater modeling are some examples of software's potential applications (Burger et al., 2016).

Extensions to EPANET 2 are available with the existing software. EPANET-MSX (Multi Species eXtension) which enables modelling of complex reactions between multiple chemical and biological species and EPANET-RTX (Real-Time eXtension) a library of classes and wrappers that provide an interoperable framework and extend the software into including data acquisition and predictive forecasting.

This study is based in EPANET and EPANET-MSX as we take advantage of all hydraulic and water-quality capabilities in order to perform complex calculations about water movement in distribution systems. In each simulation all hydraulic data (e.g. flow, velocity, pressure in pipes etc.) are computed in order to be utilized by EPANET-MSX for the quality analysis.

3.1.1 Epanet-MSX

EPANET-MSX is an extension to the original EPANET that allows it to model any system of multiple, interacting chemical/biological/physical species. The software supports two physical phases of species: bulk water species and species attached to pipe surface. Examples of bulk species may involve individual compounds or ions, organic compounds such as TOC, and other biological or chemical components such as microorganisms and forms of iron attached in pipes.

In EPANET-MSX chemical reactions can be written as a single set of ordinary differential equations (ODEs) that are integrated over time to simulate changes in species concentrations. The program offers several choices of numerical integration methods for solving the reaction system's ODEs. These include a forward Euler method, a fifth order Runge-Kutta method, and a second order Rosenbrock method (Shang et al., 2008a)

```
[TITLE]
  <title line>

[OPTIONS]
 AREA_UNITS  FT2/M2/CM2
 TIME_UNITS  SEC/MIN/HR/DAY
 SOLVER      EUL/RK5/ROS2
 COUPLING    FULL/NONE
 TIMESTEP    <seconds>
 ATOL        <value>
 RTOL        <value>

[SPECIES]
 BULK        <specieID>    <units>    (<atol>  <rtol>)
 WALL        <specieID>    <units>    (<atol>  <rtol>)

[COEFFICIENTS]
 PARAMETER   <paramID>     <value>
 CONSTANT    <constID>     <value>

[TERMS]
 <termID>    <expression>

[PIPES] or [TANKS]
 EQUIL       <specieID>    <expression>
 RATE        <specieID>    <expression>
 FORMULA     <specieID>    <expression>

[SOURCES]
 <type>   <nodeID>   <specieID>   <strength>   (<patternID>)

[QUALITY]
 GLOBAL      <specieID>    <value>
 NODE        <nodeID>      <bulkSpecieID>    <value>
 LINK        <linkID>      <wallSpecieID>    <value>

[PARAMETERS]
 PIPE        <pipeID>      <paramID>     <value>
 TANK        <tankID>      <paramID>     <value>

[PATTERNS]
 <patternID> <multiplier> <multiplier> ...

[REPORT]
 NODES       ALL
 NODES       <node1ID>     <node2ID>  ...
 LINKS       ALL
 LINKS       <link1ID>     <link2ID>  ...
 SPECIES     <speciesID>   YES/NO  (<precision>)
 FILE        <filename>
 PAGESIZE    <lines>
```

Figure 3-1: EPANET-MSX input file template

In order to run a multi-species analysis, the user must prepare two input files. The first file is a standard EPANET input file describing the hydraulic characteristics of the network being analyzed. The second file is a special EPANET-MSX file (Figure 3-1) that describes all the information is essential for a multi-species simulation. These include the import of species, and their distinction in either physical phase (water bulk or fixed in pipe surface), coefficients and parameters, chemical reaction differential equations that govern their dynamics for pipes and tanks, nodes' and pipes' quality initial conditions, sources and computational options. This file can be achieved using a plain text editor and following a specific format. The final step to run a network simulation is by issuing some commands in the Command Prompt window in

Windows. A text file with will be reported, providing the simulation results such as species concentration or water age of each separate specie over time the intervals.

3.1.2 Epanet Programmer's toolkit

EPANET can be used in two ways: 1) as a stand-alone executable program or, as well as 2) a toolkit library of functions that programmers can use to build custom applications. As a shared object, e.g. Dynamic Link Library (DLL) for Windows, the user can call EPANET functions through a programming interface by external software in different programming languages (such as C/C++, Python, MATLAB, Pascal, Visual Basic). Through Epanet Programmer's toolkit, the user is able to produce more complex operations and customize EPANET's computational engine for their own specific needs.

In the current thesis, we exploit EPANET's and EPANET-MSX's shared object library as we used Epanet-MATLAB Toolkit through MALTAB programming interface to modify all system parameters and control total simulation configuration

3.2 EPANET- MATLAB Toolkit

MALTAB is a programming platform designed specifically for engineers and scientists. It integrates computation, visualization, and programming in an easy-to-use environment (Figure 3-2) where problems and solutions are expressed in familiar mathematical notation. MATLAB is an interactive system whose basic data element is an array that does not require dimensioning. It allows you to solve many technical computing problems, especially those with matrix and vector formulations, in a fraction of the time it would take to write a program in a scalar noninteractive language such as C or Fortran.

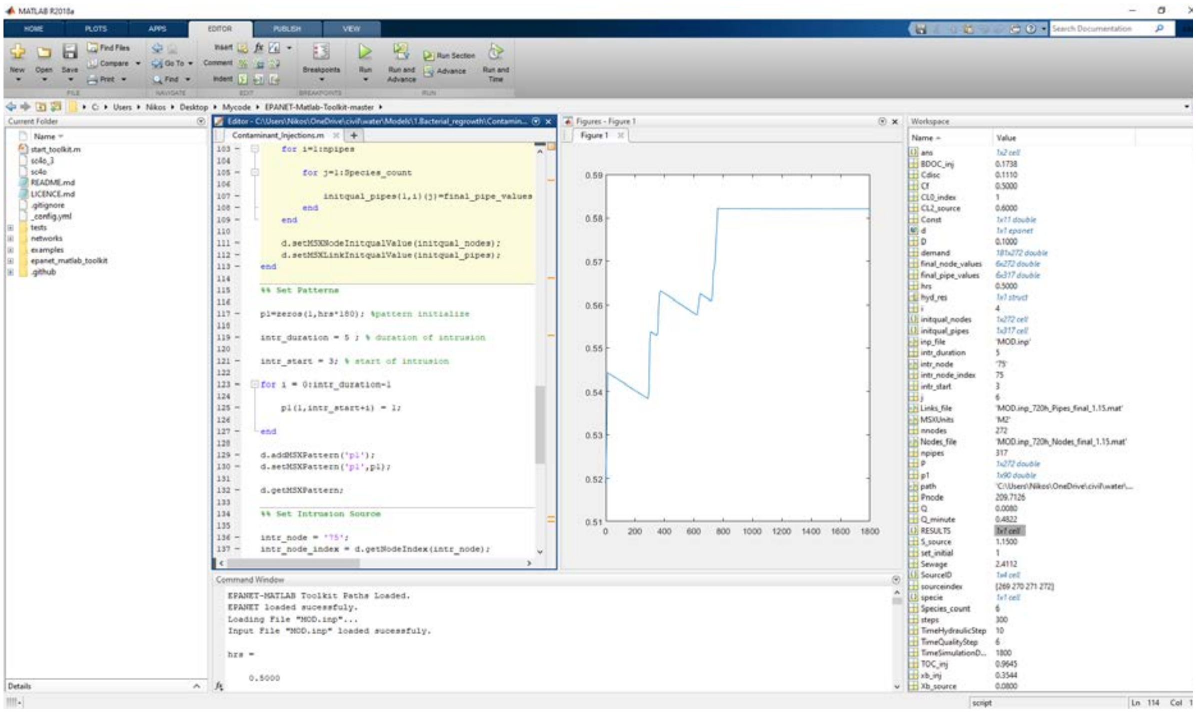

Figure 3-2: MATLAB user interface (version R2018a)

In this study, we take advantage of MATLAB's design to operate primarily on matrices and arrays. Large amount of data was included in numerous matrix formulations that allowed effortless visualization through its friendly programming environment, as well as uncomplicated matrix processes, such as concatenating matrices, expanding, re-arrange of the rank of columns and rows and straightforward operations. In addition, we exploited MATLAB's optimized for interaction graphical output, as it offers multiple functions in order to plot the data easily, and customize the colors, sizes or scales.

EPANET- MATLAB toolkit (Eliades et al., 2016) is an open-source software, developed by the KIOS Research Center for Intelligent Systems and Networks of the University of Cyprus which operates within the MATLAB environment, for providing a programming interface for the EPANET and EPANET Multi Species Extensions, a with programming platform MATLAB. The EPANET-Matlab Toolkit features easy to use commands/wrappers for viewing, modifying, simulating and plotting results produced by the EPANET libraries. The toolkit adopts an Object-Oriented Programming approach, providing a common data structure in order to successfully share data between different function modules and applications.

The toolkit is based on a MATLAB Class, which contains all properties of the input network model, static properties and a sum of functions either addressed to MATLAB directly or addressed to EPANET/EPANET-MSX (Eliades et al., 2016). The basic purpose of the class is to define an object that encapsulates data and the operations performed on that data, **epanet object.** The element d is an object that contains all the static variables of the water distribution system such as: number of nodes and pipes, skeletonization, pipe size (D and L), pipe roughness, dynamic variables such as: pump control, demand patterns, quality data, and options about the simulation process.

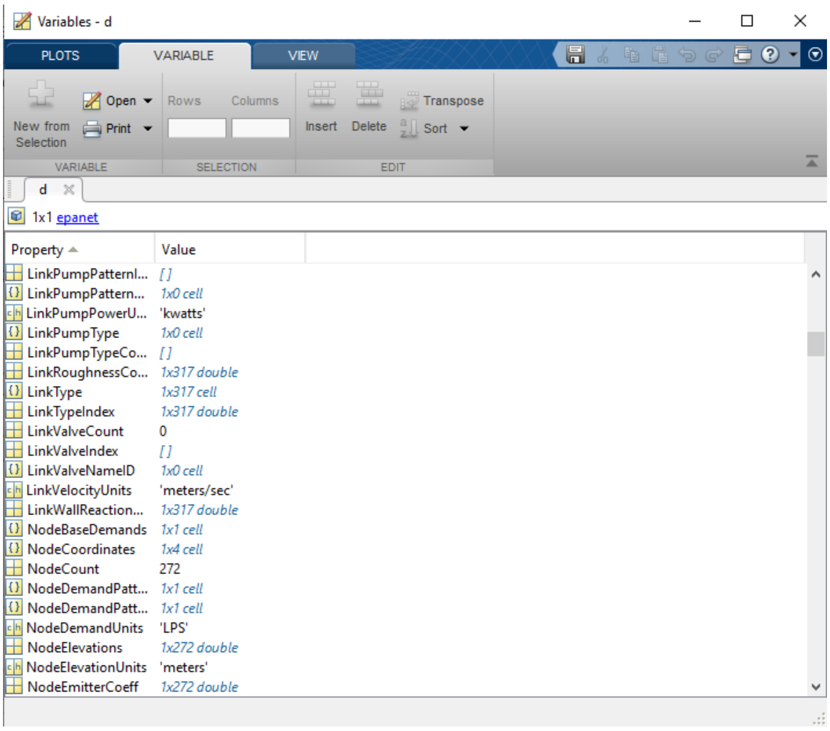

Figure 3-3: Epanet object structured by epanet MATLAB toolkit in MATLAB interface

When the object is constructed the user can call numerous toolkit functions which allow updating of all parameters in the network model, data visualization, hydraulic and quality dynamics solving, and loading of an EPANET-MSX file. The functions can be separated in two main categories: those which are used to received data starting with word -get- and functions used to change the set different factors of the simulation starting with -set-. During this thesis, we use an ample of those toolkit functions in order to adjust the dynamic variables of the system during multiple simulations. Some of these functions are provided in Table 3-1.

Table 3-1:List of EPANET-MATLAB Toolkit Class functions

Functions	Description
getComputedHydraulicTimeSeries:	Computed Hydraulic Time Series
getNodeActualDemand	Retrieves the computed value of all actual demands
setOptionsPatternDemandMultiplier	Sets the value of pattern demand multiplier
setTimeQualityStep	Sets the quality step
setPatternMatrix	Sets all of the multiplier factors for all patterns
initializeMSXQualityAnalysis	Initializes the MSX system before solving for water quality results in step-wise fashion
setMSXPattern	Sets all of the multiplier factors for a specific time pattern
getMSXComputedQualitySpecie	Retrieves the quality values for specific specie

4 Development of water quality model

4.1 Model overview

To simulate realistic deliberate injections of organic load in water distribution systems we integrate a chlorine decay model capable of interacting with organic compounds into a bacterial regrowth model. In the current study the contaminant, which is assumed a mixture of organic compounds (dissolved, suspended, biodegradable, non-biodegradable), is measured in total organic carbon (TOC) and biomass (bacteria) and will rapidly diffuse into distribution pipes from a starting point. In water supply systems, two situations may occur in practice: (a) chlorine is in excess over the reactive compounds that can react with it; or (b) the reactive compounds are in excess over chlorine (Vieira et al., 2004). At the moment where the organic substrate disperses into the system, the chlorine residual will react in an rapid rate (Brown et al., 2011; Haas and Karra, 1984) causing instant decay. The loss of the disinfectant concentration levels combined with the entry of organic nutrients from the contaminant are expected to accelerate microbial processes aggravating the total impact to consumers.

4.2 Bacterial regrowth model

The mathematical model used for describing bacterial regrowth in water distribution systems during a deliberate injection of organic load is based, on the work of Zhang, et al.,(2004). The model was adopted because it fits well for the particular experimental simulations since it contains bacterial and biodegradable dissolved organic carbon kinetics equations, which are highly determined by chlorine residual concentration. The bacterial regrowth model equations are implemented unmodified, except its chlorine modeling kinetic equation, a first order kinetic equation with a constant coefficient, that is replaced due to its failure to interpret any alterations in bulk water composition. Main advantages of the model are: (1) the microbial and chemical processes are linked with a hydraulic model and non-steady state hydraulic conditions, contrary to previous similar models (Bois et al., 1997), (2) the model contains a simplified number of system constants (11) that strongly influence prediction of bacteria and restricts secondary parameters that may lead to uncertainty and (3) there are separate microbial processes for free and attached growth (biofilm). The processes are depicted in Figure 4-1.

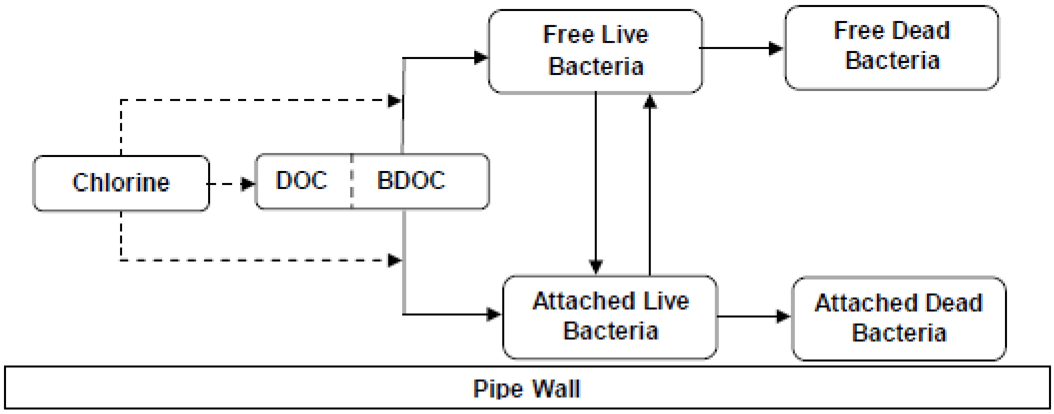

Figure 4-1: Conceptual diagram of bacterial regrowth within a pipeline. Solid arrows represent transformation processes while dashed arrows represent reactions with chlorine. | Source: Uber, (2011)

The dependent variables are free bacteria in the bulk water (X_b), attached bacteria on the inner surface of the pipe walls (X_a), biodegradable dissolved organic carbon (S) and free chlorine (CL_2) in the bulk water. The model operates as detailed below:

The net growth of free bacteria and attached bacteria utilize the biodegradable dissolved organic carbon as a growth substrate. The following rate equations, used to describe this growth are based on Monod kinetics:

$$\left.\frac{dX}{dt}\right|_{growth} = \mu X \qquad (1)$$

$$\frac{dS}{dt} = -\mu X / Y \qquad (2)$$

where X is the mass concentration of either free or attached bacteria, S is the mass concentration of BDOC, μ is the specific growth rate coefficient of bacteria and Y is the bacterial yield coefficient. From literature it is known that many parameters affect bacterial growth rate μ (Zhang et al., 2004). In the model are only considered the most important ones, which are the organic substrate concentration, the chlorine concentration and the temperature, consequently only these are considered in the model. It is essential to underline that temperature and disinfectant contribution are inserted in the equations as empirical approaches in order to describe laboratory observations, as they have not been studied extensively so far. The following equations account for the effect of all three factors on the specific growth rate:

$$\mu = \begin{cases} \mu_{max}\left(\frac{S}{S+K_s}\right)\exp\left(-\frac{Cl_2 - Cl_{2,t}}{Cl_{2,c}}\right)\exp\left(-\left(\frac{T_{opt}-T}{T_{opt}-T_i}\right)^2\right), when\ Cl_2 > Cl_{2,t} \\ \mu_{max}\left(\frac{S}{S+K_s}\right)\exp\left(-\left(\frac{T_{opt}-T}{T_{opt}-T_i}\right)^2\right) \qquad , when\ Cl_2 \leq Cl_{2,t} \end{cases} \tag{3}$$

where μ_{max} is maximum growth rate coefficient of biomass, Ks is the half–saturation constant T_{opt} is optimal temperature for bacterial activity, T_i is a temperature dependent shape parameter, T is in situ temperature; $Cl_{2,\,t}$ is threshold above which chlorine affects bacterial activity, and $Cl_{2,\,c}$ is a characteristic chlorine concentration that scales the degree of specific growth inhibition.

The bacterial mortality rate is accounted a first order rate

$$\left.\frac{dX}{dt}\right|_{decay} = -k_d X \tag{4}$$

where k_d = a decay rate constant.

The interaction of bulk bacteria and attached bacteria is accounted a first order rate reaction.

$$\left.\frac{dX_b}{dt}\right|_{deposition} = -k_{dep} X_b \tag{5}$$

$$\left.\frac{dX_b}{dt}\right|_{detachment} = k_{det} X_b U \tag{6}$$

where equation (5) denotes the deposition of free bacteria cells on to the surface of pipe walls while (6) is the detachment of attached bacteria into the bulk water with respect to flow velocity (U). K_{dep} and K_{det} denote the deposition rate constant and detachment rate constant accordingly.

Comments and notes of clarification are mentioned bellow:

1 Recent research has shown that bacteria utilize assimilable organic carbon (AOC), that is only a fraction of biodegradable dissolved organic carbon (BDOC) as a growth substrate (LeChevallier et al., 1988; van der Kooij et al., 1995; Volk and LeChevallier, 2000). In the model, AOC is neglected for reasons of simplicity. This simplification is assumed reasonable as AOC and BDOC show significant correlation in water samples according to researches (Volk and LeChevallier, 2000). Moreover, the model also does not account for other nutrients such as phosphorus and nitrogen as they are in a negligible amount with respect to organic carbon.

2 The inhibition factors for chlorine in equation (3) are empirical and were used in the SANCHO model (Laurent et al., 1997). Higher chlorine concentration leads to smaller inhibition factor resulting in smaller bacterial growth rates.

3 Due to the fact that biofilms are more resistant to inactivation by chlorine, different growth coefficients μ are used for bulk bacteria and attached bacteria (Eq. 3). Therefore $Cl_{2,\,t}$ for attached bacteria will be greater.

4 Temperature impact on bacterial regrowth rate coefficient μ is denoted. Results showed that temperature effect is insignificant in bacteria growth rate during a low timeframe intrusion event. In situ temperature is assumed bacterial optimal. As a consequence, it is neglected for simplicity and computability reduction.

5 Zhang's publication does not mention the type of bacteria being examined. In this thesis we consider that the bacteria regrowth can be measured by heterotrophic plate count (HPC) method, so as to be comparable in relation to the maximum allowable limit of the legislative provisions.

6 Values of parameters used in the bacterial regrowth model are listed in Table 4-1 as presented by Zhang et al., (2004). An exception is chlorine threshold concentration for free bacteria ($Cl_{2,t,b}$) that was replaced from 0.03 to a more conservative value 0.08 mg/L (Thøgersen & Dahi, 1996).

Table 4-1: Values of all parameters in the bacterial regrowth model. Values revised by the author are marked with an asterisk.

Parameter	Symbol	Value	Unit	Reference
Maximum growth rate of free bacteria	$\mu_{max, b}$	0.20	h^{-1}	Camper, (1996)
Maximum growth rate of attached bacteria	$\mu_{max, a}$	0.20	h^{-1}	Camper, (1996)
Chlorine threshold concentration for free bacteria *	$Cl_{2,t,b}$	0.08	mg/L	Thøgersen and Dahi, (1996)
Chlorine threshold concentration for attached bacteria	$Cl_{2,t,a}$	0.10	mg/L	Laurent et al., (1997)
Characteristic chlorine concentration	$Cl_{2,t,c}$	0.20	mg/L	Laurent et al., (1997)
Monod half saturation coefficient	K_s	0.40	mg/L	Laurent et al., (1997)
First-order kinetic constant for detachment *	K_{det}	0.04	h^{-1}	Bois et al., (1997)
First-order kinetic constant for deposition	K_{dep}	0.25	h^{-1}(m/s)	Zhang and DiGiano, (2002)
Bacterial mortality rate	K_d	0.06	h^{-1}	Zhang and DiGiano, (2002)
Bacterial yield coefficient	Y_g	0.15	mg/mg	Laurent et al., (1997)

4.3 Chlorine residual model

In order to complement the bacterial model described previously with a sufficient chlorine decay model that will allow realistic organic load injection simulations in WDSs, an extended literature review was conducted. Over the last decades, considerable research has been made concerning the best fitting chlorine decay model by evaluating different kinetic models in laboratory experiments. It is agreed by a significant part of the scientific community that first parallel chlorine decay model (Table 4-2) provided the best results among different models (Brown et al., 2011; Haas and Karra, 1984; Helbling and Vanbriesen, 2009; Vieira et al., 2004). Consequently, the same model was used in the current thesis.

Table 4-2: Parallel first order chlorine decay model

Model name	Model form	Analytical Solution	Parameters
Parallel first order	$\frac{dC_{fast}}{dt} = -k_1 C_{fast}$ $\frac{dC_{slow}}{dt} = -k_2 C_{slow}$ $C_{0,fast} = zC_0$ $C_{0,slow} = (1-z)C_0$	$C = C_0 z exp(-k_1 t) + C_0(1-z)\exp(-k_2 t)$	k_1, k_2, z

4.3.1 Influence of water quality on chlorine decay

The parameters of the parallel first order model that must be defined are k_1, k_2 and z. These symbolize a fast decay rate constant (k_1) of a compound (z) of chlorine concentration, and a slow rate constant (k_2) of the remaining compound. These coefficients were estimated by Vieira et al., (2004) in laboratory experiments performed on water samples. Vieira's research was based on water samples collected upstream of chlorination in a water treatment plant near the city of Almada (Portugal). Three series of bottle tests were carried out with the aim of evaluating the influence of (1) chlorine initial dosage, (2) organic matter (TOC) addition, (3) iron addition, and (4) temperature. Results showed existence of high correlation between constants and those variables. Specifically, when chlorine was in excess and no other chemical substance was added, k_1 and k_2 coefficients were found correlating well (r >0.79) with $1/C_0$ for three different temperature conditions (24.5 C, 20.0 C and 14.6 C) (Figure 4-2).

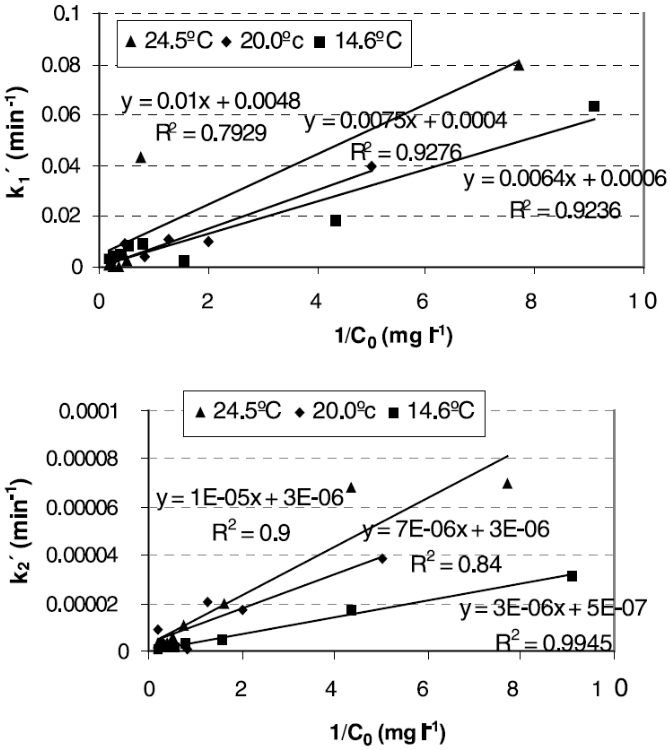

Figure 4-2: Decay constants as a function of the inverse of initial chlorine concentration, $1/C_0$ |Source: Vieira et al., (2004)

In our model, we used the linear relationships referred to 14.6 C as it meets more accurately the annual mean temperature in Europe and specifically in Modena, Italy (13.4 C, climate-dara.org) which is our case study.

In contrast, research has shown that when sufficient organic content (TOC) is added in water, chlorine decay is directly correlated to TOC concentration due to immediate chemical reactions. Linear relationships between TOC and kinetic constants were extracted for bottle samples with initial chlorine concentration 2 and 0.2 mg/L for temperature conditions of 14.6 °C (Figure 4-3). In water distribution network systems, chlorine concentration should range between 0.2 and 1 mg/L as expressed in *Guidelines for Drinking-water Quality* (World Health Organization, 2003). Consequently, for our model implementation we adopted the linear relationships extracted by experiments with initial chlorine concentration of 2mg/L as a more realistic scenario.

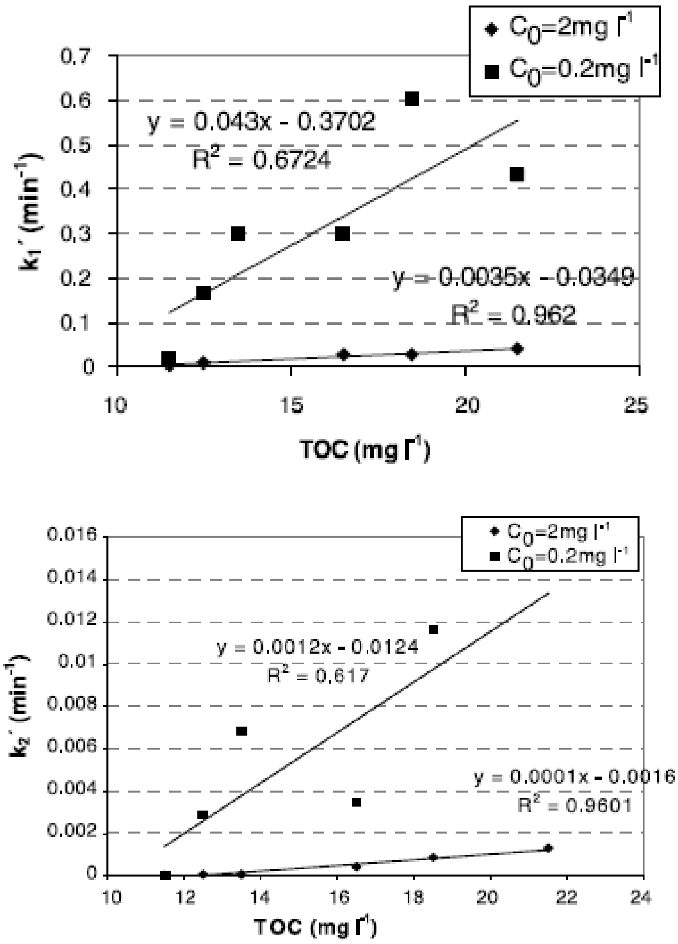

Figure 4-3: Influence of TOC on chlorine decay constants | Source: Vieira et al., (2004)

In order to estimate parameter z, we exploited the data provided by Vieira's graphs showing correlation between x and initial concentration C_0 in absence of any other substrate in excess and between z with TOC when TOC is added. These graphs did not include any mathematical relationships between fraction *z* and any compound. For this reason, we reproduced the graphs in a spreadsheet and conducted a regression analysis. In case of no added TOC, a second order polynomial trendline displayed the highest R-squared value (R^2=0.95) where fraction z decreases with initial disinfectant concentration (Figure 4-4). When organic matter is in excess over the disinfectant, results depicted a slow increase of fraction *z* with TOC, but no regression model could determine strong relationship between the variables (Figure 4-5).

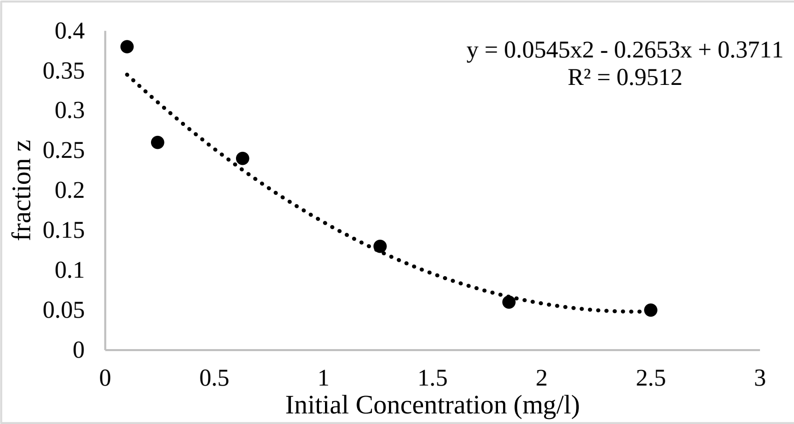

Figure 4-4: Influence of initial chlorine concentration on the fraction z (no addition of organic matter – temperature conditions: 14.6 C) | Data: Vieira et al., (2004)

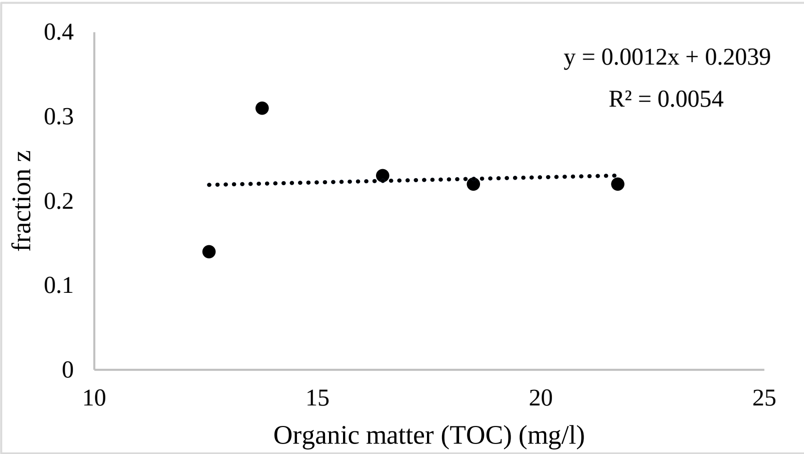

Figure 4-5: Influence of organic content on the fraction z (temperature conditions: 14.6 C, Initial chlorine concentration: 2.0 mg/L) | Data: Vieira et al., (2004)

Considering all above, it is noticeable that in case of an organic injection (TOC addition) in water supplies, chlorine decay rates are increasing radically. An example is shown in Figure 4-6 where three different decay curves are illustrated in a sample of 0.7 mg/L

The first curve results from first order chlorine decay as presented by Zhang et al., (2004) in bacterial regrowth model, the second results from parallel first order chlorine decay without any added substances and the third one depicts chlorine decay when sufficient TOC addition (50 mg/L) is injected in the sample. Decay rate values are shown in the following table:

Table 4-3: Differences in parameter values among chlorine decay models. Chlorine initial concentration is assumed 0.7 mg/L

Model	**Parameters**	**Substance depended on**	**Values**	
First order decay model	k_b	-	0.020	(1/5min)
First parallel order decay model (no added substance)	k_1,	Initial chlorine concentration	0.048	(1/5min)
	k_2		0.00005	(1/5min)
	z		0.212	-
First parallel order decay model (50mg/L TOC added)	k_1,	Total Organic Carbon	0.70	(1/5min)
	k_2		0.017	(1/5min)
	z		0.264	-

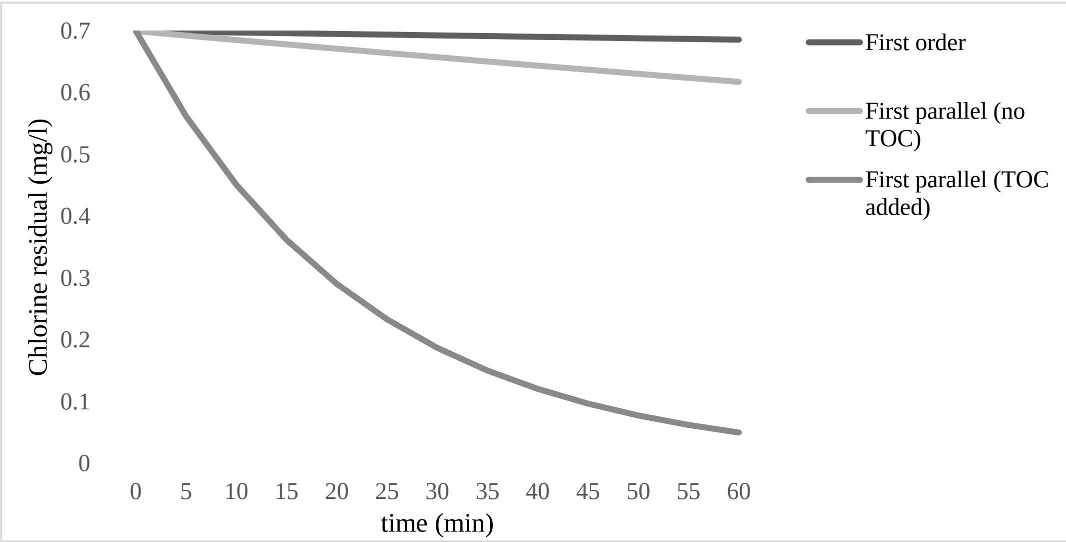

Figure 4-6: Examples of chlorine decay curves for conditions described in Table 4-3

Finally, yet importantly, a question regarding when TOC addition is assumed in sufficient quantity in order to impact chlorine decay rates. In other words, when we should consider mathematical relationships between the parameters (k_1, k_2, z) and C_{0-} (Figure 4-2 and Figure 4-4) and when between the parameters and TOC (Figure 4-3 and Figure 4-5). A practical solution is given by detecting the lower bound of TOC concentration which equalizes the fast decay rate (k_1) to the same value as when there is no TOC addition (see values in color in Table 4-4). Because, the results differ with respect to C_0, a mean value was considered. The following table shows the results:

Table 4-4: TOC sufficient concentration lower bounds.

Chlorine initial concen. *(mg/L)*	0.5	0.6	0.7	0.8	0.9	
No TOC addition -Parameters with respect to chlorine initial concentration						
k1 *(1/min)*	0.0134	0.0113	0.0097	0.0086	0.0077	
k2 *(1/min)*	0.000	0.000	0.000	0.000	0.000	
fraction z	0.252	0.232	0.212	0.194	0.176	
TOC addition- Parameters with respect to TOC						
TOC *(mg/L)*	**13.8**	**13.2**	**12.74**	**12.43**	**12.17**	**12.90**
k1 *(1/min)*	0.0134	0.0113	0.0097	0.0086	0.0077	
k2 *(1/min)*	0.000	0.000	0.000	0.000	0.000	
fraction z	0.220	0.220	0.219	0.219	0.219	

4.4 Model adaptation to Epanet-MSX

In order to run quality simulations using EPANET-MSX the next step is to prepare the MSX input file that defines the individual water quality species of our model and the reaction expressions that govern their dynamics. This can be done using a text editor and following the format described in EPANET-MSX manual. The resulting MSX input file, named *bacterial.msx,* will be expanded in the next lines.

```
[TITLE]
Contaminant injection model in water distribution systems
[OPTIONS]
  AREA_UNITS CM2             ;Surface concentration is mass/cm2
  RATE_UNITS HR             ;Reaction rate units are concentration/hour
  SOLVER     EUL
```

```
TIMESTEP   360          ;360 sec (6 min) solution time step
RTOL       0.001        ;Relative concentration tolerance
ATOL       0.0001       ;Absolute concentration tolerance
```

Area units are set to cm^2 as determined by the bacterial regrowth model. The forward standard Euler integrator (EUL) was chosen for numerical integration method, since it is best applied to non-stiff, linear reaction systems. All options can be modified using the EPANET MATLAB toolkit, thus it is of minor importance to determine them in the MSX file.

```
[SPECIES]
BULK   CL2   MG       ;chlorine
BULK   S     MG       ;organic substrate
BULK   Xb    UG       ;bulk biomass (ug/l)
WALL   Xa    UG       ;attached biomass (ug/(cm2))
BULK   Nb    log(N)   ;number of free bacteria
WALL   Na    log(N)   ;number of attached bacteria

[COEFFICIENTS]
CONSTANT CL0 1 ; INITIAL CL0 (mg/l)

CONSTANT  CL2C    0.20   ;characteristic CL2 (mg/L)
CONSTANT  CL2Tb   0.08   ;threshold CL2 for Xb (mg/L)
CONSTANT  CL2Ta   0.10   ;threshold CL2 for Xa (mg/L)
CONSTANT  MUMAXb  0.20   ;max. growth rate for Xb (1/hr)
CONSTANT  MUMAXa  0.20   ;max. growth rate for Xa (1/hr)
CONSTANT  Ks      0.40   ;half saturation constant (mg/L)
CONSTANT  Kd      0.06   ;bacterial decay constant (1/hr)
CONSTANT  Kdep    0.25   ;deposition rate constant (1/hr)
CONSTANT  Kdet    0.04   ;detachment rate constant (1/hr/((cm2)/s))
CONSTANT  Yg      0.15   ;bacterial yield coefficient (mg/mg)
```

The species being simulated are, as mentioned, chlorine (CL_2) in mg/L, biodegradable dissolved organic carbon (S) in mg/L, bacteria in the bulk water (X_b)in μg/L, and bacteria attached in the pipe surface (X_a) in $\mu g/cm^2$. In the MSX file we add N_b and N_a, which represent the total numbers of bulk bacterial cells and attached bacterial cells accordingly. Species are separated in BULK and WALL in order to define their units, mass per volume or mass per area, respectively.

In the [COEFFICIENTS] section the parameters of Table 4-1 are placed, plus the CL_0 constant with a default value of 1 mg/L. This value must be changed in every discrete simulation in order to be equal with the water supply sources' chlorine concentration value. This parameter is used in the chlorine first parallel decay model, which uses this constant in order to adjust the decay rates when no substance is added in the water system.

Next is presented the [TERMS] section which allows us to define intermediate mathematical terms in the model's description so that the rate equations can be expressed more clearly and compactly and [PIPES] section for describing the rate equations.

```
[TERMS]
Ib   EXP(-STEP(CL2-CL2Tb)*(CL2-CL2Tb)/CL2C)         ;Xb inhibition coeff.
Ia   EXP(-STEP(CL2-CL2Ta)*(CL2-CL2Ta)/CL2C)         ;Xa inhibition coeff.
MUb  MUMAXb*S/(S+Ks)*Ib                            ;Xb growth rate coeff.
MUa  MUMAXa*S/(S+Ks)*Ia                            ;Xa growth rate coeff.
TOC  5.55*S

K1_TOC   (0.0035*TOC - 0.0349)*60                   ; (i)
K2_TOC   (0.0001*TOC - 0.0012)*60                   ; (ii)
Z_TOC    (0.0012*TOC + 0.2039)                      ; (iii)

K1_CL2 (1/CL0*0.0064+ 0.0006)*60                    ; (iv)
K2_CL2 (3*10^(-6)/CL0 +5*10^(-7))*60                ; (v)
Z_CL2  0.0545*CL0^2 - 0.2653*CL0 +0.3711            ; (vi)

K1 STEP(TOC-12.9)*K1_TOC + STEP(12.9-TOC)*K1_CL2     ; (vii)
K2 STEP(TOC-12.9)*K2_TOC + STEP(12.9-TOC)*K2_CL2     ; (viii)
Z  STEP(TOC-12.9)*Z_TOC + STEP(12.9-TOC)*Z_CL2       ; (ix)
```

The effect of chlorine on limiting the number of viable bacterial cells is modeled by applying an inhibition factor I to the bacterial specific growth rates as:

$$I = \exp(\frac{-(C - C_t)}{C_c}) \tag{7}$$

Here C is the chlorine concentration and C_t , C_c are the threshold and characteristic chlorine concentrations accordingly. The special EPANET-MSX function STEP(x) is used in the definitions of the inhibition factors I_b and I_a and is internally evaluated to 1 when x>0 and 0 otherwise.

Equations (i)–(iii) calculate the chlorine decay constants with the respect to TOC, while equations (iv)-(vi) calculate them with respect to initial chlorine concentration CL_0. Lastly, the decision of which set of three parameters (k_1, k_2, z) will enter the chlorine rate equation each time step is determined in equations (vii)-(ix) considering whether current TOC concentration is over 12.9 milligrams per liter.

Total organic carbon (TOC) is not defined in the MSX file as a specie, thus its kinetic equations are not described directly. To overcome this, TOC concentration is measured as BDOC concentration since BDOC consists a fraction of TOC with a **ratio of 18%**. This percentage resulted from literature review and a combination of sources since no value was found for this actual proportion. The calculation of the percentage and the sources we based on are shown in the Table 4-5.

Table 4-5: Literature review of carbon fractions ratios aimed in estimating the BDOC/TOC ratio.

Substances Ratio	Value	Reference	Description
DOC/TOC	0.50 (range: 21-70%)	Yang et al., (2014)	In this study 22 domestic wastewater treatment plants were explored for TOC, DOC, BOD and COD by monitoring the changes of fluorescent components.
BDOC/DOC	0.35 (range: 11-59%)	Pierre et al., (1987)	This paper demonstrated that most DOC is not biodegradable. For all the water samples (e.g. sewage, sea, river, forest stream and tap water), BDOC were observed to be 35%
Consequently			
BDOC/TOC	0.35 ×0.50 = **0.18**		

```
[PIPES]
RATE    CL2    -(Z*K1 + K2*(1-Z))*CL2
RATE    S      -(MUa*Xa*Av + MUb*Xb)/Yg/1000
RATE    Xb     (MUb-Kd)*Xb + Kdet*U*Xa*Av - Kdep*Xb
RATE    Xa     (MUa-Kd)*Xa - Kdet*U*Xa + Kdep*Xb/Av
FORMULA Nb     LOG10(1.0e6*Xb)
FORMULA Na     LOG10(1.0e6*Xa)
```

In the [PIPES] section all species are calculated under the equations described in the Bacterial regrowth model except of N_b and N_a. For these, a simple expression is used to convert micrograms of bacterial carbon to logarithmic cell counts. It is assumed that there are 10^6 cells per microgram of carbon in the cell biomass (Shang et al., 2008b).

The variables U and A_v are reserved symbols in EPANET-MSX that represent flow velocity and pipe surface are per unit volume, respectively, and their values are automatically computed by the program. Whenever the surface bacteria species appears in the expression for bulk bacteria it is multiplied by A_v to convert from areal density to volumetric concentration. Likewise, bulk bacteria are divided by A_v in rate expression for attached bacteria to convert it to an areal density.

Finally, the [TANKS] kinetic rate expressions do not include any terms involving X_a since it is assumed that surface species do not exist within storage facilities. The [SOURCES], [QUALITY] and [PATTERNS] sections are left blank in the MSX file as they are defined through EPANET MATLAB toolkit in the MATLAB interface.

```
[TANKS]
RATE    CL2    -K1*Z*CL2 - K2*(1-Z)*CL2
RATE    S      -MUb*Xb/Yg/1000
RATE    Xb     (MUb-Kd)*Xb
FORMULA Nb     LOG10(1.0e6*Xb)

[SOURCES]
[QUALITY]
[PATTERNS]
```

---

5 Case study

5.1 Methodology overview

In this case study we examine the vulnerability of municipal water distribution systems to deliberate organic load contamination under realistic hydraulic and water-quality conditions. The multispecies water-quality model introduced in previous paragraph is integrated to a hydraulic water distribution network model and utilized to describe the movement and interaction of water quality species (chlorine, biodegradable dissolved organic carbon, bacteria in bulk water, attached bacteria) through the network pipes, before and during the simulation injections. The contaminant is a soluble conservative substance consisting of organic carbon (measured in TOC) and heterotrophic plate count (HPC) bacteria, assuming domestic wastewater proportion 1.47×10^{6} CFU/ gram TOC (Cyprowski et al., 2018). The release of this substance in high amounts leads to significant water contamination by either high TOC or bacterial concentration while at the same time chlorine reacts with TOC and decays rapidly.

The experimental phase has two objectives. The first objective is to develop and demonstrate a vulnerability assessment to examine network's response and potential consumers' harm under the biochemical contaminant assaults intruded in different points of the network. The second objective is to investigate the sensitivity of network's response to three (3) dynamic variables, two of them depended on the intruder (injection mass, injection duration) and the last one depended on the water operators (BDOC concentration in processed water). The last variable in turn, influences the total water quality of the network.

5.2 Network topology

The water distribution network of Modena, Italy which was hydraulically modeled by Bragalli et al., (2008) is considered our study site. The input hydraulic data, which are provided by

OpenWaterAnalytics[1]. were acquired from the web. The system provides a complex network consisting of 272 nodes, 336 pipes that cover almost 72 km, and 4 source reservoirs (a main source and three minor ones), all mainly serving residential users with an average systemwide demand of 20 million L/day (243 L/s). It was mostly preferred due to its complex structure and high variability of base demands, pipe lengths and water flows, creating this way a broad reach of different hydraulic and water quality conditions available for experimental simulations. The water consumption at any node is known and used to estimate numbers of consumers connected to each node in the network (Figure 5-2). Assuming that people averagely consume 180 litres per day (European Parliament, 2019), then approximately 195.000 consumers are served.

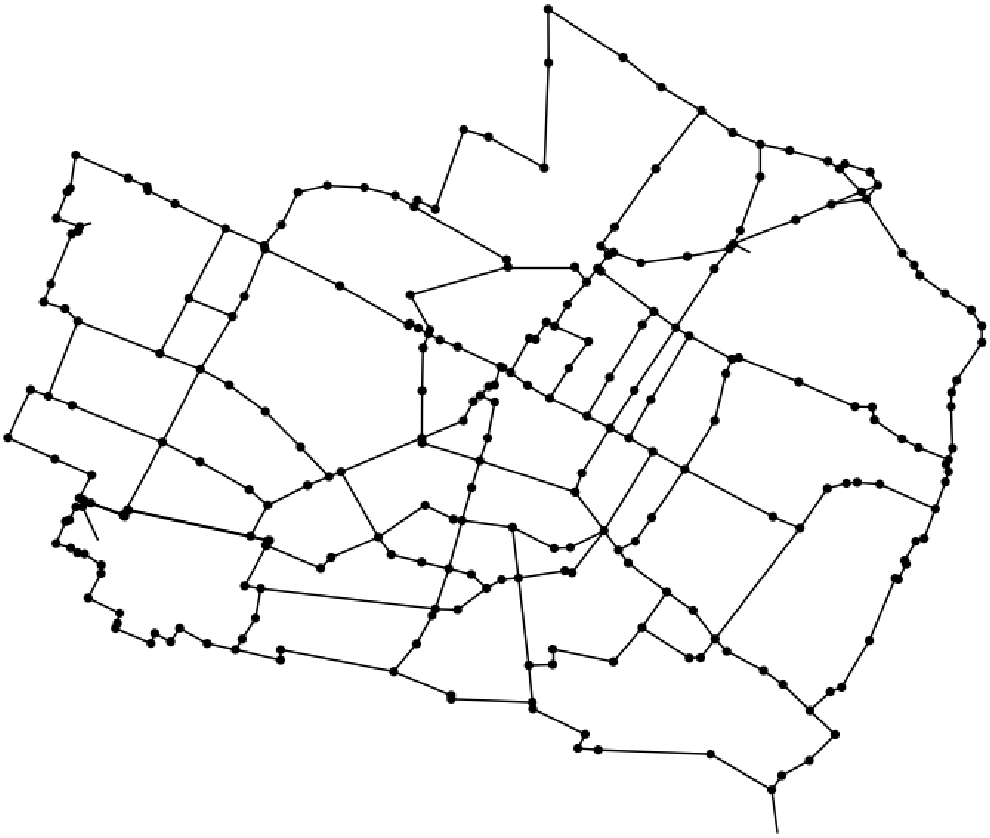

Figure 5-1: Network of Modena study site. Discontinuity in pipes denote the existence of

The layout of the Modena water distribution system consists of mostly closed-loop links with main and sub-lines, while dead-end links do not exist. The network does not include storage

[1] https://github.com/OpenWaterAnalytics/EPANET-Matlab-Toolkit

tanks for equalizing water supply, as the three minor reservoirs are spatially distributed in the network, thus function to distribute the required volume in the most isolated areas. In addition, the system is capable of transferring the flow capacity, without any water pumps despite possible demand fluctuations.

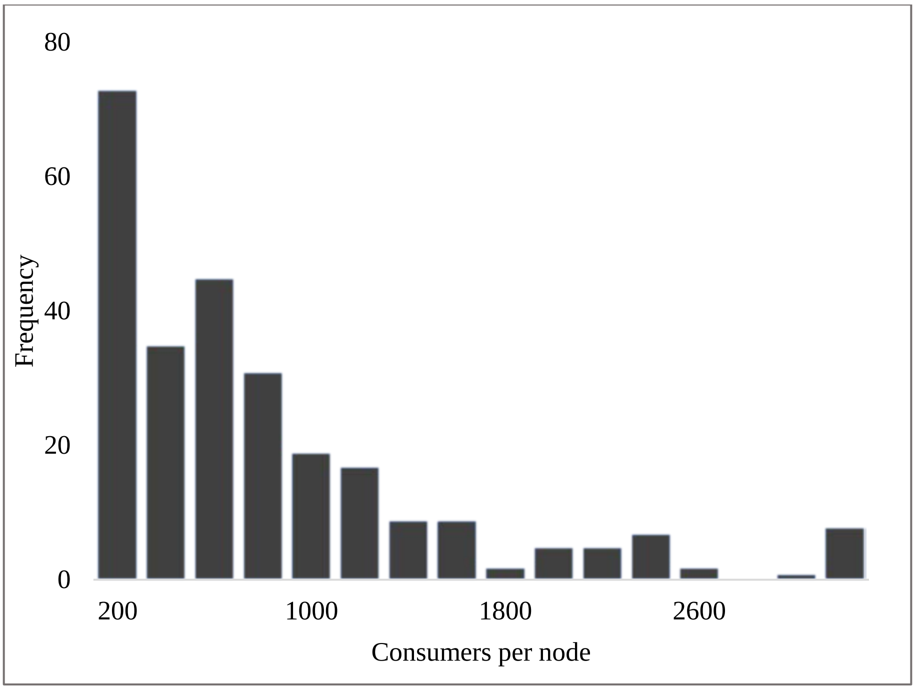

Figure 5-2: Distribution of number of consumers at each network node of total 268, estimated from the water demand at these nodes

An EPANET hydraulic analysis was set under constant base demand for all nodes for 24 hours to ensure that no errors such as negative pressures occur during the solution. The range of main static characteristics and dynamic variables resulted from the simulation are presented in Table 5-1. Exception is pipe roughness coefficient, which is invariable in all pipes of the system with a value of 130 in terms of Hazen-Williams formula and indicates that pipe material is cast iron (Rossman, 2000).

Table 5-1: Modena network main characteristics and hydraulic parameters range for base-case EPANET simulation under constant base demand for all nodes. *Roughness coefficient remains invariable in all pipes.

Parameters	Range		Units
Nodes			
Elevation	30.59	41.83	m
Base Demand	0.01	9.47	L/s
Reservoirs Elevation	72.00	74.50	m
Pressure	27.13	39.05	m
Pipes			
Length	6.03	1094.73	m
Diameter	100	350	mm
Roughness*	130		-
Velocity	0.01	1.25	m/s
Flow	0.08	130.03	m^3/s

5.3 Contaminant event simulations

The objectives of this thesis are based on observations made on multiple contaminant event simulations. The attacks are simulated as a deliberate injection of a soluble biochemical substance pumped each time into a node on the trunk line of the Modena drinking water distribution system. The injection is set using EPANET's mass booster source option, which allows to input a steady mass rate per minute. Since the contaminant substance consists of TOC and bacteria, the mass booster option is used separately for the two substances.

An example **demonstration** of an attack scenario is presented below, providing some basic steps for the construction of an organic load contamination event through EPANET-MATLAB-toolkit. The complete source code is provided in the Appendix p. 113.

The EPANET Input and MSX file are loaded, constructing the **epanet** object d.

```
inp_file = 'MOD.inp';
d = epanet(inp_file); %Load network and use the EPANET library
d.loadMSXFile('bacterial_kinetics.msx') % Load MSX file with reactions
```

The location (node 52) and the duration of the intrusion (30 minutes) are declared as:

```
intr_node = '52';
intr_node_index = d.getNodeIndex(intr_node);
inj_time  = 30;     %(min)
```

The duration of the simulation is set to 4 hours and the pattern step to 1 minute. The pattern step is used to define the duration of the intrusion by creating a matrix ('p1') of elements equal to total pattern time step intervals. The matrix is filled with ones and zeros, one for time intervals in which injection occurs and zero in the opposite case.

```
hrs = 4
d.setTimeSimulationDuration(hrs*60*60); %Set simulation duration
d.setTimePatternStep(30*60);% Set pattern step
p1=zeros(1,hrs*3600/TimePatternStep); % p1 matrix initialize
intr_start = 3; % start minute of intrusion
for i = 0:inj_time-1
      p1(1,intr_start+i) = 1; % p1 matrix filled
end
d.setMSXPattern('p1',p1) % Set p1 matrix as the 'p1' time pattern
```

Lastly, the intrusion source characteristics are defined. Assuming a total 6 kg biochemical mass is injected in the network, then the contaminant enters the network with a steady rate of 200 g/minute. The total bacterial and BDOC injected masses used as an input to the model are calculated based on the assumptions previously described.

```
total_TOC = 6000; % Total mass of contaminant substance (g)
TOC_inj = total_TOC/(inj_time); % (gr/min)
```

```
BDOC_inj = TOC_inj/5.55; %(gr/min) TOC conversion to BDOC (18% BDOC/TOC
ratio)
xb_inj = 1.47*TOC_inj ; %(ug/min) microbial load per TOC grams
d.setMSXSources(intr_node,'S','MASS',BDOC_inj*10^3,'p1');
d.setMSXSources(intr_node,'Xb','MASS',xb_inj,'p1');
```

After the injection, the biochemical substance is dispersed into the water distribution system reaching other downstream nodes. The TOC and bacteria concentration of the polluted water reaching each node depends on the hydraulic conditions (e.g. flow, velocity) in the downstream pipes as well as the continual reactions occurring between the species involved. Figures 5-2 and 5-3 show the chlorine residual and BDOC concentration in two downstream nodes during the simulation. Node 50 is placed 200 m after the intrusion and the contamination reached the node only 12 minutes after the beginning of the injection. In contrary, node 104 distances 1.3 km from the injection point and the polluted water reaches it after 1:50 hours with almost zero chlorine concentration due to its decay.

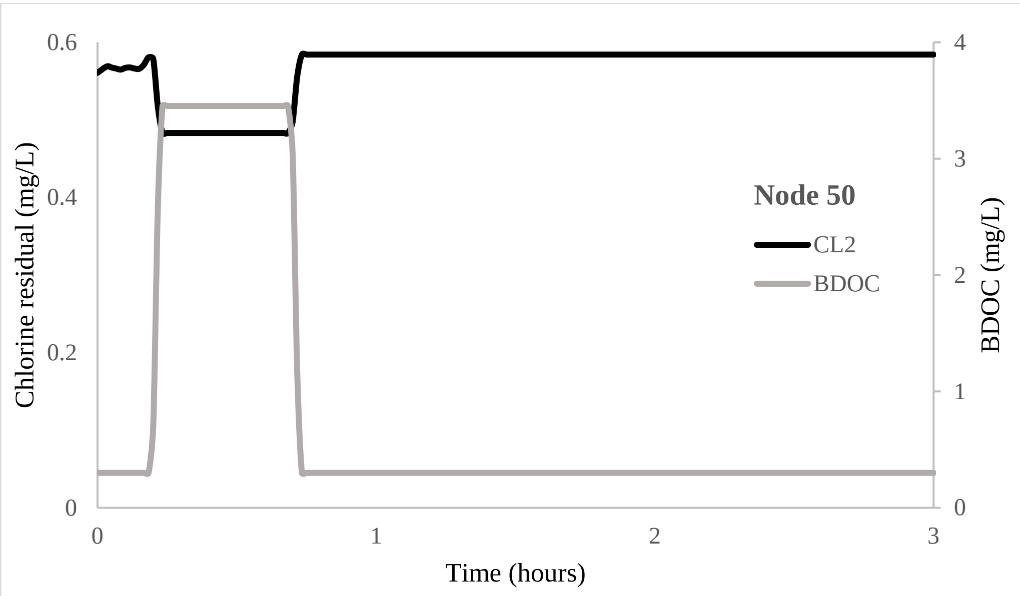

Figure 5-3: Chlorine residual and BDOC concentration in node 50 (upstream) during the attack demonstration example simulation

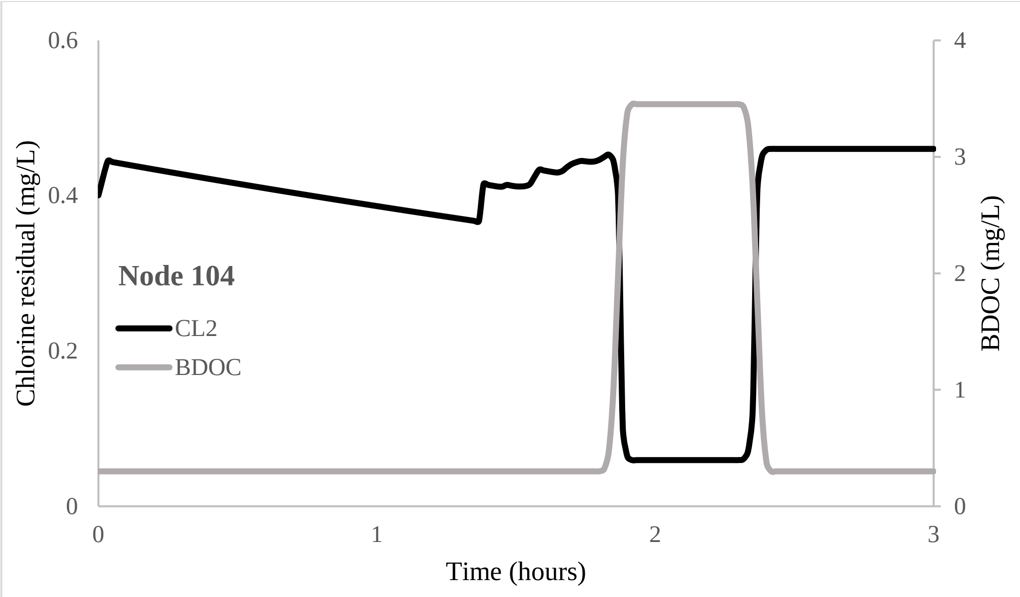

Figure 5-4: Figure 5-5: Chlorine residual and BDOC concentration in nodes 104 (downstream) during the attack demonstration example simulation

5.4 Initial conditions

Realistic water-quality conditions that exist in our site study water distribution system are necessary in order to extract more accurate results about how organic load injections effect in a case of deliberate intrusion. Under common conditions, bacteria entering the bulk water are inactivated if the disinfectant residual is sufficient. However, bacteria that attach on the surface of pipe materials still grow even in the presence of disinfectant. In this case, there is no negative impact on the consumer even though bacterial regrowth occurs on the pipe surface. On the other hand, if the loss of disinfectant residual in the bulk water is significant (e.g. due to large water residence times), then bacteria that are released from biofilm will not be inactivated quickly but they will grow in bulk water causing potential harm to consumers. Considering all the above, firstly, we examine which is the lowest chlorine dose that ensures that chlorine concentration does not drop below a certain target across the whole network and secondary, we conduct a hydraulic and quality simulation, in which concentrations of chlorine (CL2), biodegradable dissolved organic carbon (BDOC) and bulk bacteria (X_b) enter the system from the sources, interact across all the pipes combined with the hydraulic conditions, and finally reach an equilibrium considering the establishment of biofilm in the pipes surface. The final concentrations of chlorine residual, free bacteria, and attached bacteria are inserted as initial conditions to each network element (nodes, pipes) for the injection simulations.

5.4.1 Investigation of minimum chlorine dose

Many studies argue that a minimum chlorine level of 0.2 mg/L or more and its preservation throughout the system is required to maintain good quality drinking water (Ridgway and Olson, 1982; Vasconcelos et al., 1997). This opinion is debatable according to other studies which demonstrated that disinfection of bacteria by 2 mg/L of chlorine might not be effective enough under microbial load (LeChevallier et al., 1984). In this study, we set a minimum chlorine target 0.3 mg/L throughout the system to ensure low bacterial activity. To determine the chlorine level dose needed in the sources in order to preserve the chlorine target a MATLAB program was created, of which the flowchart is presented in Figure 5-4. The chlorine decay rate equations are described in the MSX file which is set as an input to the program and are described in paragraph 4.3.

Table 5-2: Input parameters for minimum chlorine dose program

Features	**Details**
Simulation Duration	100 hours
EPANET hydraulic step	1 hour
EPANET quality step	6 minutes
Chlorine residual target	0.3 mg/L
Start-up duration	20 hours
Initial chlorine decay parameter CL_0	1 mg/L

The program is based on two repetitive processes (loops). Initially we set the chlorine decay parameter CL_0 to 1 mg/L, a value that actually represents the concentration of water while exiting the sources. Then a chlorine source dose of 0.3 mg/L is set and EPANET investigates if this dose is sufficient to cover the network with water of concentration greater than the target (0.3 mg/L) after 100 hours of simulation. The target is only checked after a start-up duration of 20 hours to ensure that chlorine concentration is equalized in all points of the network. If the dose is not acceptable, then 0.05 mg/L is added to and the simulation runs over until chlorine dose is sufficient. Afterwards, the decay parameter (CL_0) is set equal to the source dose and the simulations start over until chlorine source dose and chlorine decay parameter (CL_0) have equal values. The process is visualized in the following flowchart.

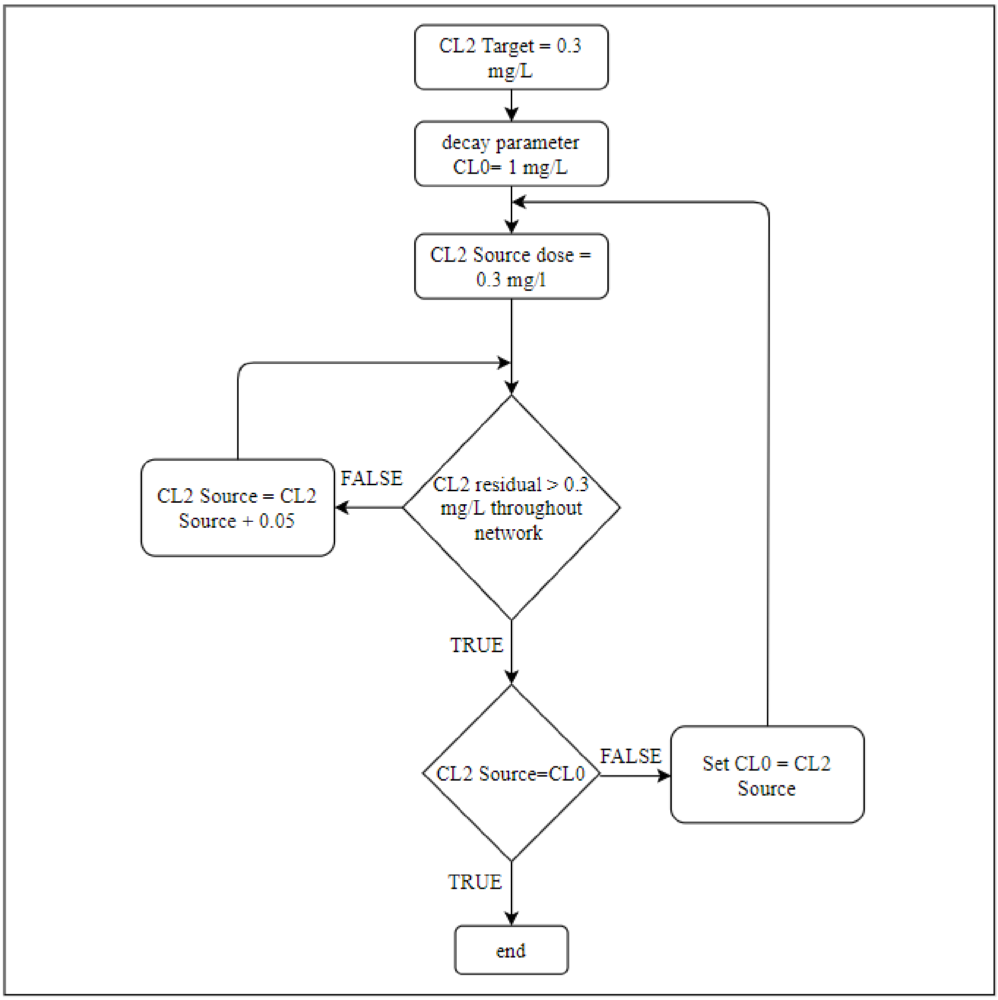

Figure 5-6: Flowchart of minimum chlorine dose program, used to investigate the sufficient chlorine concentration exiting the sources in order to ensure chlorine residual greater than 0.3 mg/l throughout the network.

Results show that chlorine concentration dose of **0.6 mg/L** set in all network sources is sufficient to prevent any points with water of lower concentration than the target 0.3 mg/L. The lowest chlorine concentration point is in Node 265 with chlorine residual concentration of 0.32 mg/l. In total, 9 nodes have lower concentration of 0.4 mg/L, 146 nodes between 0.4-0.5 mg/l and 113 nodes have greater than 0.5 mg/L.

5.4.2 Development of biofilm on pipe wall

The development of biofilm on pipe walls in water distribution systems is caused by a number of factors including the nature of water transport mechanisms (e.g. the importance of dispersion compared to advection), the existence and concentration of an electron acceptor, the concentration of the disinfectant and the characteristics of a growth substrate (Zhang et al., 2004). According to other studies (Bois et al., 1997; Servais et al., 1992) even low levels of biodegradable organic matter are sufficient to support biofilm growth in water infrastructure. In this case study, a simulation is conducted in which chlorine, biodegradable carbon and bulk bacterial concentration enter the network from the sources. By the end of the simulation the final values for each node and pipe (four species per element) will be saved to a MATLAB file in order to be applied as **initial conditions** for the organic load injection simulations in the first objective of the vulnerability assessment.

The simulation is conducted by setting only the species concentration (chlorine, organic matter, bacteria) in the entrance of the network. The concentration of chlorine is set to **0.6 mg/L** as the minimum dose needed to ensure that no system point's chlorine concentration gets lower than 0.3 mg/L. Biodegradable dissolved organic carbon concentration is set to **0.3 mg/L**. This value is adopted from the study of Volk and LeChevallier, (2000), who monitored BDOC concentration in finished water at 95 water plants across US and Canada and concluded that the geometric mean for all the sites was 0.32 mg/l. Last but not least, bacterial concentration value is based on legislation so it does not exceed the recommended limits. Several countries, among which, Germany, Australia, the Netherlands and Japan include a limit of 100 CFU/mL, while EU does not set numerical values for HPC bacteria (Chowdhury, 2012). Therefore, the microbial value is set to 80 CFU/mL. Assuming there are 10^6 cells per microgram of carbon in the cell biomass (Shang et al., 2008b), **0.08 μg/L** is set as the concentration of bulk bacteria in the entrance of the water distribution system. Apart from concentration in the sources, the initial conditions within all links of the network are zero for any species (chlorine, BDOC, bulk bacteria, attached bacteria) and base demand in all nodes is assumed invariable. The simulation lasted 30 days in order to reach a steady state with respect to attached bacteria (biofilm) in all pipes of the network. Simulation's hydraulic step is set 1 hour, the quality step is 12 minutes and total computation time is 12 minutes using a 2.55 GHz CPU PC.

Results show that the geometric mean of bacteria in bulk water in all nodes of the network is 0.06 μg/mL (60 CFU/ml). As expected, the bacterial regrowth in bulk water has been controlled under the disinfectant sufficient concentration in all points of the network. On the other hand, **sufficient bacterial growth** has occurred in the surface of pipes. The geometric mean of biofilm in pipes is 6.70 μg/cm^2 (6.70×10^6 CFU/cm^2). Table 5-3 displays the four pipes with most attached bacteria growth and the lower four pipes along with their hydraulic characteristics.

Table 5-3: Pipes with greater and lower concentration of attached bacteria after 30 days of simulation

Pipe No.	Biofilm (μg/cm^2)	Diameter (mm)	Flow (L/s)
269	786.29	100	0.04
335	16.16	400	222.25
291	14.05	350	162.66
290	13.87	350	161.43
250	0.79	100	0.82
117	0.73	100	1.25
252	0.52	100	0.89
215	0.48	100	2.33

The fact of extremely biofilm growth in pipe 269 can be justified by investigating the hydraulic conditions in it. Precisely, pipe 269 constitutes a sub-line pipe transferring only 0.04 L/sec with a velocity of nearly zero (0.0054 m/s) and low chlorine concentration 0.17 mg/L. Therefore, detachment of attached bacteria is insignificant as water velocity does not produce enough shear stress in the surfaces and that combined with low chlorine residual and water stagnation, lead to higher growth rates.

Below are illustrated the time series of all species (chlorine, BDOC, bulk bacteria, attached bacteria) for three nodes of different biofilm growth after 30 days simulation.

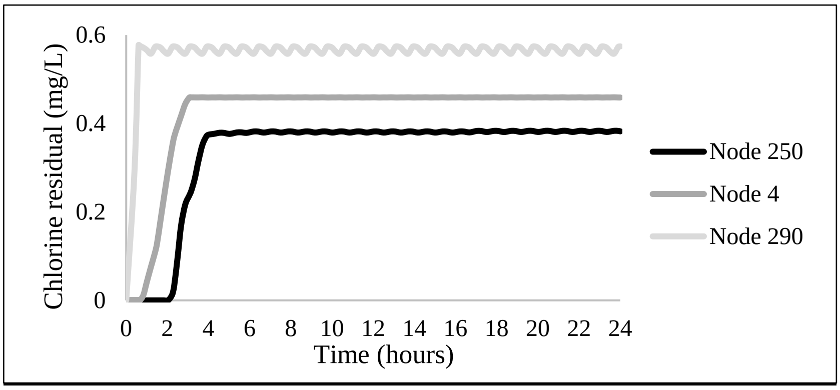

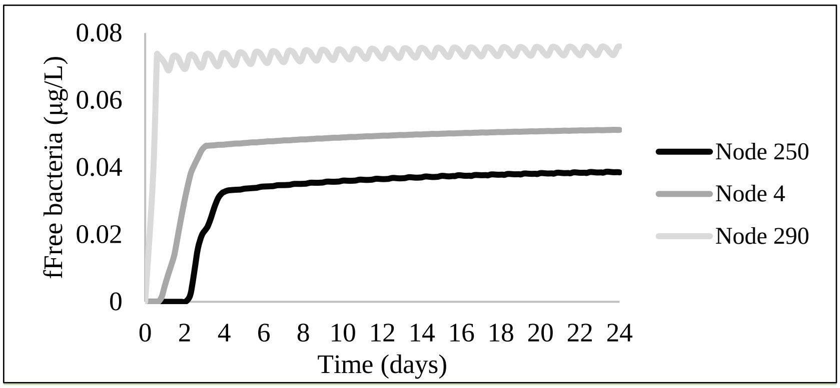

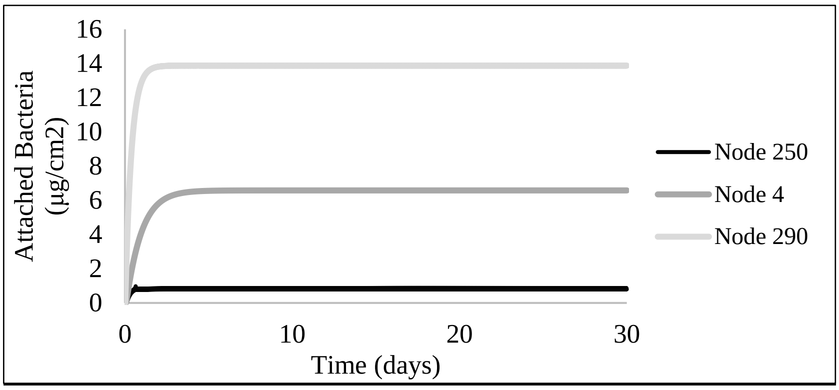

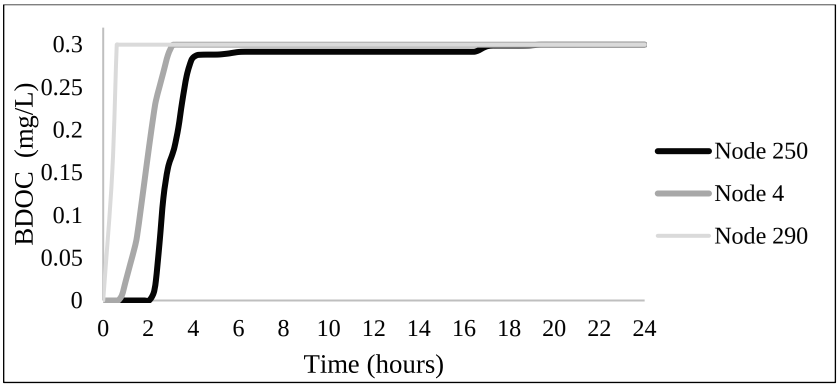

Figure 5-7: Timeseries of chlorine, free bacteria, attached bacteria (biofilm) and BDOC in three different nodes.

5.5 Investigation of network response to contamination events

In this chapter the two parts of the vulnerability assessment investigation are analyzed. The concept of part I investigation has four main tasks: (1) Simulate a biochemical assault on the pipe network and repeat the exact same attack scenario node by node at all 268 nodes in the pipe network through EPANET-MATLAB toolkit as described in paragraph 5.3, (2) in each case attack, measure the total effect of the intrusion, using different indexes for quantification of impact (total population exposed, consumer-minutes exposure, TOC per consumer, HPC bacteria per consumer, duration of water contamination), (3a) construct distribution functions of exposures for demonstrating system vulnerability according to the indexes of previous task and (3b) construct zone of influence (ZOI) and zone of exposure (ZOE) maps, which categorize network injection nodes on the basis of their potential to expose downstream consumers and, their likelihood of being exposed by injections of other nodes respectively.

In part II of the investigation, a sensitivity analysis is performed at the most influencing injection node found from the previous part, to determine the sensitivity of network response to four (4) dynamic network variables. The three variables denote different characteristics of the contamination action that are determined by the intruder (total mass injected, duration of the attack, water demand based on time of the attack). The fourth variable is determined by water operators and is the concentration of biodegradable dissolved organic carbon

(BDOC) in the end-use water exiting from the treatment plants (sources). This parameter determines the total water quality conditions (biofilm accumulation, chlorine residual) of the network, and it is investigated to gauge these conditions' effect in a contamination event. Each step of the investigation is outlined below.

5.5.1 Attack scenario

The attacks are simulated as a deliberate injection of the conservative soluble biochemical substance consisting of organic carbon and heterotrophic bacteria. Organic carbon is measured in TOC and bacteria in μg/l or colony-forming units (CFU/ml) assuming that there are 10^6 cells per microgram of carbon in the cell biomass (Shang et al., 2008b). All network simulations run a base-case event in which 7000 g of TOC and 10.3 mg of bacteria are injected into a single node with a steady rate for 30 minutes. The demand multiplier is set to 1.0 assuming average consumption throughout the simulation, thus, the simulation start time is not necessary to be defined as there are not fluctuations in the water demand. The total simulation period is 4 hours, long enough to cover the whole contamination event as determined by multiple trials. Before each simulation all nodes and pipes are set with initial conditions of the four species: chlorine, BDOC, bulk bacteria and attached bacteria. The initial conditions have been computed in a 30 days simulation, assuming chlorine, BDOC, bacteria source of 0.6 mg/L, 0.3 mg/L and 0.08 μg/L respectively as already mentioned in chapter 5.4.2. The default EPANET and EPANET-MSX parameters used for each simulation are summarized in Table 5-4. All 268 network nodes are selected one at a time as injection points.

Table 5-4: Default EPANET and EPANET-MSX Input Parameters for Base-Case Simulation

Features	Details
EPANET	
Total simulation period	4 h
Hydraulic time step	1 h
Quality time step	6 min
Demand multiplier	1.0
Base demand	14.580 Lpm
EPANET-MSX	
Differential equation solver	Euler method
Pattern time step	60 sec
Total chemical mass injected	7000 g TOC
Injection source type	Mass booster
Injection duration	30 min
	CL2: 0.6 mg/l
Source species concentration	BDOC: 0.3 mg/l
	Bacteria: 0.08 μg/l
Initial conditions	In all nodes & links

5.5.2 Vulnerability assessment

For each injection point, the total downstream contaminated nodes are detected; hence total consumers associated with the contamination event are counted. A node is labeled "contaminated" when either of the three bellow conditions occurs:

- Chlorine concentration drops below 0.2 mg/L (World Health Organization, 2003).
- Any abnormal (higher)TOC concentration than sources' (World Health Organization, 2017)
- Bacterial concentration is above 100 CFU/mL (Chowdhury, 2012).

The percentage of population exposed due to a contamination event which started in the k^{th} injection node is calculated as shown in Eq. 8

$$P_k = \sum_{n=1}^{N} f_n I_{k,n} \tag{8}$$

In Eq. (8), $N= 268$ total network nodes, f_n is the fraction of the network's population residing at Node n, ($\sum_{n=1}^{268} f_n = 1$), and $I_{k,n}$ is a dummy variable, indicating whether a node n is contaminated ($I_n =1$) or whether is clean ($I_n=0$). In this point, it should be highlighted that it is unlikely that all residents at a contaminated node will be exposed, as water can be used for different reasons apart from drinking Thus this index represents the upper bound of the fraction of the total population that would be exposed to the contaminant.

To get a more detailed perspective of the network's response to contamination, some more types of vulnerability measures are proposed. Although, percentage of total population exposed is a key measurement to evaluate the consequences of an attack event, the comparison of the percentages might not always indicate the most harmful intrusion. For example, assume that the intrusion in two different nodes contaminate the same number of customers. What if the intrusion in the first node affects them for longer time? To involve this parameter, consumer-minutes exposure (CME_k), as shown in Eq. (9) is proposed to get an absolute value of consumers exposed multiplied by the time they are exposed.

$$CME_k = \sum_{n=1}^{N} t_{cl2,n} \cup t_{BDOC,n} \cup t_{bact,n} \times \Pi_n \tag{9}$$

In Eq. (9) $t_{cl2,n}$ is the total duration of time that water reaches n node undergoing the first contamination condition. $t_{BDOC,n}$ and $t_{bact,n}$ are total time durations for the second and third contamination conditions accordingly. Π_n expresses the total number of consumers that are associated with node n. CME index offers an objective criterion, by comparing attacks of seemingly different scale and revealing the real magnitude of a contamination event.

Organic carbon and bacteria cause different effects on human health if consumed. For this reason, each contamination event is examined in terms of how many consumers are affected from the two substances separately ($\Pi_{TOC,k}$, $\Pi_{bact,k}$) as well as it is calculated the weighted average TOC exposure ($A_{TOC,k}$) measured in mg/L per consumer and bacterial exposure ($A_{bact,k}$) measured in CFU/mL per consumer from the k^{th} injection node. (Eq. 10-11).

$$A_{TOC,k} = (\sum_{n=1}^{N} C_{TOC,n,k} * \Pi_n)/\Pi_{TOC,k} \tag{10}$$

$$A_{bact,k} = (\sum_{n=1}^{N} C_{bact,n,k} * \Pi_n)/\Pi_{bact,k} \tag{11}$$

where $C_{toc,n,k}$ and $C_{bact,n,k}$ are average TOC and bacterial concentrations reaching n node during the $t_{BDOC,n}$ and $t_{bact,n}$ total time durations respectively and $\Pi_{TOC,k}$, $\Pi_{bact,k}$ are total consumers exposed to TOC and bacteria respectively. The total contaminant loads $W_{TOC,n,k}$ and $W_{bact,n,k}$ are calculated by using Eq. (12-13)

$$W_{TOC,n,k} = \sum_{t_{TOC,n}} C_{TOC,n}(t) \times Q_n(t) \times \Delta t \tag{12}$$

$$W_{bact,n,k} = \sum_{t_{BDOC,n}} C_{bact,n}(t) \times Q_n(t) \times \Delta t \tag{13}$$

where $Q_n(t)$ = corresponding nodal demand (L^3/T) and Δt (T) is the quality time step.

Lastly, the total contamination event (T_k) is measured by defining and summing all the distinct simulation time steps in which at least one node was exposed for at least a contamination condition (Eq. 14).

$$T_k = \bigcup_{1}^{N} t_{cl2,n} \cup t_{BDOC,n} \cup t_{bact,n} \tag{14}$$

The indexes P_k, CME_k, $W_{TOC,k}$, $W_{bact,k}$, $A_{TOC,k}$, $A_{bact,k}$ and T_k are calculated for each of the injection nodes (k), producing seven (7) arrays of 268 values.

5.5.3 Construction of demonstration tools

Statistical graphs

To allow the inspection of the results of the total system response, the vulnerability indexes P_k, $A_{TOC,k}$, CME_k $A_{bact,k}$ and T_k introduced in previous chapter are plotted in an empirical relative frequency distribution diagram (histogram) and its corresponding cumulative distribution function (CDF) diagram. In each data array, a Weibull distribution is fitted in order to generalize and conclude the total outcome of this experimental method. For the construction of the histogram, array values of each vulnerability index, are split into intervals (classes) of equal width and in each class, are corresponded the total number of data points whose value is beneath the width. The exposure CDF was introduced by Propato and Uber, (2004) to gauge the effectiveness of a disinfectant residual against a pathogen intrusion. In this study, the exposure CDF is generated by plotting the ranked values of the arrays of the vulnerability indexes on the *x-axis* against a point estimate of the nonexceedance probability on the *y-axis.* The nonexceedance probability is given by the empirical distribution function (Eq. 14).

$$F(x) = \frac{number\ of\ elements\ in\ the\ sample \leq x}{K+1} \tag{14}$$

where K is the total number of data points (K = 268 injection nodes in this case). The Weibull fitting distribution parameters for each fit curve are retrieved using MATLAB curve fitting toolbox.

Zone of Influence

The zone of influence (ZOI) (Khanal et al., 2006) is constructed by corresponding the set of population exposure values (P_k) onto their respective nodes. The nodes are divided into three groups depended on their ability to expose downstream nodes with the contamination conditions previously introduced:

- Red zone (high influence) = injection nodes with $P_k \geq 30\%$
- Orange zone (moderate influence) = injection nodes with $10\% < P_k < 30\%$
- Yellow zone (low influence) = injection nodes with $5\% < P_k \leq 10\%$
- Green zone (very low influence) = injection nodes with $P_k \leq 5\%$

Zone of influence colors the points of the network based on their criticality of potentially being a contaminant injection point. Future research (e.g. for optimal sensors placement) but also on municipal authorities' plans for enhanced physical security potentially could consult this map to determine the zones of the network that cause the highest damage.

Zone of Exposure

In contrast to Zone of Influence, the Zone of Exposure (ZOE) demonstrates the vulnerability of each network point by corresponding each node to the likelihood of being infected from a contamination event in any point of the network. This is succeeded by making an assumption that each node of the network has the same probability of being attacked. The ZOE map is constructed by corresponding each node to the times that has been influenced from total 268 simulation events.

5.5.4 Sensitivity analysis

A sensitivity analysis is conducted to determine the total effect variability of the simulations compared with different variables of the water distribution system. The variables in a network can be broadly categorized into two groups: static variables and dynamic variables (Khanal et al., 2006) (Table 5-5). Static variables are properties of the network that are not ordinarily affected by human behavior (e.g. skeletonization, pipe length), while dynamic variables are features of the network that are constantly changing between a range and depended by the behavior of consumers, utilities or accidental events (e.g. flow, pressure). In this study three dynamic variables are investigated (total mass injected, injection time, BDOC concentration exiting from water plant sources). The two first variables examined, are determined from the attacker whereas the third depends on the water operators. Specifically, BDOC concentration exiting the sources is responsible for biofilm growth in the surface of pipes. To examine this variable, different concentrations of BDOC are assumed, and by each of them, a different 30-day simulation was set in order to develop biofilm in pipes. The values of biofilm were set as initial conditions to the sensitivity simulations.

Table 5-5: Important variables in simulating network contamination events (Khanal et al, 2006). Bold variables are examined in the sensitivity analysis

Sources of uncertainty or variability			
Dynamic variables			Static variables
Consumer	Utility	Contamination	System features
End-user type	**Network operation**	**Duration**	Tank mixing
Water Demand	Source blending	Timing	Pipe roughness
Demand pattern	Hydrant flushing	Location	Pipe size (D and L)
Exposure	Pump schedule	**Mass**	Transport
Dose response	Tank storage	Type	Skeletonization

The impact of biofilm growth (therefore an equivalent BDOC concentration) to the total impact of a contaminant injection is investigated. It is noted that biofilm growth depends also on the bacterial and chlorine concentrations exiting the water sources, but are not examined as they would produce relevant biofilm values. Expected values of BDOC concentration are assumed to range between 0.1 to 1.15 based on the study of Volk & LeChevallier, 2000), who monitored exiting water from 31 treatment plants in different locations of US and Canada.

For this investigation, a single point of injections is determined, in order to compare the effects of each contamination event on condition that static and all other dynamic variables are constant. The selected injection point is Node 52, (red zone), located on the main transmission line downstream the main reservoir. The range of the two first variables examined is set from -40% to +40% increasing with a 10% step. The third variable BDOC concentration was examined for a wider range (-67% to 133%) as it was observed that minor fluctuations produced insignificant change of impact during an intrusion. Each simulation maintains all the characteristics and baseline values of Part I attack scenario apart from the examined variable which is set between the range. In total, eight (8) simulations are conducted for first two variables and seven (0.1 to 0.7 mg/L initial BDOC concentration) for the third one.

Table 5-6: Input variables for Sensitivity Analysis.

Variable (unit)	Range	
	Minimum	Maximum
Injection mass (g)	4200	9800
Injection duration (min)	18	42
BDOC concentration (mg/L)	0.10	0.70

In each simulation, the hydraulic behavior and the following characteristics presented, are observed and analyzed in order to determine and rank the dynamic input variables based upon their significance to the contamination output. The characteristics include the vulnerability indexes introduced for the first objective:

- Total Population exposed (P)
- Total Population exposed only from Bacteria (Π_{bact})
- Consumer-Minutes Exposure (CME)
- Average TOC concentration per Person (A_{TOC})
- Average bacterial concentration per Person (A_{bact})
- Total TOC mass reached consumers (W_{TOC})
- Total Bacterial mass reached consumers (W_{bact})

6 Results and Discussion

6.1 Vulnerability assessment

In Table 6-1 are shown vulnerability indexes *P, CME*, A_{TOC} , A_{bact} , total TOC and bacterial mass that reached consumers' taps, and total contamination duration of each contamination event occurred from the specific node for the first five injection nodes (1-5). Complete table of the results of total 268 node injections is presented in the Appendix p. 140.

Table 6-1: Results of base-case attack scenario for the nodes 1-5.

Injection Node k	**Population influenced**	P_k	CME_k	$A_{TOC,k}$ *(mg/L)*	$A_{bact,k}$ *(CFU/mL)*	**Total TOC mass** *(g)*	**Total bacterial mass** *(mg)*	**Contamination duration** T_k *(min)*
1	40125	20.5%	1.58E+06	7.98	193	7209	24	180
2	19480	10.0%	6.11E+05	16.75	274	7096	15	174
3	18783	9.6%	5.94E+05	19.22	281	7085	15	157
4	10784	5.5%	3.49E+05	66.41	359	7072	14	79
5	4509	2.3%	1.43E+05	194.86	734	7029	12	64

Results show that total population influenced (P) ranges from under 0.1% to over 55%, strongly depending on the location of the intrusion, as Zone of Influence indicates (Figure 6-1). High influencing nodes (P>30%) are all located downstream of the upper right (biggest) reservoir, connected to the main pipe line of the network. Node 52 is found to be the most critical node of the network, since a contaminant injection in this point potentially impacts up to 57.8% of the population (Figure 6-2). Moderate and low influencing nodes ($5\% < P < 10\%$ and $10\% < P < 30\%$) are located in two main zones: (1) downstream the three smaller reservoirs and (2) in the center of the network. The remaining nodes, mostly located in the exterior of town, influence less than 5% of the total population, while in 17 of them the contaminant is prevented from spreading to the network due to hydraulic gradient, thus exposing only the population of the specific neighborhood.

Figure 6-1: Zone of Influence map for Modena water distribution network

The last category of nodes (green zone) contrariwise reflects to the highest TOC and bacteria concentration exposure per person, as shown in Table 6-2, indicating that consumers influenced from these nodes potentially encounter the most serious consequences by far comparing to consumers exposed from nodes of other zones. To give an example, contamination in node 265 was found to influence the lowest fraction population (106 consumers), but in contrary each consumer was exposed to an average TOC and bacterial concentration of 3265mg/L and 5183 CFU/mL respectively, while the upper limit for bacterial concentration in potable water is 100 CFU/mL. In opposite, the other three zones have significantly lower consequences to consumers. This is attributed to the fact that, contamination events where the pollutant is diffused for longer hours and consequently at more nodes, its initial concentration will be significantly reduced and consequently consumers' impact will be considerably less.

Table 6-2: Concentrations of organic carbon and bacteria per Zone of Influence

	Number of nodes	A_{TOC} (*mg/L*)	A_{bact} (*CFU/mL*)	Contamination Duration T_k (*min*)
Green zone (P<5%)	159	347.2	1062.9	30.0
Yellow zone (5%<P<10%)	67	24.8	310.1	167.4
Orange zone (10%<P<30%)	37	12.1	239.0	182.0
Red zone (P>30%)	5	2.9	133.3	216.5

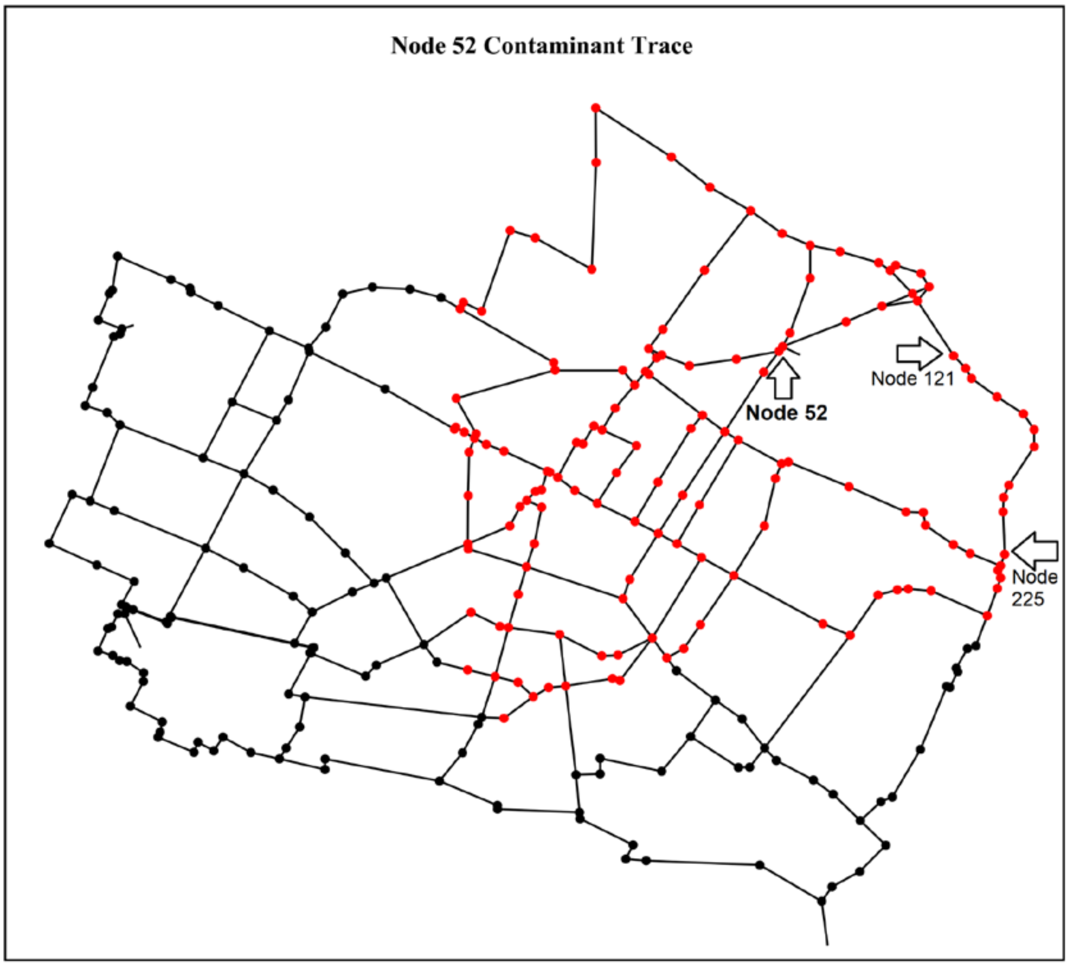

Figure 6-2: Contaminant trace of Node 52 injection

Table 6-3 presents a statistical analysis of different measurements of consumers' impact from all nodes' injections. Total TOC mass reached consumers taps in each injection has an average value of 7062 g, almost identical to the total mass of the contaminant injected (7000g). Divergence in total TOC mass (e.g. 7633 g from injection node 52) occurs due to normal TOC concentration in water exiting from the sources, which is added to the results. In contrary, although total bacterial mass injected in each case is 10.3 mg, average mass reached to consumers has increased to 14 mg, climbing up to 47.5 mg in node 52 injection. This fact denotes significant **bacterial regrowth** inside the pipes during the migration of the contaminant. Longer dispersal times lead to higher bacterial growth as evidenced in Figure 6-3. Bacterial regrowth can be attributed to the fact that high TOC concentrations, intruded during a contamination event, cause immediate reactions with chlorine, leading to its fast decay. Therefore, water deficient in chlorine is susceptible to bacterial cultivation during its transportation to remote nodes. A characteristic example is given to show bacterial regrowth during examined long-duration contamination events. It was observed that during the contamination event due to injection to node 52, node 121 (see Figure 6-2) reached a maximum bacterial concentration of 109 CFU/mL from the initial 60 CFU/mL, while chlorine concentration dropped to 0.29 mg/L from 0.49 mg/L. The same polluted flow reached Node 225, located 1.5 km in the downstream of node 121, after 80 minutes. Over the 80 minutes water travel time, chlorine concentration dropped to 0.04 mg/L and bacterial concentration raised to 190 CFU/mL from the initial 35 CFU/mL.

Table 6-3: Statistical analysis of contamination impact from all nodes' injection

	Range		Mean	Standard Deviation	Skewness
Population influenced	106	112975	11928	14159	3.8
Percentage of Population Influenced	0.1%	57.8%	6%	7%	3.8
CME	3.18E+03	4.25E+06	4.17E+05	5.33E+05	4.0
TOC/person *(g)*	0.07	66	1.78	4.34	12.4
Bacteria/person *(μg)*	0.44	97.20	3	6	12.3
Total TOC mass *(g)*	7026	7633	7062	103	0.8
Total bacterial mass *(mg)*	10.8	47.5	14	4	3.9
Pollution duration (min)	30	238	125	58	0.0

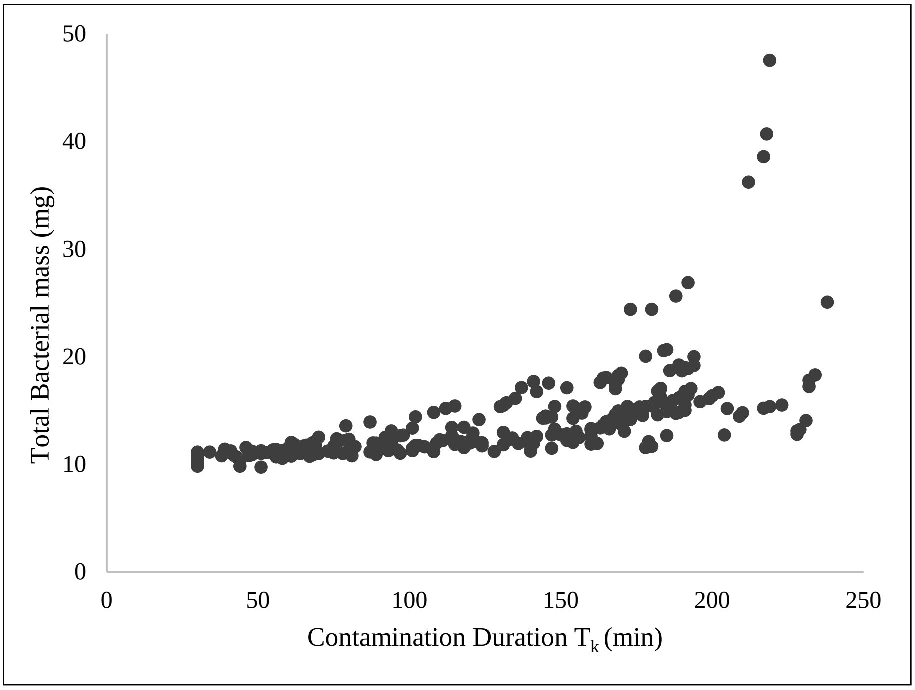

Figure 6-3: Correlation of total Bacterial mass reached consumers' taps with total contamination duration

In Figure 6-4 is presented the Zone of Exposure (ZOE) that demonstrates how frequently a node was contaminated during the total 268 injections. Results show that each node's likelihood of being contaminated is linked to the number of nodes located beneath and the reservoir from which is supplied. In total, 126 nodes were exposed less than 10 times (contamination probability ≤ 3.7%) and are mainly located in the downstream of a reservoir, because in-between there is a limited number of nodes. In contrary, nodes with a high possibility of being impacted from a contamination event, usually are supplied from two or more reservoirs. Therefore, each node located in the pipe line between the examined node and the reservoirs will potentially impact it. An example is node 266 (see Figure 6-4), which is supplied by three reservoirs. As a result, amongst total 268 injections in each node, it was contaminated from 69 of them (26.1%). Table 6-4 presents the number of nodes with their possibility of being impacted, as resulted from the base-case scenario intrusion in each of 268 nodes.

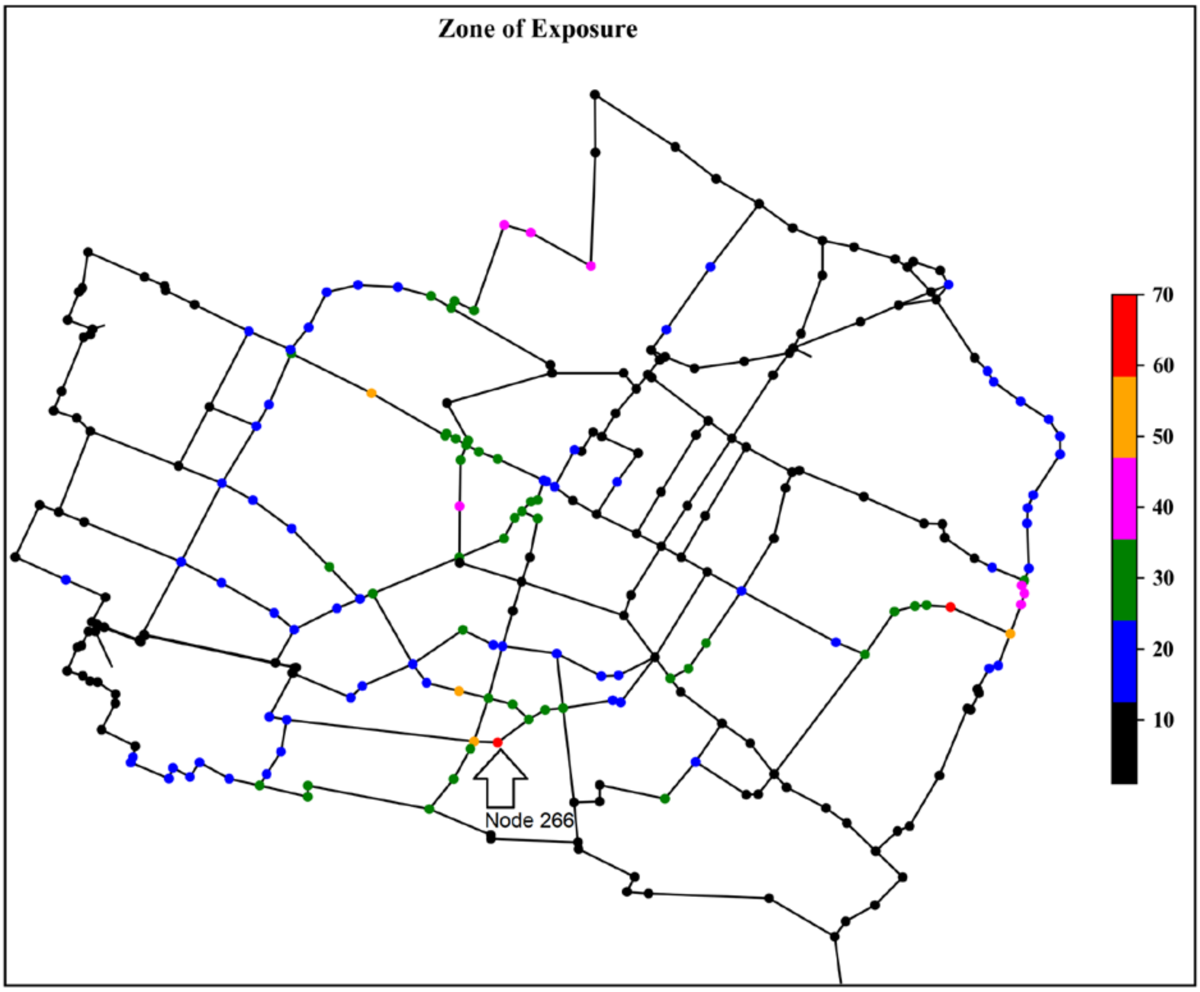

Figure 6-4: Zone of Exposure for Modena water distribution Network. Colourmap indicates the frequency in which a node was exposed to contamination from total 268 node injections

Table 6-4: Number of nodes related to possibility of being impacted as resulted from total 268 injections in all nodes of the Modena network

Possibility	**Number of nodes**
P>20%	2
10%<P<20%	37
5%<P<10%	70
P<5%	159

Figures 6-5 to 6-14 present the PDF and CDF diagrams of the vulnerability indexes introduced in paragraph 5.5.2. Both diagrams provide a simple intuitive way to interpret results of simulated contamination events. The shape of the exposure CDF offers useful insights about the network response to contaminations.

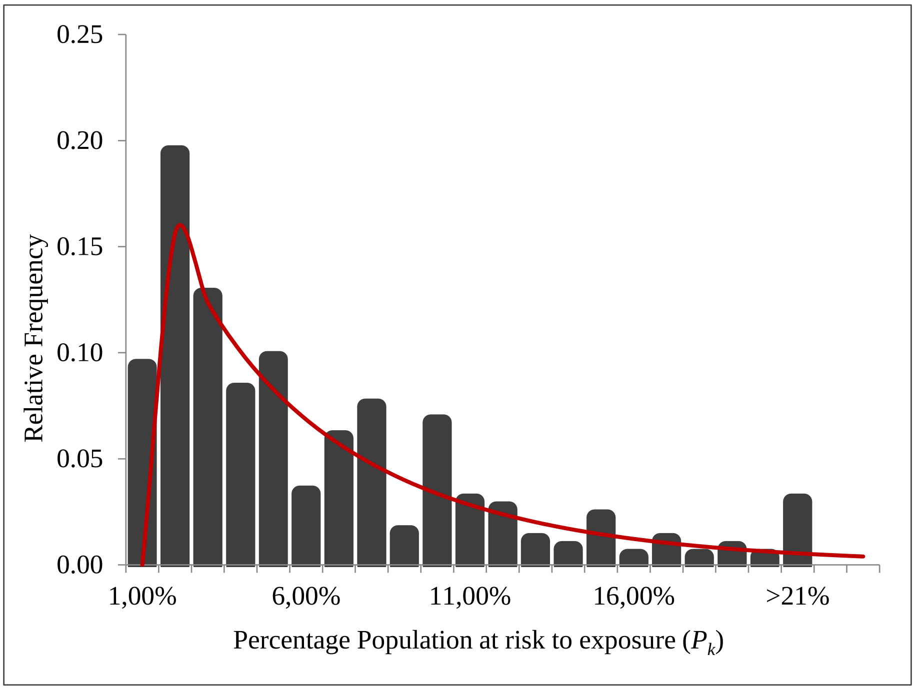

Figure 6-5: Empirical relative frequency distribution and Weibull theoretical PDF of Percentage Population at risk to exposures for base-case intrusions in Modena network.

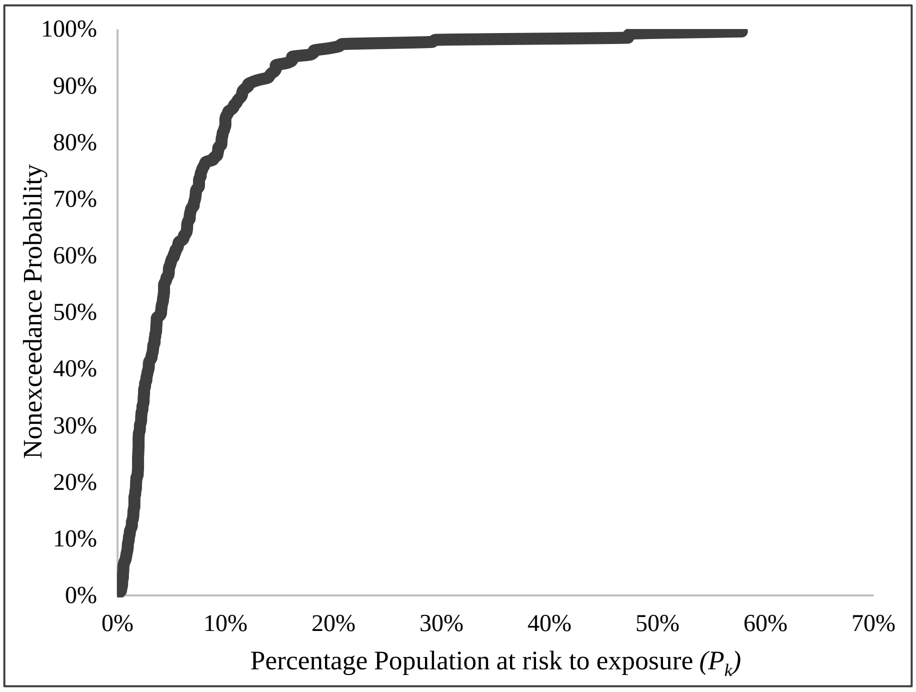

Figure 6-6: Percentage Population Exposure CDF for base-case intrusions in Modena network

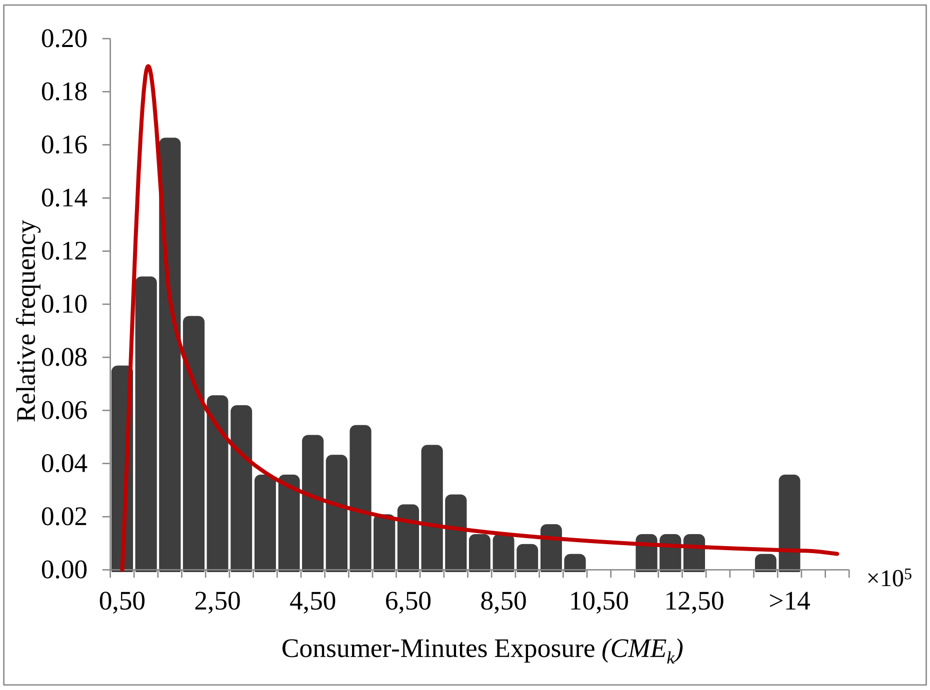

Figure 6-7: Empirical relative frequency distribution and Weibull theoretical PDF of Consumer-Minutes Exposure (CME) for base case intrusions in Modena network

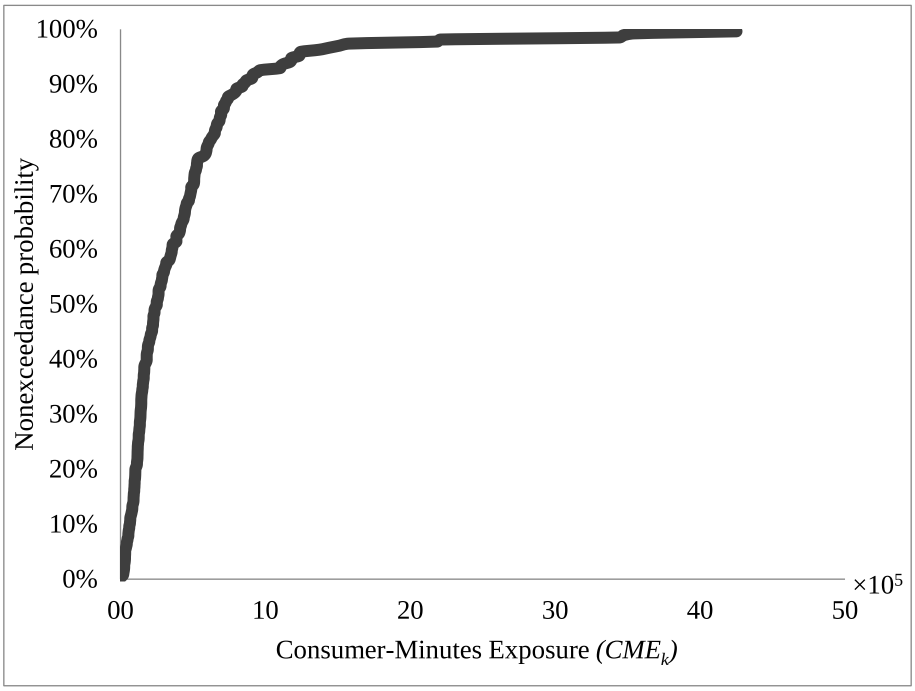

Figure 6-8: Consumer-Minutes Exposure CDF for base-case intrusions in Modena network

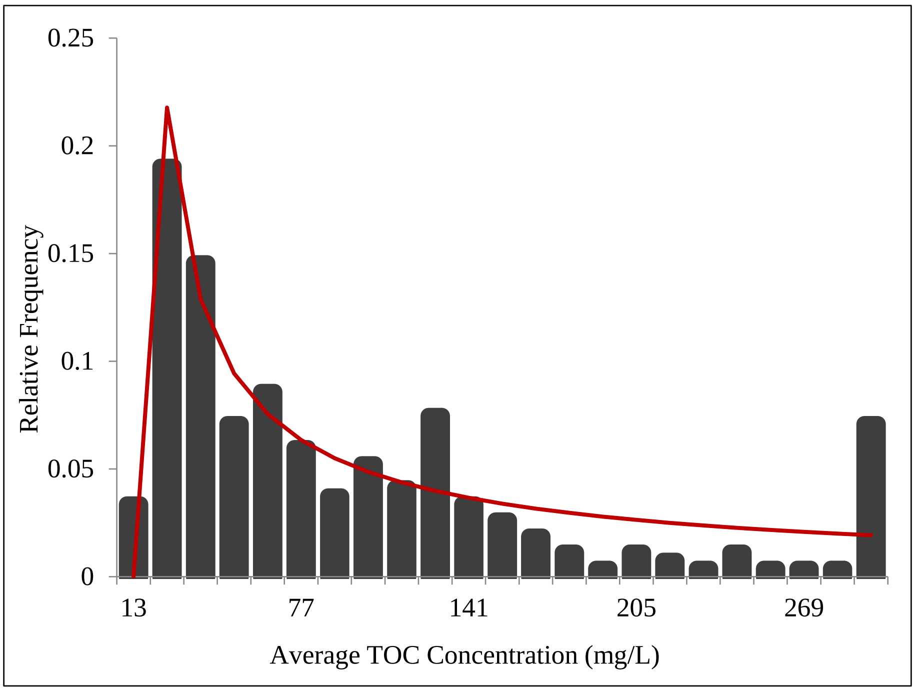

Figure 6-9: Empirical relative frequency distribution and Weibull theoretical PDF of TOC concentration per Person for base case intrusions in Modena network

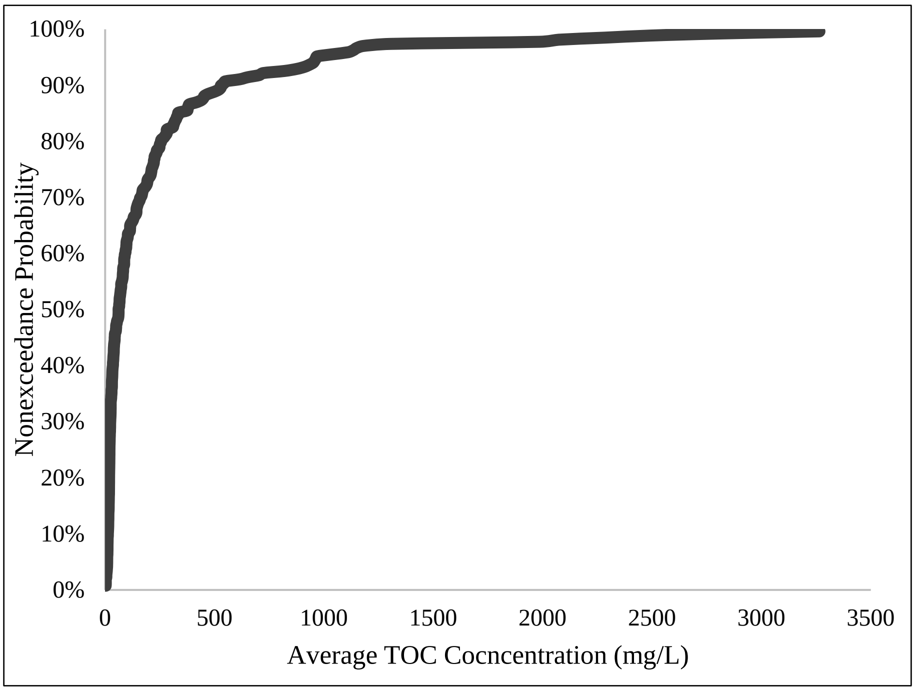

Figure 6-10: TOC concentration per Person CDF for base-case intrusions in Modena network

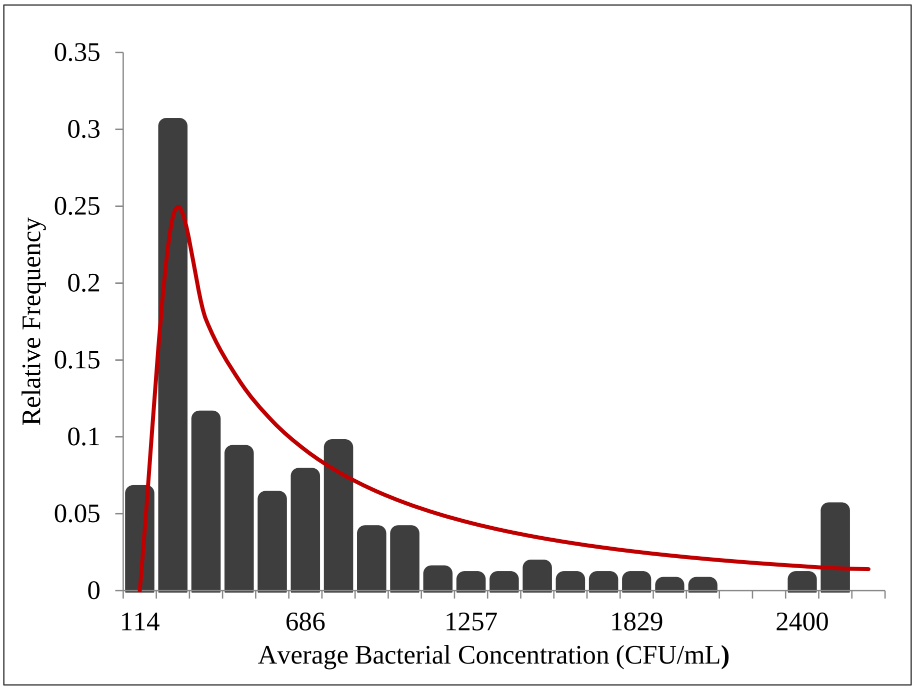

Figure 6-11: Empirical relative frequency distribution and Weibull theoretical PDF of Bacterial mass per Person for base case intrusions in Modena network

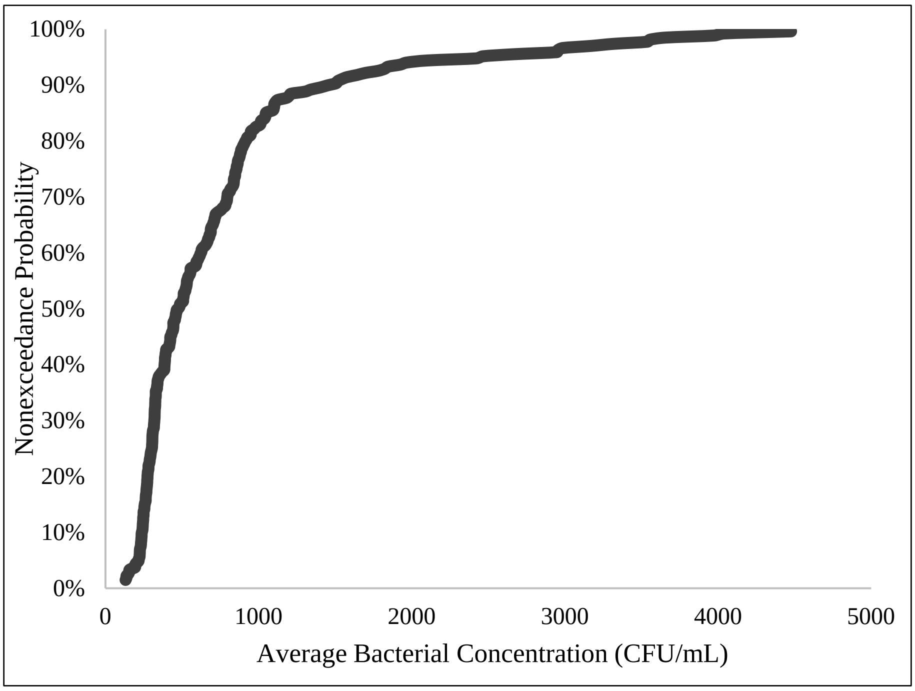

Figure 6-12: Bacterial concentration per Person CDF for base-case intrusions in Modena network

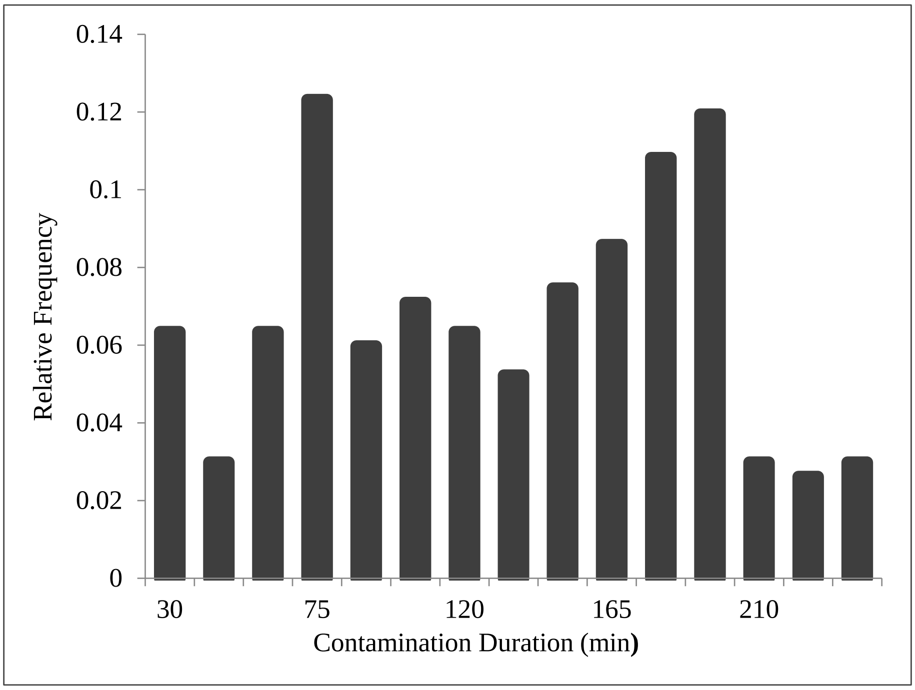

Figure 6-13: Empirical relative frequency distribution of Contamination durations for base case intrusions in Modena network

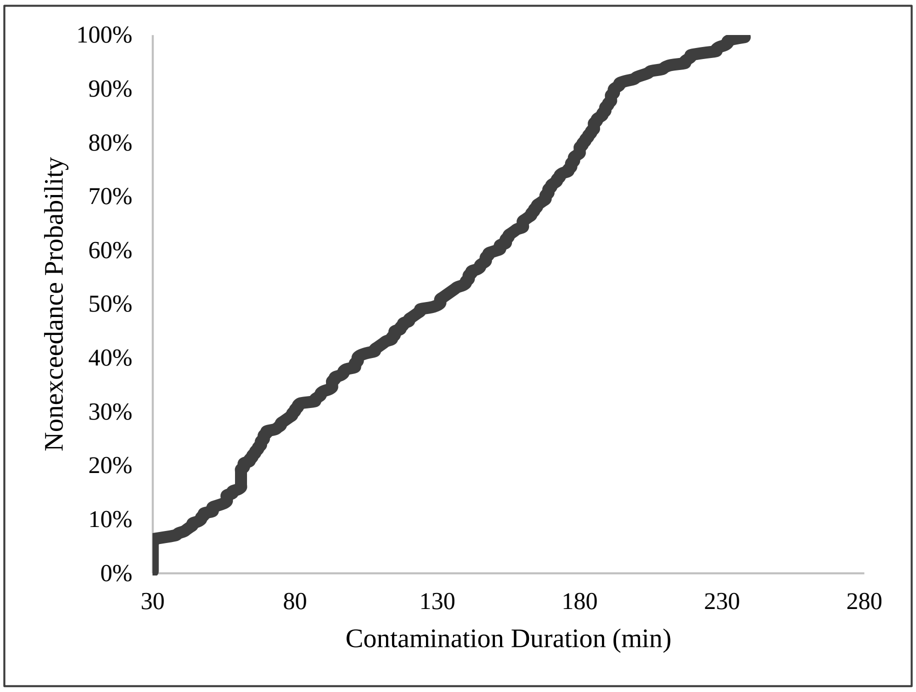

Figure 6-14: Contamination durations CDF for base-case intrusions in Modena network

6.2 Sensitivity analysis

In this part of the investigation the three dynamic variables (mass injection, injection duration, BDOC concentration in water) were examined for their overall effect to a contamination event but also for their impact on bacterial growth, which potentially puts consumers at greater risk.

6.2.1 Effect of mass injection

Results from sensitivity analysis on mass injection show that there is negligible impact on total Population exposed (*P*) (-2% and 4% for -40% and 40% mass respectively), which is responsible for the fluctuations in Consumer-Minutes exposure (*CME*) (-15% and 9% for -40% and 40% mass injection), indicating that the duration of potential exposure per consumer remained in general, invariable. As expected, total TOC mass reaching consumers' taps (W_{TOC}), is proportional to mass injection, while it greatly impacts on total bacterial mass (W_{bact}) (-45% and 54% for -40% and 40% mass injection).

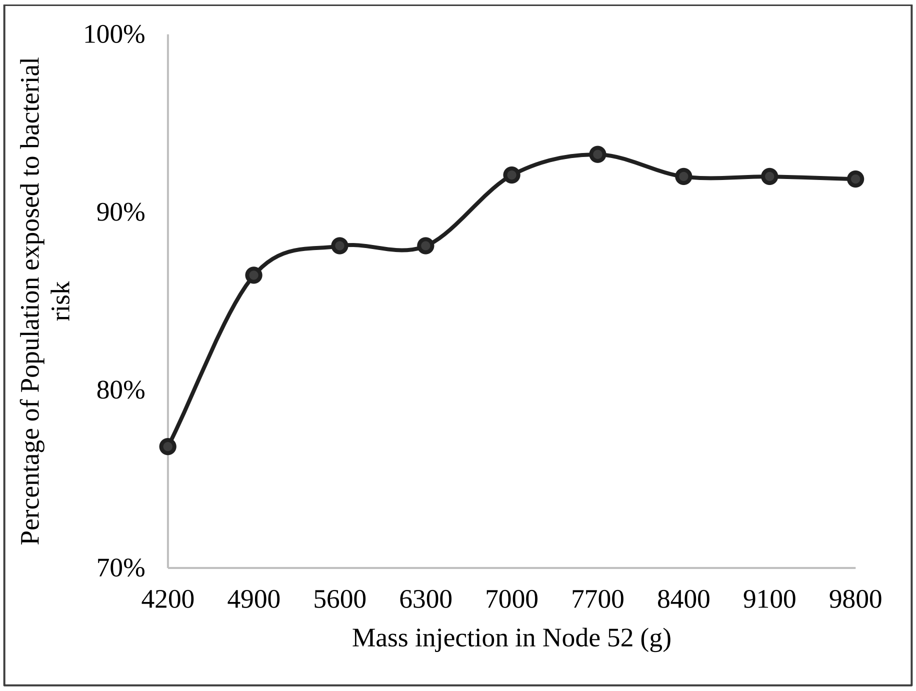

Figure 6-15: Percentage of Population at bacterial risk to total Population exposed, relative to injected mass in Node 52

These measures denote that in either case, the contaminant reaches almost a certain number of downstream nodes regardless of the mass injection. In contrary, the values of TOC concentration reaching distant nodes have a critical effect at the rate of bacterial cultivation. Larger TOC concentration (A_{TOC}) leads to faster chlorine decay and consequently faster bacterial growth rates. Thus, higher bacterial concentration (A_{bact}) is formed and more consumers are at risk to bacterial contamination. The opposite situation occurs when TOC concentration decreases. For example, in the "-40% TOC mass"case, total bacterial mass was 22.51 mg, 6.13 mg of which were injected and 16.38 mg were produced in the pipe network, whereas in the "+40% TOC mass" case the values were 63.31 mg, 14.31 mg and 49 mg respectively. To quantify the bacterial rate created in the network, in the first case bacteria growth reached 266% of injected bacteria, while in the second case it reached 376%. However, it is noted that above 7000 g mass injection, the percentage of population exposed to bacteria did not increase, but reached a peak of 92% of total population impacted (Figure 6-15).This signifies that the remainder 8% is exposed to lower TOC concentrations, which is unable to produce bacterial growth. Figure 6-16 presents the results from sensitivity analysis in each category measured for -40% -20% +20% and +40% values of injected mass. Complete table is included in the Appendix p. 149.

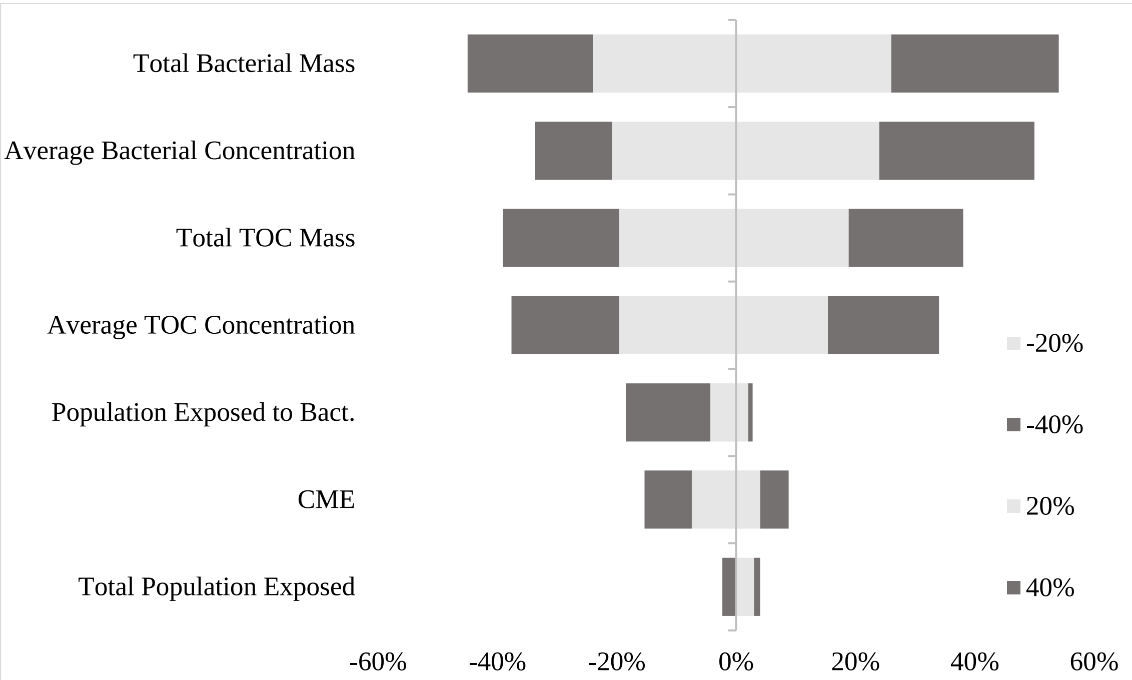

Figure 6-16: Percentage Tornado sensitivity chart for mass injection variable

6.2.2 Effect of injection duration

The fluctuations in this variable proportionally influenced the Consumer-Minutes exposure (-38% and 39% for -40% and 40% injection duration) as each node affected, was exposed for longer or shorter times proportional to the intrusion, plus that population exposed remained almost invariable although the varying of the duration. Average TOC concentration (A_{TOC}) is inversely proportional to injection duration as the total TOC mass injected is divided per minute of injection to give the rate of discharge assuming for each attack scenario. However, it was observed that the longer an injection lasted, total bacterial mass increased (W_{bact}) (-24% and 21% for – 40% and 40% injection duration respectively) explained by longer durations of bacterial growth in the pipe network. In contrary, average bacterial concentration (A_{bact}) dropped when injection duration increased and vice versa, because during shorter time injections, the contaminant entered the network with higher concentrations, thus creating a higher peak of bacterial concentration. Therefore, in longer injection durations consumers are exposed to more bacteria mass but with a lower rate and in short injection durations, consumers are exposed to high concentrations for less time. Lastly, they were not observed significant variations in the total population exposed (P), meaning that the contaminant reaches a specific number of nodes independently of the injection duration, while also Total TOC mass (A_{TOC}) reached consumers was almost invariable as expected. Complete table of the results is included in the Appendix p. 149.

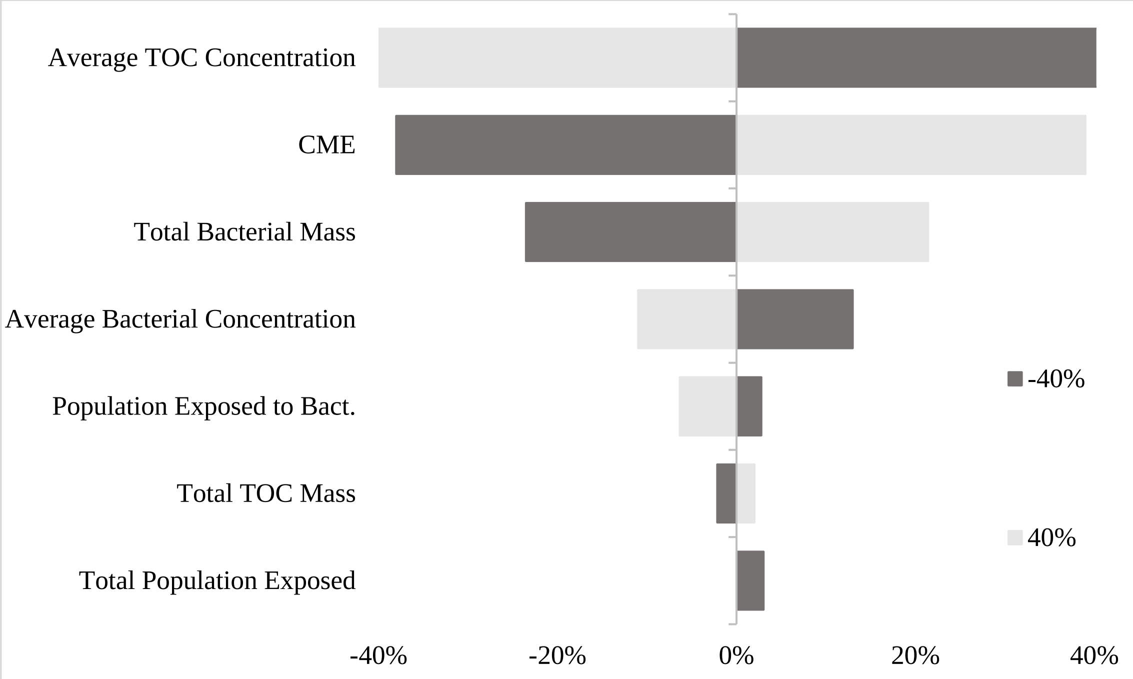

Figure 6-17: Percentage Tornado sensitivity chart for duration injection variable

6.2.3 Effect of BDOC concentration in water

The effect of BDOC concentration in water was found to be significant in the formation of biofilm (-14% and 24% for –67% and 133% BDOC concentration accordingly) as shown in Figure 6-18. However, the formation of biofilm was observed to be of negligible importance in the contamination event as every vulnerability index examined, was marginally fluctuated. Nevertheless, the slight increase or decrease in total bacterial mass (A_{TOC}) (-3% and +6% for -67% and 133% BDOC concentration) indicates that biofilm contributes to the bacterial regrowth, as water flow velocity detaches the attached cells into the bulk flow. Consequently, it is concluded that the cleanliness of water distribution systems is of minor importance in case of a deliberate organic load intrusion. Complete table of the results is included in the Appendix p. 149.

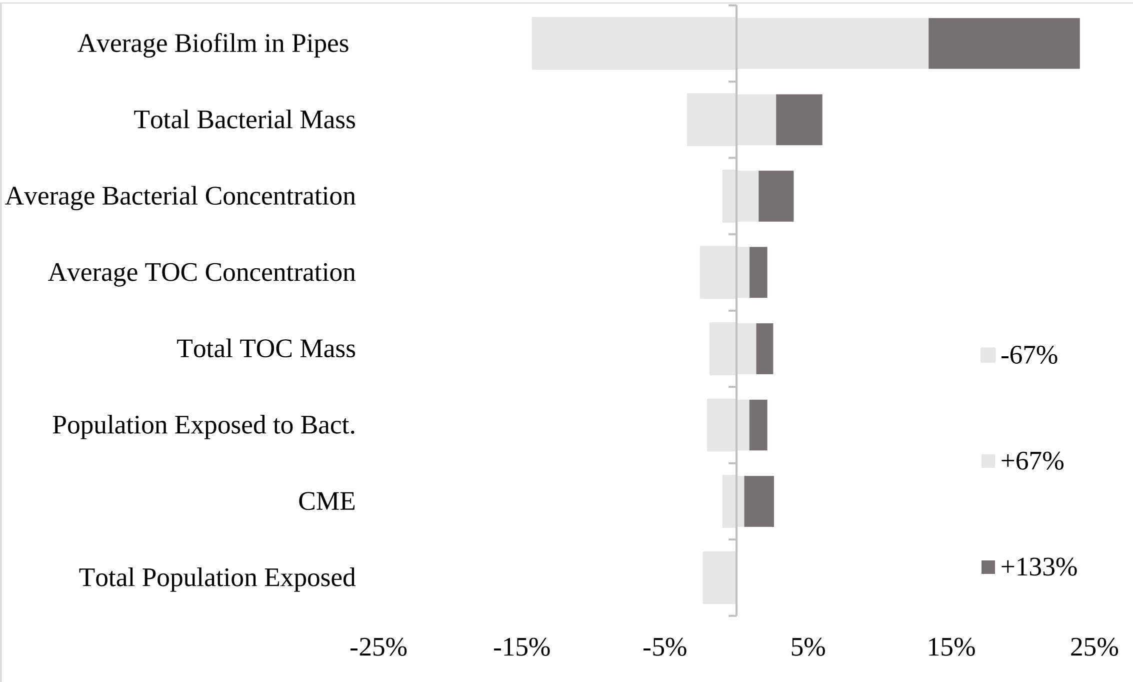

Figure 6-18: Percentage Tornado sensitivity chart for BDOC concentration in water variable

7 Summary and conclusions

This study focuses on simulating deliberate contaminant injections to water distribution systems under realistic water-quality conditions and assess their vulnerability. The key step achieved here involves the linkage of EPANET-MSX, an extension software of EPANET hydraulic solver, which allows biochemical reactions of different chemical and biological species under non-steady hydraulic conditions during the simulation. Previous studies (Khanal et al., 2006; Kenneth A. Nilsson et al., 2005) simulated contamination events in WDSs, assuming an undefined conservative biochemical polluting substance spreading the network pipes, mainly focusing on the hydraulic compounds that influence the diffusion of the contaminant. In contrary, this study was mainly centralized in modeling the quality phase of water and the reactions of the contaminant with the water quality compounds. Here, the contaminant was assumed a non-conservative organic substrate comprised of organic carbon and heterotrophic bacteria which was measured in total organic carbon (TOC).

To develop the water-quality model for simulating the contaminant intrusions, two mathematical models were adopted and conjoined together using specific modifications through EPANET-MSX. First, a bacterial regrowth model was utilized, containing bulk and surface bacteria (biofilm) kinetic equations, organic substrate kinetic equations and describing the interactions between the species and second, a chlorine decay model was used, capable of reacting with excessive organic substrate and adjusting its decay rate depended on the water quality conditions. Chlorine decay played a significant role in the bacterial growth rate as they function as an inhibition factor. Consequently, fast decaying of chlorine due to TOC, potentially could create a bacterial outbreak and thus aggravating the consequences of a contamination event from the organic substrate.

Before the simulation intrusions, initial conditions for each biochemical specie was included in the model in every point of the network. These conditions were extracted from 30-day simulations of normal system functioning in order to develop biofilm in each pipe, and a balance of all interacted species in each node and pipe. Also, a program was developed in order to estimate the required chlorine dose concentration in network's sources in order to prevent bacterial cultivation under normal conditions (that is, without counting the consequences of a contaminant injection).

The investigation of vulnerability assessment in water distribution systems was separated in two parts. In part I of the investigation, a deterministic base-case contamination event was applied individually to 268 source nodes in the study site water supply network of Modena, Italy. Several vulnerability indexes were constructed, each of them measuring a different aspect in the total impact of the contamination. These indexes included measurements of exposure to TOC, exposure to bacteria, contamination duration and population exposure Therefore, each node was assessed on the total damage produced to the system in total, and individually based on the indexes. For the visualization of the results and the better comprehending of the network response to polluting intrusions a ZOI map was constructed, categorizing each node based on their downstream impact, and also a ZOE map was constructed, categorizing each node based on their likelihood of being exposed during a contamination event starting from a random point of the network. In addition, simple statistical graphs were used to demonstrate the likelihood of different potential magnitudes from a contamination event. In the second part, dynamic variables of a contamination event starting in node 52 (red zone) were examined using a sensitivity analysis to investigate the output in system response when these values are varied.

The final conclusions considered from the vulnerability assessment in Modena WDS are presented below:

- The range of potential population exposed from a single contamination event is from 106 consumers (0.01%) to 112975 (57.8%) and is highly depended based on the location of the injection as shown in ZOI map.
- Out of 268 total injection nodes, the most influencing were located on the downstream of every reservoir source (red and orange zones) while green zone nodes are in decisive majority holding over the 59% (160/268) of the total map.
- In contrary, population affected due to injections in green zone nodes are exposed to significantly more polluting substance per person. In total an intrusion on 17 nodes

was found to affect only population residing on the injected node. Those cases leaded to highest TOC and bacterial concentrations per person.

- In base-case intrusion scenario, the polluting substance consisted of 7000 g TOC and 10mg bacterial mass. It was discovered that during the contamination event a sufficient bacterial regrowth occurred in 70% of total injections as it was measured that total bacterial mass reaching downstream nodes exceeded the initial injected dose.
- In case of an organic substrate injection, total consumers affected, have approximately 90% possibility of be exposed to water contaminated from both organic substance and bacterial mass, depended on the location the injected mass dose, the injection duration and the water demand. The remaining 10% is the possibility of infection only from the organic compound.
- ZOE map gives an overview of the most susceptible nodes in the water distribution systems. In total, 25 nodes (approximately 10% of the network) of the network, have over 10% likelihood to be influenced by an intrusion starting from any node in the network. Averagely each node has 5% chance of being exposed to a contamination.
- From the sensitivity analysis of the three variables related to the network intrusion, it was observed that total population exposed was only slightly variable or completely invariable, indicating that the contaminant reaches almost a certain number of nodes (therefore certain population, as assumed) regardless of the examined increase or decrease of the intrusion characteristics. In contrary, bacterial regrowth was significantly influenced from mass injection and injection duration.
- Cleanness of the network (depended on concentration of biofilm formation in the pipes and in turn BDOC concentration in water) proved unimportant to the total impact of deliberate organic load injections as indicated in the 3rd part of the sensitivity analysis.

Future research potential

The fundamental basis of this work on simulating attacks on water networks is the water quality model, which is a combination of a microbial growth model and a chlorine decay model. The equations of the bacterial growth model are semi-empirical and their components were formulated based on experimental procedures of prior years, which have significant discrepancies with respect to the conditions of our simulation. Therefore, for further research on the subject of organic load attacks, a new experimental procedure is proposed to extract a water model based on realistic contaminant conditions. On this occasion, more precise parameters will be given for example, the development of the microbial load given a strong dose of organic charge, the attenuation of chlorine taking into account and its reaction with the bacteria, and the contribution of biofilm to the growth of bacteria when chlorine has been completely decayed. Finally, the model shall be enriched with the incorporation of other chemical elements which can determine water quality during such an intrusion and in this model are neglected.

Moreover, in order to investigate the system vulnerability and make generalizations for its response to organic attacks, a Monte Carlo simulation is proposed, which in this work was not possible to be implemented in a reasonable time frame due to the lack of computational power. In contrast to the deterministic runs, the Monte Carlo simulations can be used to produce stochastic demands in each node that affect the behavior of the network, and generate random sampling of the systems' dynamic variables in order to extract a holistic output on network response.

Last but not least, future research on methodologies for optimal sensor placement and contaminant source location identification through sensor data, in order to minimize the impact from a deliberate organic load injection is suggested.

BIBLIOGRAPHY

Agency, U.S.E.P., 2000. Epanet 2 users manual.

Association of Metropolitan Water Agencies, 2007. Protecting the Water Sector from Security Threats, The Emerging Legal and Policy Frameworks. J. Microgr. 25, 4–6.

Batté, M., Appenzeller, B.M.R., Grandjean, D., Fass, S., Gauthier, V., Jorand, F., Mathieu, L., Boualam, M., Saby, S., Block, J.C., 2003. Biofilms in drinking water distribution systems. Rev. Environ. Sci. Biotechnol. 2, 147–168. https://doi.org/10.1023/B:RESB.0000040456.71537.29

Berry, J.W., Fleischer, L., Hart, W.E., Phillips, C.A., Watson, J.P., 2005. Sensor placement in municipal water networks. J. Water Resour. Plan. Manag. 131, 237–243. https://doi.org/10.1061/(ASCE)0733-9496(2005)131:3(237)

Bois, F.Y., Fahmy, T., Block, J.C., Gatel, D., 1997. Dynamic modeling of bacteria in a pilot drinking-water distribution system. Water Res. 31, 3146–3156. https://doi.org/10.1016/S0043-1354(97)00178-4

Bragalli, C., D'Ambrosio, C., Lee, J., Lodi, A., Toth, P., 2008. Water Network Design by MINLP. IBM Res. RC24495.

Brown, D., Bridgeman, J., West, J.R., 2011. Predicting chlorine decay and THM formation in water supply systems. Rev. Environ. Sci. Biotechnol. 10, 79–99. https://doi.org/10.1007/s11157-011-9229-8

Burger, G., Sitzenfrei, R., Kleidorfer, M., Rauch, W., 2016. Quest for a New Solver for EPANET 2 142, 1–11. https://doi.org/10.1061/(ASCE)WR.1943-5452.0000596

Burkhardt, J.B., Szabo, J., Klosterman, S., Hall, J., Murray, R., 2017. Modeling fate and transport of arsenic in a chlorinated distribution system. Environ. Model. Softw. 93, 322–331. https://doi.org/10.1016/j.envsoft.2017.03.016

Centre for European Reform [CER], 2005. The EU and National Identifications. Soc. Forces 84, 653–680.

Chowdhury, S., 2012. Heterotrophic bacteria in drinking water distribution system: A review, Environmental Monitoring and Assessment. https://doi.org/10.1007/s10661-011-2407-x

Clark, R.M., Buchberger, S.G., 2004. Responding To a Contamination Threat in a Drinking Water Network : the Potential for Modeling and Monitoring 1–26.

Cyprowski, M., Stobnicka-Kupiec, A., Ławniczek-Wałczyk, A., Bakal-Kijek, A., Gołofit-Szymczak, M., Górny, R.L., 2018. Anaerobic bacteria in wastewater treatment plant. Int. Arch. Occup. Environ. Health 91, 571–579. https://doi.org/10.1007/s00420-018-1307-6

Danneels, J.J., Finley, R.E., 2009. Assessing the Vulnerabilities of U.S. Drinking Water Systems. J. Contemp. Water Res. Educ. 129, 8–12. https://doi.org/10.1111/j.1936-704x.2004.mp129001003.x

Di Cristo, C., Leopardi, A., 2008. Pollution source identification of accidental contamination in water distribution network. J. Water Resour. Plan. Manag. 134, 197–202. https://doi.org/10.1061/(ASCE)0733-9496(2008)134:2(197)

Douterelo, I., Boxall, J.B., Deines, P., Sekar, R., Fish, K.E., Biggs, C.A., 2014a. Methodological approaches for studying the microbial ecology of drinking water distribution systems. Water Res. 65, 134–156. https://doi.org/10.1016/j.watres.2014.07.008

Douterelo, I., Boxall, J.B., Deines, P., Sekar, R., Fish, K.E., Biggs, C.A., 2014b. ScienceDirect Methodological approaches for studying the microbial ecology of drinking water distribution systems. Water Res. 65, 134–156. https://doi.org/10.1016/j.watres.2014.07.008

Eliades, D.G., Kyriakou, M., Vrachimis, S.G., Polycarpou, M.M., 2016. EPANET-MATLAB Toolkit : An Open-Source Software for Interfacing EPANET with MATLAB. Comput. Control Water Ind. CCWI 2016 1–8.

Eliades, D.G., Lambrou, T.P., Panayiotou, C.G., Polycarpou, M.M., 2014. Contamination event detection in water distribution systems using a model-based approach. Procedia Eng. 89, 1089–1096. https://doi.org/10.1016/j.proeng.2014.11.229

European Parliament, 2019. Drinking water in the EU: better quality and access [WWW

Document]. URL https://www.europarl.europa.eu/news/en/headlines/society/20181011STO15887/drinking-water-in-the-eu-better-quality-and-access

Flemming, H.C., 1998. Relevance of biofilms for the biodeterioration of surfaces of polymeric materials. Polym. Degrad. Stab. 59, 309–315. https://doi.org/10.1016/s0141-3910(97)00189-4

Gleick, P.H., 2006. Water and terrorism. Water Policy 8, 481–503. https://doi.org/10.2166/wp.2006.035

Grayman, W.M., 2013. Contamination of Water Distribution Systems. https://doi.org/10.1142/9789814531788_0031

Guan, J., Aral, M.M., Maslia, M.L., Grayman, W.M., 2006. Identification of contaminant sources in water distribution systems using simulation-optimization method: Case study. J. Water Resour. Plan. Manag. 132, 252–262. https://doi.org/10.1061/(ASCE)0733-9496(2006)132:4(252)

Haas, C.N., Karra, S.B., 1984. Kinetics demand of wastewater exertion. J. (Water Pollut. Control Fed. 56, 170–173.

Hakim, S., Blackstone, E.A., 2014. Protecting Critical Infrastructure Series Editors.

Hart, W.E., Murray, R., 2010. Review of sensor placement strategies for contamination warning systems in drinking water distribution systems. J. Water Resour. Plan. Manag. 136, 611–619. https://doi.org/10.1061/(ASCE)WR.1943-5452.0000081

Health Canada, 2013. Guidance on the Use of Heterotrophic Plate Counts in Canadian Drinking Water Supplies [WWW Document]. URL https://www.canada.ca/en/health-canada/services/publications/healthy-living/guidance-use-heterotrophic-plate-counts-canadian-drinking-water-supplies.html (accessed 1.16.20).

Helbling, D.E., Ph, D., Asce, A.M., Vanbriesen, J.M., Ph, D., Asce, A.M., 2009. Modeling Residual Chlorine Response to a Microbial Contamination Event in Drinking Water Distribution Systems 135, 918–927. https://doi.org/10.1061/(ASCE)EE.1943-7870.0000080

Helbling, D.E., Vanbriesen, J.M., 2009. Modeling residual chlorine response to a microbial contamination event in drinking water distribution systems. J. Environ. Eng. 135, 918–927. https://doi.org/10.1061/(ASCE)EE.1943-7870.0000080

Hou, D., Song, X., Zhang, G., Zhang, H., Loaiciga, H., 2013. An early warning and control system for urban, drinking water quality protection: China’s experience. Environ. Sci. Pollut. Res. 20, 4496–4508. https://doi.org/10.1007/s11356-012-1406-y

Instituto Superiore de Sanita, 2005. Security of water systems.

Janke, R., Davis, M., Taxon, T., 2012. Simulating intentional contamination events in water distribution systems: A report on the sensitivity of estimated impacts to major simulation parameters. Water Distrib. Syst. Anal. 2010 - Proc. 12th Int. Conf. WDSA 2010 568–584. https://doi.org/10.1061/41203(425)54

Jeong, H.S., Qiao, J., Abraham, D.M., Lawley, M., Richard, J.P., Yih, Y., 2006. Minimizing the consequences of intentional attack on water infrastructure. Comput. Civ. Infrastruct. Eng. 21, 79–92. https://doi.org/10.1111/j.1467-8667.2005.00419.x

Khanal, N., Buchberger, S.G., McKenna, S.A., 2006. Distribution system contamination events: Exposure, influence, and sensitivity. J. Water Resour. Plan. Manag. 132, 283–292. https://doi.org/10.1061/(ASCE)0733-9496(2006)132:4(283)

King, C.H., Shotts, E.B., Wooley, R.E., Porter, K.G., 1988. Survival of Coliforms and Bacterial Pathogens within Protozoa during Chlorinationt 54, 3023–3033.

Krause, A., Leskovec, J., Guestrin, C., VanBriesen, J., Faloutsos, C., 2008. Efficient sensor placement optimization for securing large water distribution networks. J. Water Resour. Plan. Manag. 134, 516–526. https://doi.org/10.1061/(ASCE)0733-9496(2008)134:6(516)

Laird, C.D., Biegler, L.T., van Bloemen Waanders, B.G., Bartlett, R.A., 2005. Contamination source determination for water networks. J. Water Resour. Plan. Manag. 131, 125–134. https://doi.org/10.1061/(ASCE)0733-9496(2005)131:2(125)

Laurent, P., Servais, P., Prévost, M., Gatel, D., Clément, B., 1997. the SANCHO model on distribution systems 8, 92–103. https://doi.org/10.1002/j.1551-8833.1997.tb08262.x

LeChevallier, M.W., Cawthon, C.D., Lee, R.G., 1988. Factors promoting survival of bacteria in chlorinated water supplies. Appl. Environ.

Microbiol. 54, 649–654.

LeChevallier, M.W., Hassenauer, T.S., Camper, A.K., McFeters, G.A., 1984. Disinfection of bacteria attached to granular activated carbon. Appl. Environ. Microbiol. 48, 918–923. https://doi.org/10.1128/aem.48.5.918-923.1984

Lindley, T.R., Buchberger, S.G., 2002. Assessing intrusion susceptibility in distribution systems. J. / Am. Water Work. Assoc. 94, 66–69. https://doi.org/10.1002/j.1551-8833.2002.tb09490.x

Maiolo, M., Pantusa, D., 2018. Infrastructure Vulnerability Index of drinking water systems to terrorist attacks. Cogent Eng. 5, 1–21. https://doi.org/10.1080/23311916.2018.1456710

Nilsson, Kenneth A, Buchberger, S.G., Clark, R.M., 2005. Simulating Exposures to Deliberate Intrusions into Water Distribution Systems 131, 228–236.

Nilsson, Kenneth A., Buchberger, S.G., Clark, R.M., 2005. Simulating exposures to deliberate intrusions into water distribution systems. J. Water Resour. Plan. Manag. 131, 228–236. https://doi.org/10.1061/(ASCE)0733-9496(2005)131:3(228)

Niquette, P., Servais, P., Savoir, R., 2000. Impacts of pipe materials on densities of fixed bacterial biomass in a drinking water distribution system. Water Res. 34, 1952–1956. https://doi.org/10.1016/S0043-1354(99)00307-3

Ostfeld, A., Uber, J.G., Salomons, E., Berry, J.W., Hart, W.E., Phillips, C.A., Watson, J.-P., Dorini, G., Jonkergouw, P., Kapelan, Z., di Pierro, F., Khu, S.-T., Savic, D., Eliades, D., Polycarpou, M., Ghimire, S.R., Barkdoll, B.D., Gueli, R., Huang, J.J., McBean, E.A., James, W., Krause, A., Leskovec, J., Isovitsch, S., Xu, J., Guestrin, C., VanBriesen, J., Small, M., Fischbeck, P., Preis, A., Propato, M., Piller, O., Trachtman, G.B., Wu, Z.Y., Walski, T., 2008. The Battle of the Water Sensor Networks (BWSN): A Design Challenge for Engineers and Algorithms. J. Water Resour. Plan. Manag. 134, 556–568. https://doi.org/10.1061/(ASCE)0733-9496(2008)134:6(556)

Pedersen, K., 1990. Biofilm development on stainless steel and pvc surfaces in drinking water. Water Res. 24, 239–243. https://doi.org/10.1016/0043-1354(90)90109-J

Percival, S.L., Knapp, J.S., Edyvean, R.G.J., Wales, D.S., 1998. Biofilms, mains water and stainless steel. Water Res. 32, 2187–2201. https://doi.org/10.1016/S0043-1354(97)00415-6

Powell, J.C., Hallam, N.B., West, J.R., Forster, C.F., Simms, J., 2000. Factors which control bulk chlorine decay rates. Water Res. 34, 117–126. https://doi.org/10.1016/S0043-1354(99)00097-4

Prévost, M., Rompré, A., Coallier, J., Servais, P., Laurent, P., Clément, B., Lafrance, P., 1998. Suspended bacterial biomass and activity in full-scale drinking water distribution systems: Impact of water treatment. Water Res. 32, 1393–1406. https://doi.org/10.1016/S0043-1354(97)00388-6

Propato, M., Uber, J.G., 2004. Vulnerability of water distribution systems to pathogen intrusion: How effective is a disinfectant residual? Environ. Sci. Technol. 38, 3713–3722. https://doi.org/10.1021/es035271z

Qiu, M., Salomons, E., Ostfeld, A., 2020. A framework for real-time disinfection plan assembling for a contamination event in water distribution systems. Water Res. 115625. https://doi.org/10.1016/j.watres.2020.115625

Reasoner, D.J., 1990. Monitoring Heterotrophic Bacteria in Potable Water 452–477. https://doi.org/10.1007/978-1-4612-4464-6_22

Ridgway, H.F., Olson, B.H., 1982. Chlorine resistance patterns of bacteria from two drinking water distribution systems. Appl. Environ. Microbiol. 44, 972–987. https://doi.org/10.1128/aem.44.4.972-987.1982

Sankary, N., Ostfeld, A., 2019. Bayesian Localization of Water Distribution System Contamination Intrusion Events Using Inline Mobile Sensor Data. J. Water Resour. Plan. Manag. 145, 1–10. https://doi.org/10.1061/(ASCE)WR.1943-5452.0001086

Schwartz, R., Lahav, O., Ostfeld, A., 2014. Integrated hydraulic and organophosphate pesticide injection simulations for enhancing event detection in water distribution systems. Water Res. 63, 271–284. https://doi.org/10.1016/j.watres.2014.06.030

Schwartz, T., Hoffmann, S., Obst, U., 1998. Formation and bacterial composition of young, natural biofilms obtained from public bank-filtered drinking water systems. Water Res. 32, 2787–2797. https://doi.org/10.1016/S0043-

1354(98)00026-8

Servais, P., Billen, G., Hascoët, M.C., 1987. Determination of the biodegradable fraction of dissolved organic matter in waters. Water Res. 21, 445–450. https://doi.org/10.1016/0043-1354(87)90192-8

Servais, P., Billen, G., Laurent, P., Levi, Y., Randon, G., 1992. Studies of BDOC and bacterial dynamics in the drinking water distribution system of the northern Parisian suburbs. Rev. des Sci. l'Eau 5, 69–89. https://doi.org/10.7202/705154ar

Seth, A., Klise, K.A., Siirola, J.D., Haxton, T., Laird, C.D., 2016. Testing contamination source identification methods for water distribution networks. J. Water Resour. Plan. Manag. 142, 1–11. https://doi.org/10.1061/(ASCE)WR.1943-5452.0000619

Shang, F., Uber, J.G., Rossman, L.A., 2008a. Modeling reaction and transport of multiple species in water distribution systems. Environ. Sci. Technol. 42, 808–814. https://doi.org/10.1021/es072011z

Shang, F., Uber, J.G., Rossman, L.A., 2008b. Modeling Reaction and Transport of Multiple Species in Water Distribution Systems. Environ. Sci. Technol. 42, 808–814. https://doi.org/10.1021/es072011z

Th�gersen, J., Dahi, E., 1996. Chlorine decay and bacterial inactivation kinetics in drinking water in the tropics. World J. Microbiol. Biotechnol. 12, 549–556. https://doi.org/10.1007/BF00419471

van der Kooij, D., Veenendaal, H.R., Baars-Lorist, C., van der Klift, D.W., Drost, Y.C., 1995. Biofilm formation on surfaces of glass and Teflon exposed to treated water. Water Res. 29, 1655–1662. https://doi.org/10.1016/0043-1354(94)00333-3

Vasconcelos, J.J., Rossman, L.A., Grayman, W.M., Boulos, P.F., Clark, R.M., 1997. Kinetics of chlorine decay. J. / Am. Water Work. Assoc. 89, 54–65. https://doi.org/10.1002/j.1551-8833.1997.tb08259.x

Vieira, F.C.S., Nahas, E., 2005. Comparison of microbial numbers in soils by using various culture media and temperatures. Microbiol. Res. 160, 197–202. https://doi.org/10.1016/j.micres.2005.01.004

Vieira, P., Coelho, S.T., Loureiro, D., 2004. Accounting for the influence of initial chlorine concentration, TOC, iron and temperature when modelling chlorine decay in water supply. J. Water Supply Res. Technol. - AQUA 53, 453–467. https://doi.org/10.2166/aqua.2004.0036

Volk, C.J., LeChevallier, M.W., 2000. Assessing biodegradable organic matter. J. / Am. Water Work. Assoc. 92, 64–76. https://doi.org/10.1002/j.1551-8833.2000.tb08945.x

Wolfe, R.L., Ward, N.R., Olson, B.H., 1985. Inactivation of heterotrophic bacterial populations in finished drinking water by chlorine and chloramines. Water Res. 19, 1393–1403. https://doi.org/10.1016/0043-1354(85)90306-9

World Health Organization, 2017. Drinking Water Parameter Cooperation Project - Support to the revision of Annex I Council Directive 98/83/EC on the Quality of Water Intended for Human Consumption 1–240.

World Health Organization, W.H.O., 2003. Antimony in Drinking-water. Background document for development of WHO Guidelines for Drinking-water Quality. Who 2, 1–9. https://doi.org/WHO/SDE/WSH/03.04/74

Yang, L., Shin, H.S., Hur, J., 2014. Estimating the concentration and biodegradability of organic matter in 22 wastewater treatment plants using fluorescence excitation emission matrices and parallel factor analysis. Sensors (Switzerland) 14, 1771–1786. https://doi.org/10.3390/s140101771

Zechman, E.M., Ranjithan, S.R., 2009. Evolutionary computation-based methods for characterizing contaminant sources in a water distribution system. J. Water Resour. Plan. Manag. 135, 334–343. https://doi.org/10.1061/(ASCE)0733-9496(2009)135:5(334)

Zhang, W., DiGiano, F.A., 2002. Comparison of bacterial regrowth in distribution systems using free chlorine and chloramine: A statistical study of causative factors. Water Res. 36, 1469–1482. https://doi.org/10.1016/S0043-1354(01)00361-X

Zhang, W., Miller, C.T., DiGiano, F.A., 2004. Bacterial Regrowth Model for Water Distribution Systems Incorporating Alternating Split-Operator Solution Technique. J. Environ. Eng. 130, 932–941. https://doi.org/10.1061/(ASCE)0733-9372(2004)130:9(932)

Zyl, J.E. Van, Borthwick, J., Hardy, A., 2015. OOTEN : An Object-oriented programmers toolkit for EPANET OOTEN : An object-oriented programmers toolkit for Epanet.

APPENDICES

APPENDIX I

1. **MATLAB code and functions used for simulations and extracting of the results**
2. **EPANET-MSX input file for organic attacks**
3. **EPANET input file for Modena water distribution system**

1. MATLAB code and functions used for simulations and extracting of the results

A. Chlorine residual sufficient dose

```
%% CHLORINE RESIUDAL MODELING IN EPANET-MSX

%% Clear
clear; close('all'); clc;
start_toolkit;

%% Load a network and run Hydraulics
d = epanet('MOD.inp');
% Set simulation time duration and hydraulic time Step
hrs = 100;
TimeSimulationDuration = hrs*3600;
d.setTimeSimulationDuration(TimeSimulationDuration);
TimeHydraulicStep = 1*3600; %in sec
d.setTimeHydraulicStep(TimeHydraulicStep);
% Get the number of nodes
nnodes = d.getNodeCount;

%% Hydraulic analysis using the functions ENopenH, ENinit, ENrunH,
ENgetnodevalue/&ENgetlinkvalue, ENnextH, ENcloseH
% (This function contains events)
hyd_res = d.getComputedHydraulicTimeSeries;

%% Load EPANET-MSX files
d.loadMSXFile('chlorine_res.msx')
% .inp Units
 if d.Units_US_Customary == 1
     setMSXAreaUnitsFT2(d)
 else
     setMSXAreaUnitsM2(d)
 end

%MSX TIMESTEP in seconds
TimeQualityStep = 360; %in sec
d.setMSXTimeStep(TimeQualityStep);
Total_Q_Steps = TimeSimulationDuration/TimeQualityStep;
% Set Ctarget
Ctarget = 0.3;
% Source node id
SourceID = d.getNodeReservoirNameID;
for i =1:d.getNodeReservoirCount
    sourceindex(i) = d.getNodeIndex(SourceID{i});
end
% set Start-up Duration
sud = 20*3600; %in sec
% Obtain an MSX hydraulic solution
d.solveMSXCompleteHydraulics;
%Set const. value of CL0
CL0_index = d.getMSXConstantsIndex('CL0');
d.setMSXConstantsValue(0.6);  %change in second run. Default is 1
CL0 = d.getMSXConstantsValue

%% Begin the search for the source concentration
csource = 0.0;
tleft = 1;
t_steps = zeros(Total_Q_Steps,1);
violation = 1;
while (violation && (csource <= 1.3))
    % Update source concentration to next level
    csource = csource + 0.05;
    c = zeros(Total_Q_Steps,nnodes); %Node concentrations for each time step
    for i =1:d.getNodeReservoirCount
        d.setMSXSources(SourceID{i},'CL2','CONCEN',csource,0);
```

```
    end
    % Run WQ simulation checking for target violations
    d.initializeMSXQualityAnalysis(0); %new
    j = 1;
    violation = 0;
    while (~violation && (tleft > 0))
        [t, tleft]=d.stepMSXQualityAnalysisTimeLeft;
        t_steps(j) = t;
            for i=1:nnodes
                 c(j,i) = d.getMSXSpeciesConcentration(0,i,1); %den ipologizetai to
reservoir, 0 gia nodes anti links, i ta nodes, 1 to CL2
                 if (t > sud)
                    if (c(j,i) < Ctarget)
                        violation = 1;
                        break;
                    end
                 end
            end
      j = j+1;
    end
end
csource

%% Unload library
d.unloadMSX
d.unload
```

B. Base case attack scenario in total 268 nodes

```
%% contaminant injections. Base-case scenario in total 268 nodes

%% Clear
clear; close('all'); clc;
start_toolkit;
 %% loops = nnodes;
for q =1:268 %TOTAL node Junctions

% Load a network and run Hydraulics
inp_file = 'MOD.inp';
d = epanet(inp_file);

% Set simulation time duration and hydraulic time Step
hrs = 4;
TimeSimulationDuration = hrs*3600;
d.setTimeSimulationDuration(TimeSimulationDuration);
TimePatternStep = 60 ;
d.setTimePatternStep(TimePatternStep); %1min time step
TimeHydraulicStep = 1*3600; %in sec
d.setTimeHydraulicStep(TimeHydraulicStep);

% Get the number of nodes and pipes
nnodes = d.getNodeCount;
npipes = d.getLinkPipeCount;

%% Hydraulic analysis using the functions ENopenH, ENinit, ENrunH,
ENgetnodevalue/&ENgetlinkvalue, ENnextH, ENcloseH
hyd_res = d.getComputedHydraulicTimeSeries;

%% Load EPANET-MSX files
d.loadMSXFile('bacterial_3.msx')

% .inp Units
 if d.Units_US_Customary == 1
```

```
     setMSXAreaUnitsFT2(d)
 else
     setMSXAreaUnitsM2(d)
 end

%MSX TIMESTEP in seconds
TimeQualityStep = 60; %in sec. Prosoxi sti diairesi
d.setMSXTimeStep(TimeQualityStep);

%Time_steps
steps = ceil(TimeSimulationDuration/TimeQualityStep);

% Source node id & index
SourceID = d.getNodeReservoirNameID;
for i =1:d.getNodeReservoirCount
    sourceindex(i) = d.getNodeIndex(SourceID{i});
end

% Obtain an MSX hydraulic solution
d.solveMSXCompleteHydraulics; %new
Species_count = d.getMSXSpeciesCount;

%Set const. value of CL0
CL0_index = d.getMSXConstantsIndex('CL0');
d.setMSXConstantsValue(0.6);  %apo chlorine_residual.m 2nd run
Const = d.getMSXConstantsValue;

%% Set Reservoir Source
CL2_source = 0.6; % (mg/l) apo chlorine_residual.m 2nd run
S_source = 0.3; % (mg/l) Volk et. al
Xb_source = 0.08; % (ug/l)  CANADA <100 cfu/ml
for i =1:d.getNodeReservoirCount
    d.setMSXSources(SourceID{i},'CL2','CONCEN',CL2_source,0);
    d.setMSXSources(SourceID{i},'S','CONCEN',S_source,0);
    d.setMSXSources(SourceID{i},'Xb','CONCEN',Xb_source,0);
end

%% Set Initial Conditions
set_initial = 1
if  set_initial
    Nodes_file =strcat(inp_file,'_720h_Nodes_final_0.6_0.3_0.08.mat');
    Links_file = strcat(inp_file,'_720h_Pipes_final_0.6_0.3_0.08.mat');
    path = 'C:\Users\...';
    load(strcat(path,Nodes_file)); %file named as final_node_values
    load(strcat(path,Links_file)); %file named as final_pipe_values
    initqual_nodes = d.getMSXNodeInitqualValue;
    initqual_pipes = d.getMSXLinkInitqualValue;
    for i=1:nnodes
        for j=1:Species_count
            initqual_nodes{1,i}(j)=final_node_values(j,i);
        end
    end
    for i=1:npipes
        for j=1:Species_count
            initqual_pipes{1,i}(j)=final_pipe_values(j,i);
        end
    end
    d.setMSXNodeInitqualValue(initqual_nodes);
    d.setMSXLinkInitqualValue(initqual_pipes);
end

%% Set Intrusion Source
total_TOC = 7000; %(gr)
inj_time  = 30;     %(mim)
TOC_inj = total_TOC/(inj_time); % (gr/min)
BDOC_inj = TOC_inj/5.55; %(gr/min)
xb_inj = 1.47*TOC_inj ; %(ug/min)
```

```
%% Set Patterns

p1=zeros(1,hrs*3600/TimePatternStep); %pattern initialize
intr_duration = inj_time; % duration of intrusion
intr_start = 3; % start of intrusion
for i = 0:intr_duration-1
    p1(1,intr_start+i) = 1;
end
d.addMSXPattern('p1');
d.setMSXPattern('p1',p1);
d.getMSXPattern;
intr_node = q;
%% set sources
d.setMSXSources(intr_node,'S','MASS',BDOC_inj*10^3,'p1');
d.setMSXSources(intr_node,'Xb','MASS',xb_inj,'p1');

%% results
for a =[1:2,5:6]
    specie = d.getMSXSpeciesNameID(a);
    RESULTS{q,a} = d.getMSXComputedQualitySpecie(specie{1});
end

%% Unload library
d.unloadMSX
d.unload
end
```

C. Quest of a contamination event impact

```
function [matrix1] = contaminated_nodes(a,b) %a = node injection. b = results

sz =size(b{1,1}.NodeQuality) ;
matrix=cell(sz(2));
k=0;
for j=1:sz(2)
    k=k+1;
        for i=1:sz(1)
            if 0.1 > b{a,1}.NodeQuality(i,j)
                matrix{k,1}=j;
                matrix{k,2}= [matrix{k,2},i];
            end
                if b{a,2}.NodeQuality(i,j) > 1.05
                matrix{k,1}=j;
                matrix{k,3}=[matrix{k,3},i];
                matrix{k,9}= [matrix{k,9},b{a,2}.NodeQuality(i,j)];
            end
                if b{a,5}.NodeQuality(i,j) > 5
                matrix{k,1}=j;
                matrix{k,4}=[matrix{k,4},i];
                matrix{k,10}= [matrix{k,10},b{a,5}.NodeQuality(i,j)];
            end
        end
end
matrix1={0,0,0,0};
k=0;
for i=1:sz(2)
   if matrix{i,1}~= 0
       matrix1{1+k,1}=matrix{i,1};
       matrix1{1+k,2}=matrix{i,2};
       matrix1{1+k,3}=matrix{i,3};
       matrix1{1+k,4}=matrix{i,4};
       matrix1{1+k,9}=matrix{i,9};
       matrix1{1+k,10}=matrix{i,10};
       k=k+1;
   end
end
```

```
sz2= size(matrix1);
for i =1:sz2(1)
    min_cl2 = min(b{a,1}.NodeQuality(:,matrix1{i,1}));
    max_S   = max(b{a,2}.NodeQuality(:,matrix1{i,1}));
    max_Xb  = max(b{a,5}.NodeQuality(:,matrix1{i,1}));
    init_cl2 = b{a,1}.NodeQuality(1,matrix1{i,1});
    init_S   = b{a,2}.NodeQuality(1,matrix1{i,1});
    init_Xb  = b{a,5}.NodeQuality(1,matrix1{i,1});
    matrix1{i,5} = min_cl2;
    matrix1{i,6} = max_S;
    matrix1{i,7}  = max_Xb;
    matrix1{i,12} = init_cl2;
    matrix1{i,13} = init_S;
    matrix1{i,14} = init_Xb;
end
end
```

D. Quest of vulnerability indexes from an attack scenario

```
function [toc,xb,pop_TOC,pop_xb,matrix] = substances_per_person(time,k,popul) %TOC
per person.
% popul = population;
% k     = contaminated_nodes func;
% time  = TimeQualityStep;
%toc = toc per person
%xb  = xb per person
%pop_TOC = total population exposed to TOC
%pop_xb  = total population exposed to xb
k_size = size(k);
matrix = zeros(k_size(1),2);
pop_TOC =0;
pop_xb  =0;
for i = 1:k_size(1)
    [cancel,toc_time] = size(k{i,3});
    [cancel,xb_time ] = size(k{i,4});
     pop_TOC = pop_TOC + popul(1,k{i,1});
        matrix(i,1) = toc_time*time*popul(4,k{i,1})*mean(k{i,9}); % mg per node.

%number_of_time_intervals*time_interval*litres_per_seconds_in_node*toc_concentratio
n -->
    % sec*litres/sec*mg/litres = mg
    if ~isempty(k{i,10})
        matrix(i,2) = xb_time*time*popul(4,k{i,1})*bact(mean(k{i,10}));
        pop_xb = pop_xb + popul(1,k{i,1});
    end
end
toc = sum(matrix(1:k_size(1,1)))/pop_TOC;
xb  = sum(matrix(1:k_size(1),2))/pop_xb;

function [duration,duration_matrix] = attack_duration(k)

% k =  contaminated_nodes func
% popul = popul_demand func

x = [k{:,2} k{:,3} k{:,4}];

duration_matrix = unique(x);
duration = numel(duration_matrix);

function [cm_final] = customer_minutes(k,popul)
% k =  contaminated_nodes func
% popul = popul_demand func
sz = size(k);
for i = 1:sz(1)
     I = (k{i,1}(1,1));
     cl_time = k{i,2};
```

```
     s_time  = k{i,3};
     xb_time = k{i,4};
     x = [cl_time s_time xb_time]
     time_exposed = unique(x);
     time_exposed_array{i} = time_exposed;
     time_size=size(time_exposed);
     popul_exposed_per_attacked_node(i) = popul(1,I);
     cm(i) = numel(time_exposed)*popul_exposed_per_attacked_node(i);
end
cm_final = sum(cm);
```

E. 30-day simulation for the setting of initial conditions

```
%% Getting initial conditions IN EPANET-MSX

%% Clear
clear; close('all'); clc;
start_toolkit;
%% Load a network and run Hydraulics
inp_file = 'MOD.inp';
d = epanet(inp_file);

% Set simulation time duration and hydraulic time Step
hrs = 30*24
TimeSimulationDuration = hrs*3600;
d.setTimeSimulationDuration(TimeSimulationDuration);

TimeHydraulicStep = 1*3600; %in sec
d.setTimeHydraulicStep(TimeHydraulicStep);

% Get the number of nodes and pipes
nnodes = d.getNodeCount;
npipes = d.getLinkPipeCount;

%% Hydraulic analysis using the functions ENopenH, ENinit, ENrunH,
ENgetnodevalue/&ENgetlinkvalue, ENnextH, ENcloseH
% (This function contains events)
hyd_res = d.getComputedHydraulicTimeSeries;

%% Load EPANET-MSX files
d.loadMSXFile('bacterial_2.msx')

% .inp Units
 if d.Units_US_Customary == 1
     setMSXAreaUnitsFT2(d)
 else
     setMSXAreaUnitsM2(d)
 end

 MSXUnits = d.getMSXAreaUnits;

%MSX TIMESTEP in seconds

TimeQualityStep = 720; %in sec. Prosoxi sti diairesi
d.setMSXTimeStep(TimeQualityStep);

%Time_steps

steps = ceil(TimeSimulationDuration/TimeQualityStep);


% Source node id & index
SourceID = d.getNodeReservoirNameID;

for i =1:d.getNodeReservoirCount
    sourceindex(i) = d.getNodeIndex(SourceID{i});
```

```
end

% Obtain an MSX hydraulic solution
d.solveMSXCompleteHydraulics; %new

Species_count = d.getMSXSpeciesCount;

%Set const. value of CL0
CL0_index = d.getMSXConstantsIndex('CL0');
d.setMSXConstantsValue(0.6);  %apo chlorine_residual.m 2nd run
Const = d.getMSXConstantsValue;

%% Set Source Initial Conditions

CL2_source = 0.6;   % (mg/l) apo chlorine_residual.m 2nd run
S_source   = 0.3;   % (mg/l) %VOLK 0.1, 0,3, 0.7
Xb_source  = 0.08;  % (ug/l) CANADA <100 cfu/ml

for i =1:d.getNodeReservoirCount
    d.setMSXSources(SourceID{i},'CL2','CONCEN',CL2_source,0);
    d.setMSXSources(SourceID{i},'S','CONCEN',S_source,0);
    d.setMSXSources(SourceID{i},'Xb','CONCEN',Xb_source,0);
end

%% Run Quality
QUAL_RES_FINAL = struct;

final_node_values  = zeros(Species_count,nnodes);
final_pipe_values  = zeros(Species_count,npipes);

for i=1:Species_count

    specie = d.getMSXSpeciesNameID(i);
    QUAL_RES_FINAL(i).qual_res= d.getMSXComputedQualitySpecie(specie{1});

    for j=1:nnodes
        final_node_values(i,j)  = QUAL_RES_FINAL(i).qual_res.NodeQuality(steps,j);


    end

    for k=1:npipes

        final_pipe_values(i,k)  = QUAL_RES_FINAL(i).qual_res.LinkQuality(steps,k);

    end

end

%% Save final conditions

path = 'C:\...';
nname =
strcat(path,inp_file,'_',num2str(hrs),'h','_','Nodes_final','_',num2str(CL2_source)
,'_',num2str(S_source),'_',num2str(Xb_source),'.mat');
save(nname,'final_node_values');

pname =
strcat(path,inp_file,'_',num2str(hrs),'h','_','Pipes_final','_',num2str(CL2_source)
,'_',num2str(S_source),'_',num2str(Xb_source),'.mat');
save(pname,'final_pipe_values');



%% Unload library
d.unloadMSX
d.unload
```

2. EPANET-MSX input file for organic load attacks

```
[TITLE]
Water quality model. Initial conditions, sources and patterns are not considered in the MSX file
[OPTIONS]
  AREA_UNITS CM2          ;Surface concentration is mass/cm2
  RATE_UNITS HR           ;Reaction rates are concentration/hour
  SOLVER     EUL          ;
  TIMESTEP   360          ;360 sec (6 min) solution time step
  RTOL       0.001        ;Relative concentration tolerance
  ATOL       0.0001       ;Absolute concentration tolerance
[SPECIES]
BULK   CL2   MG     ;chlorine
BULK   S     MG     ;organic substrate
BULK   Xb    UG     ;bulk biomass (ug/l)
WALL   Xa    UG     ;attached biomass (ug/(ft2 or m2))
BULK   Nb    log(N)          ;number of free bacteria
WALL   Na    log(N)          ;number of attached bacteria
[COEFFICIENTS]
CONSTANT CL0 1 ; INITIAL CL0 (mg/l)
CONSTANT  CL2C    0.20   ;characteristic CL2 (mg/L)
CONSTANT  CL2Tb   0.08   ;threshold CL2 for Xb (mg/L)
CONSTANT  CL2Ta   0.10   ;threshold CL2 for Xa (mg/L)
CONSTANT  MUMAXb  0.20   ;max. growth rate for Xb (1/hr)
CONSTANT  MUMAXa  0.20   ;max. growth rate for Xa (1/hr)
CONSTANT  Ks      0.40   ;half saturation constant (mg/L)
CONSTANT  Kd      0.06   ;bacterial decay constant (1/hr)
CONSTANT  Kdep    0.25   ;deposition rate constant (1/hr)
CONSTANT  Kdet    0.04   ;detachment rate constant (1/hr/(m2)/s))
CONSTANT  Yg      0.15   ;bacterial yield coefficient (mg/mg)
[TERMS]
Ib   EXP(-STEP(CL2-CL2Tb)*(CL2-CL2Tb)/CL2C)        ;Xb inhibition coeff.
Ia   EXP(-STEP(CL2-CL2Ta)*(CL2-CL2Ta)/CL2C)        ;Xa inhibition coeff.
MUb  MUMAXb*S/(S+Ks)*Ib                            ;Xb growth rate coeff.
MUa  MUMAXa*S/(S+Ks)*Ia                            ;Xa growth rate coeff.
TOC  5.55*S
K1_TOC   (0.0035*TOC - 0.0349)*60
K2_TOC   (0.0001*TOC - 0.0012)*60
Z_TOC    (0.0012*TOC + 0.2039)
K1_CL2 (1/CL0*0.0064+ 0.0006)*60
```

K2_CL2 (3*10^(-6)/CL0 +5*10^(-7))*60
Z_CL2 0.0545*CL0^2 - 0.2653*CL0 +0.3711
K1 STEP(TOC-12)*K1_TOC + STEP(12-TOC)*K1_CL2
K2 STEP(TOC-12)*K2_TOC + STEP(12-TOC)*K2_CL2
Z STEP(TOC-12)*Z_TOC + STEP(12-TOC)*Z_CL2
[PIPES]
RATE CL2 -(Z*K1 + K2*(1-Z))*CL2
RATE S -(MUa*Xa*Av + MUb*Xb)/Yg/1000
RATE Xb (MUb-Kd)*Xb + Kdet*U*Xa*Av - Kdep*Xb
RATE Xa (MUa-Kd)*Xa - Kdet*U*Xa + Kdep*Xb/Av
FORMULA Nb LOG10(1.0e6*Xb)
FORMULA Na LOG10(1.0e6*Xa)
[TANKS]
RATE CL2 -K1*Z*CL2 - K2*(1-Z)*CL2
RATE S -MUb*Xb/Yg/1000
RATE Xb (MUb-Kd)*Xb
FORMULA Nb LOG10(1.0e6*Xb)

[SOURCES]
;CONC/MASS/FLOW/SETPOINT <nodeID> <specieID> <strength> (<tseriesID>)

[QUALITY]

[PATTERNS]

3. EPANET input file for Modena water distribution system

[TITLE]
Modena water distribution system -- Bragalli, D'Ambrosio, Lee, Lodi, Toth (2008)
[JUNCTIONS]

;ID	Elev	Demand	Pattern	
1	39.49	0.06		;
2	39.62	1.45		;
3	38.70	5.13		;
4	37.25	2.76		;
5	36.27	0.96		;
6	35.95	0.78		;

7	35.95	1.03	;
8	36.09	2.12	;
9	36.18	1.16	;
10	37.00	1.78	;
11	36.50	0.44	;
12	37.39	0.03	;
13	38.07	0.57	;
14	37.02	0.36	;
15	41.26	3.30	;
16	39.35	0.03	;
17	39.53	2.10	;
18	36.59	4.67	;
19	36.76	0.00	;
20	37.72	1.53	;
21	37.31	4.61	;
22	37.62	1.06	;
23	36.99	1.32	;
24	35.20	2.74	;
25	35.11	0.59	;
26	34.65	0.45	;
27	34.33	0.64	;
28	36.15	7.11	;
29	36.30	0.93	;
30	36.10	0.04	;
31	36.14	0.02	;
32	35.80	2.93	;
33	33.26	2.34	;
34	33.34	1.94	;
35	33.51	1.19	;
36	32.70	1.41	;
37	32.65	2.98	;
38	32.56	2.11	;
39	33.56	7.74	;
40	31.59	4.29	;
41	31.38	7.78	;
42	32.67	3.75	;
43	33.50	2.37	;
44	33.57	1.42	;
45	33.77	0.32	;
46	34.14	1.14	;

47	33.68	1.23	;
48	33.71	1.37	;
49	31.68	1.18	;
50	33.34	1.81	;
51	32.83	0.97	;
52	32.78	0.55	;
53	39.28	2.77	;
54	37.12	0.65	;
55	36.48	1.38	;
56	36.42	8.28	;
57	36.13	1.22	;
58	36.05	3.85	;
59	36.77	2.62	;
60	35.48	2.78	;
61	35.05	1.56	;
62	35.10	1.16	;
63	37.95	1.22	;
64	38.44	2.93	;
65	37.81	1.13	;
66	38.22	1.12	;
67	38.73	0.48	;
68	38.95	1.37	;
69	39.70	2.26	;
70	40.59	1.31	;
71	40.81	1.06	;
72	41.06	0.38	;
73	41.45	1.76	;
74	41.83	0.56	;
75	41.44	0.00	;
76	41.09	4.64	;
77	40.74	1.03	;
78	38.60	3.08	;
79	36.91	1.60	;
80	36.75	4.49	;
81	36.81	1.25	;
82	37.05	0.87	;
83	35.88	0.72	;
84	36.45	0.49	;
85	36.16	3.92	;
86	34.99	0.94	;

87	35.61	3.33	;
88	34.89	4.17	;
89	35.59	1.44	;
90	35.70	1.84	;
91	35.20	2.00	;
92	35.64	2.24	;
93	35.93	0.20	;
94	37.64	2.27	;
95	37.17	1.44	;
96	37.10	2.67	;
97	36.97	0.60	;
98	37.00	2.76	;
99	36.74	0.05	;
100	34.78	2.06	;
101	34.26	3.19	;
102	33.66	4.69	;
103	33.78	1.70	;
104	33.75	0.02	;
105	33.38	0.10	;
106	34.85	1.11	;
107	34.27	1.02	;
108	34.30	0.88	;
109	33.95	2.33	;
110	33.92	0.31	;
111	32.32	0.45	;
112	34.76	2.96	;
113	34.21	8.12	;
114	34.92	1.76	;
115	32.96	5.96	;
116	30.69	0.00	;
117	30.59	6.34	;
118	30.73	0.00	;
119	30.70	0.00	;
120	31.02	3.03	;
121	31.03	1.85	;
122	31.75	1.77	;
123	32.00	1.48	;
124	32.05	0.00	;
125	32.10	1.32	;
126	33.76	2.24	;

127	32.27	1.26	;
128	31.86	5.39	;
129	32.42	1.00	;
130	33.00	1.61	;
131	33.63	4.71	;
132	36.37	2.64	;
133	35.69	2.11	;
134	35.52	1.51	;
135	35.56	0.84	;
136	35.92	1.05	;
137	35.37	1.16	;
138	35.06	2.45	;
139	34.12	1.66	;
140	39.35	0.00	;
141	39.10	0.00	;
142	39.84	0.00	;
143	39.84	0.80	;
144	39.45	0.33	;
145	39.70	0.34	;
146	37.95	1.02	;
147	37.61	1.23	;
148	37.95	0.09	;
149	35.69	0.43	;
150	35.32	1.56	;
151	35.81	0.80	;
152	35.81	1.38	;
153	36.02	0.53	;
154	38.25	0.59	;
155	37.50	2.33	;
156	37.54	0.03	;
157	37.08	0.31	;
158	36.76	8.49	;
159	35.88	0.32	;
160	35.77	0.21	;
161	34.70	0.02	;
162	35.37	1.23	;
163	34.99	0.99	;
164	35.93	0.55	;
165	36.27	0.78	;
166	32.67	0.27	;

167	32.75	0.27	;
168	32.88	0.07	;
169	34.09	9.47	;
170	36.09	2.64	;
171	36.05	1.02	;
172	36.04	0.88	;
173	36.02	0.49	;
174	31.76	0.00	;
175	31.91	1.12	;
176	31.80	0.00	;
177	31.48	0.00	;
178	31.12	0.01	;
179	31.10	0.00	;
180	31.19	0.00	;
181	30.39	0.00	;
182	30.55	0.01	;
183	31.13	1.84	;
184	31.81	0.04	;
185	32.34	1.68	;
186	32.83	2.37	;
187	33.69	0.09	;
188	33.17	1.23	;
189	33.23	3.90	;
190	33.34	1.17	;
191	33.77	1.70	;
192	33.77	2.15	;
193	32.20	4.00	;
194	34.41	4.46	;
195	33.39	0.05	;
196	34.34	0.01	;
197	35.03	4.12	;
198	34.44	0.39	;
199	34.53	0.15	;
200	34.94	1.82	;
201	34.70	3.43	;
202	36.70	0.62	;
203	36.20	4.17	;
204	35.03	2.26	;
205	36.77	1.01	;
206	36.20	0.54	;

207	37.88	0.77	;
208	38.03	0.33	;
209	36.86	1.15	;
210	37.24	1.53	;
211	36.66	0.00	;
212	36.49	0.30	;
213	37.30	0.32	;
214	40.30	0.56	;
215	39.85	0.00	;
216	41.00	0.19	;
217	41.16	1.42	;
218	35.05	0.59	;
219	33.92	1.48	;
220	32.14	0.92	;
221	34.17	0.33	;
222	35.10	0.06	;
223	31.55	0.46	;
224	31.75	0.72	;
225	32.07	0.00	;
226	31.94	0.00	;
227	31.66	0.20	;
228	31.04	0.08	;
229	31.05	1.30	;
230	38.49	1.07	;
231	35.68	1.03	;
232	35.39	0.03	;
233	34.89	1.15	;
234	34.86	1.43	;
235	34.99	4.86	;
236	32.54	4.71	;
237	34.41	1.34	;
238	36.16	1.87	;
239	35.30	0.82	;
240	35.17	0.94	;
241	32.92	0.09	;
242	33.07	1.28	;
243	31.91	0.43	;
244	32.00	0.51	;
245	32.05	0.00	;
246	32.05	0.01	;

247	30.70	0.01	;
248	31.33	0.00	;
249	36.30	1.75	;
250	35.83	1.03	;
251	36.95	1.26	;
252	38.01	1.36	;
253	36.65	0.14	;
254	36.91	0.00	;
255	36.77	1.96	;
256	31.50	2.21	;
257	38.65	0.62	;
258	39.54	0.00	;
259	39.58	0.50	;
260	39.58	0.11	;
261	40.55	0.12	;
262	40.79	0.22	;
263	40.95	1.28	;
264	37.76	0.19	;
265	35.96	0.22	;
266	36.81	1.19	;
267	36.21	1.69	;
268	35.61	0.43	;

[RESERVOIRS]

;ID	Head	Pattern	
269	72.00		;
270	73.80		;
271	73.00		;
272	74.50		;

[TANKS]

;ID Elevation InitLevel MinLevel MaxLevel Diameter MinVol VolCurve

[PIPES]

;ID	Node1	Node2	Length	Diameter	Roughness	MinorLoss	Status
1	1	16	46.84	125.00	130.00	0.00	
2	16	2	267.68	100.00	130.00	0.00	
3	2	3	541.07	100.00	130.00	0.00	
4	3	4	542.29	100.00	130.00	0.00	
5	4	5	404.72	100.00	130.00	0.00	

6	5	206	151.67	100.00	130.00	0.00
7	206	6	341.57	100.00	130.00	0.00
8	1	140	39.91	100.00	130.00	0.00
9	140	143	269.73	100.00	130.00	0.00
10	143	145	45.92	100.00	130.00	0.00
11	145	146	890.09	100.00	130.00	0.00
12	146	148	33.79	100.00	130.00	0.00
13	148	63	6.03	100.00	130.00	0.00
14	63	149	367.92	125.00	130.00	0.00
15	149	150	97.66	125.00	130.00	0.00
16	150	60	322.19	100.00	130.00	0.00
17	60	61	359.48	100.00	130.00	0.00
18	61	218	199.59	100.00	130.00	0.00
19	1	141	57.06	200.00	130.00	0.00
20	141	142	223.41	200.00	130.00	0.00
21	142	144	47.03	200.00	130.00	0.00
22	144	257	782.67	200.00	130.00	0.00
23	257	53	231.87	125.00	130.00	0.00
24	53	251	279.84	100.00	130.00	0.00
25	251	57	145.70	100.00	130.00	0.00
26	57	58	81.10	100.00	130.00	0.00
27	58	59	550.17	100.00	130.00	0.00
28	53	230	155.63	100.00	130.00	0.00
29	230	252	357.81	100.00	130.00	0.00
30	252	3	267.32	100.00	130.00	0.00
31	3	13	612.50	100.00	130.00	0.00
32	13	12	160.50	100.00	130.00	0.00
33	12	11	531.71	100.00	130.00	0.00
34	1	258	41.91	200.00	130.00	0.00
35	258	259	95.22	200.00	130.00	0.00
36	259	260	25.13	200.00	130.00	0.00
37	260	215	158.12	200.00	130.00	0.00
38	215	261	95.40	200.00	130.00	0.00
39	261	77	52.92	200.00	130.00	0.00
40	77	262	44.92	200.00	130.00	0.00
41	262	216	127.05	200.00	130.00	0.00
42	216	263	56.68	200.00	130.00	0.00
43	263	76	181.29	200.00	130.00	0.00
44	76	217	220.90	200.00	130.00	0.00
45	217	75	67.65	200.00	130.00	0.00

46	75	74	36.06	200.00	130.00	0.00
47	74	73	242.29	150.00	130.00	0.00
48	73	72	70.45	150.00	130.00	0.00
49	72	71	112.83	150.00	130.00	0.00
50	71	70	105.72	150.00	130.00	0.00
51	70	69	199.42	150.00	130.00	0.00
52	69	68	180.64	125.00	130.00	0.00
53	68	78	288.76	125.00	130.00	0.00
54	78	154	69.26	100.00	130.00	0.00
55	154	79	718.45	100.00	130.00	0.00
56	79	155	390.78	100.00	130.00	0.00
57	155	156	24.00	125.00	130.00	0.00
58	156	95	504.52	125.00	130.00	0.00
59	95	96	41.78	150.00	130.00	0.00
60	96	97	367.93	150.00	130.00	0.00
61	97	157	101.86	150.00	130.00	0.00
62	157	98	125.36	150.00	130.00	0.00
63	98	158	699.76	150.00	130.00	0.00
64	158	136	448.05	200.00	130.00	0.00
65	136	159	114.29	200.00	130.00	0.00
66	159	160	197.30	200.00	130.00	0.00
67	160	137	235.98	200.00	130.00	0.00
68	137	135	224.87	200.00	130.00	0.00
69	135	222	176.73	125.00	130.00	0.00
70	222	161	76.44	100.00	130.00	0.00
71	161	131	356.94	100.00	130.00	0.00
72	131	242	443.79	100.00	130.00	0.00
73	242	130	20.55	100.00	130.00	0.00
74	130	241	113.33	100.00	130.00	0.00
75	241	168	25.96	100.00	130.00	0.00
76	168	167	145.04	100.00	130.00	0.00
77	167	166	55.24	100.00	130.00	0.00
78	166	129	208.22	100.00	130.00	0.00
79	129	125	190.43	100.00	130.00	0.00
80	125	246	70.98	100.00	130.00	0.00
81	246	245	52.04	100.00	130.00	0.00
82	245	124	34.03	100.00	130.00	0.00
83	124	225	79.47	100.00	130.00	0.00
84	225	226	277.99	100.00	130.00	0.00
85	176	227	86.03	100.00	130.00	0.00

86	227	177	296.25	100.00	130.00	0.00
87	177	180	111.30	100.00	130.00	0.00
88	180	178	123.37	100.00	130.00	0.00
89	178	179	196.27	100.00	130.00	0.00
90	179	228	198.46	100.00	130.00	0.00
91	228	229	75.62	100.00	130.00	0.00
92	229	121	110.14	100.00	130.00	0.00
93	121	118	423.57	100.00	130.00	0.00
94	118	117	116.57	100.00	130.00	0.00
95	117	181	100.61	100.00	130.00	0.00
96	181	182	164.84	100.00	130.00	0.00
97	182	116	47.49	100.00	130.00	0.00
98	116	247	87.54	100.00	130.00	0.00
99	49	184	189.27	150.00	130.00	0.00
100	184	41	244.80	150.00	130.00	0.00
101	41	248	293.47	150.00	130.00	0.00
102	248	40	308.64	150.00	130.00	0.00
103	40	39	566.57	150.00	130.00	0.00
104	226	176	95.14	100.00	130.00	0.00
105	247	183	248.55	100.00	130.00	0.00
106	183	49	187.78	100.00	130.00	0.00
107	39	38	357.67	125.00	130.00	0.00
108	38	37	700.57	100.00	130.00	0.00
109	37	193	404.46	100.00	130.00	0.00
110	193	36	160.86	125.00	130.00	0.00
111	36	194	557.42	125.00	130.00	0.00
112	194	27	127.02	150.00	130.00	0.00
113	27	26	46.66	150.00	130.00	0.00
114	26	195	674.32	150.00	130.00	0.00
115	195	33	50.76	125.00	130.00	0.00
116	26	196	138.54	100.00	130.00	0.00
117	196	25	199.33	100.00	130.00	0.00
118	25	232	231.12	100.00	130.00	0.00
119	232	24	187.06	100.00	130.00	0.00
120	24	231	240.64	100.00	130.00	0.00
121	231	7	173.44	125.00	130.00	0.00
122	7	6	23.58	100.00	130.00	0.00
123	6	28	526.74	125.00	130.00	0.00
124	28	249	500.72	100.00	130.00	0.00
125	249	29	15.29	100.00	130.00	0.00

126	7	8	265.92	125.00	130.00	0.00
127	8	23	355.51	125.00	130.00	0.00
128	23	207	189.78	125.00	130.00	0.00
129	207	208	28.18	125.00	130.00	0.00
130	208	22	129.34	125.00	130.00	0.00
131	22	21	361.24	125.00	130.00	0.00
132	21	264	223.52	150.00	130.00	0.00
133	20	210	185.17	150.00	130.00	0.00
134	210	209	154.95	150.00	130.00	0.00
135	209	19	34.71	200.00	130.00	0.00
136	264	20	31.14	150.00	130.00	0.00
137	19	253	42.52	200.00	130.00	0.00
138	253	18	356.45	200.00	130.00	0.00
139	18	211	128.82	200.00	130.00	0.00
140	211	212	140.66	200.00	130.00	0.00
141	212	11	113.32	200.00	130.00	0.00
142	11	10	555.23	150.00	130.00	0.00
143	10	4	272.68	150.00	130.00	0.00
144	59	203	315.88	100.00	130.00	0.00
145	203	202	284.93	100.00	130.00	0.00
146	202	31	97.93	125.00	130.00	0.00
147	265	32	262.94	100.00	130.00	0.00
148	32	33	635.82	100.00	130.00	0.00
149	33	34	415.73	150.00	130.00	0.00
150	34	35	122.60	150.00	130.00	0.00
151	265	31	29.56	100.00	130.00	0.00
152	59	205	33.80	100.00	130.00	0.00
153	205	88	377.12	100.00	130.00	0.00
154	88	89	629.17	150.00	130.00	0.00
155	89	90	133.28	200.00	130.00	0.00
156	90	91	348.05	200.00	130.00	0.00
157	91	234	292.89	300.00	130.00	0.00
158	234	109	488.99	300.00	130.00	0.00
159	138	235	289.88	100.00	130.00	0.00
160	235	110	486.72	100.00	130.00	0.00
161	102	106	260.92	200.00	130.00	0.00
162	106	91	163.58	200.00	130.00	0.00
163	48	108	424.07	200.00	130.00	0.00
164	108	109	173.66	200.00	130.00	0.00
165	109	110	99.55	150.00	130.00	0.00

166	110	111	307.92	150.00	130.00	0.00
167	59	204	283.84	100.00	130.00	0.00
168	204	200	141.49	125.00	130.00	0.00
169	200	100	58.27	125.00	130.00	0.00
170	100	199	79.59	150.00	130.00	0.00
171	199	198	39.41	150.00	130.00	0.00
172	198	101	126.25	150.00	130.00	0.00
173	29	30	61.39	100.00	130.00	0.00
174	30	31	73.73	100.00	130.00	0.00
175	31	250	83.16	125.00	130.00	0.00
176	250	197	118.22	150.00	130.00	0.00
177	197	101	297.21	150.00	130.00	0.00
178	101	221	17.08	200.00	130.00	0.00
179	221	139	58.11	200.00	130.00	0.00
180	139	219	135.50	200.00	130.00	0.00
181	139	192	255.85	100.00	130.00	0.00
182	192	191	40.65	100.00	130.00	0.00
183	219	102	161.59	200.00	130.00	0.00
184	191	190	136.29	100.00	130.00	0.00
185	190	105	57.23	125.00	130.00	0.00
186	105	189	164.02	125.00	130.00	0.00
187	189	35	192.86	125.00	130.00	0.00
188	105	104	234.58	100.00	130.00	0.00
189	104	103	215.82	100.00	130.00	0.00
190	102	103	231.93	100.00	130.00	0.00
191	91	138	134.12	150.00	130.00	0.00
192	138	112	175.33	150.00	130.00	0.00
193	112	113	231.12	150.00	130.00	0.00
194	112	92	607.94	100.00	130.00	0.00
195	257	147	122.13	150.00	130.00	0.00
196	147	63	40.06	150.00	130.00	0.00
197	63	64	301.37	150.00	130.00	0.00
198	64	65	102.07	125.00	130.00	0.00
199	65	80	1094.73	100.00	130.00	0.00
200	65	66	199.73	100.00	130.00	0.00
201	66	67	160.59	100.00	130.00	0.00
202	67	68	82.49	100.00	130.00	0.00
203	80	266	137.42	100.00	130.00	0.00
204	266	84	229.41	100.00	130.00	0.00
205	84	267	111.38	125.00	130.00	0.00

206	267	85	105.08	125.00	130.00	0.00
207	85	173	292.34	125.00	130.00	0.00
208	173	172	47.39	125.00	130.00	0.00
209	172	92	324.07	125.00	130.00	0.00
210	93	268	120.76	100.00	130.00	0.00
211	268	114	187.57	100.00	130.00	0.00
212	89	92	314.62	150.00	130.00	0.00
213	92	93	157.18	100.00	130.00	0.00
214	93	238	103.32	100.00	130.00	0.00
215	238	133	308.21	100.00	130.00	0.00
216	133	239	205.05	100.00	130.00	0.00
217	239	134	234.72	100.00	130.00	0.00
218	134	162	109.11	150.00	130.00	0.00
219	162	163	262.04	150.00	130.00	0.00
220	163	240	152.57	150.00	130.00	0.00
221	240	135	240.23	150.00	130.00	0.00
222	114	113	381.95	100.00	130.00	0.00
223	113	115	374.77	100.00	130.00	0.00
224	115	236	318.59	125.00	130.00	0.00
225	236	111	104.73	125.00	130.00	0.00
226	111	220	43.25	100.00	130.00	0.00
227	220	122	406.87	100.00	130.00	0.00
228	122	123	386.74	100.00	130.00	0.00
229	123	175	106.49	100.00	130.00	0.00
230	175	174	85.64	100.00	130.00	0.00
231	174	223	214.06	100.00	130.00	0.00
232	223	224	117.61	100.00	130.00	0.00
233	224	124	203.24	100.00	130.00	0.00
234	16	17	29.27	100.00	130.00	0.00
235	17	214	170.94	100.00	130.00	0.00
236	214	15	252.74	100.00	130.00	0.00
237	15	213	325.90	100.00	130.00	0.00
238	213	14	350.99	100.00	130.00	0.00
239	14	12	118.26	100.00	130.00	0.00
240	4	54	207.60	125.00	130.00	0.00
241	54	55	285.73	125.00	130.00	0.00
242	55	56	322.72	125.00	130.00	0.00
243	56	57	265.11	100.00	130.00	0.00
244	10	9	406.85	100.00	130.00	0.00
245	9	8	518.87	100.00	130.00	0.00

246	9	5	397.02	100.00	130.00	0.00
247	58	60	493.32	100.00	130.00	0.00
248	60	151	140.28	100.00	130.00	0.00
249	151	152	195.40	100.00	130.00	0.00
250	152	83	175.12	100.00	130.00	0.00
251	83	153	145.50	100.00	130.00	0.00
252	153	84	132.26	100.00	130.00	0.00
253	218	62	54.37	100.00	130.00	0.00
254	62	87	317.19	100.00	130.00	0.00
255	87	171	294.19	125.00	130.00	0.00
256	171	170	100.68	125.00	130.00	0.00
257	170	92	238.22	150.00	130.00	0.00
258	85	87	339.22	100.00	130.00	0.00
259	85	94	585.54	100.00	130.00	0.00
260	95	94	247.16	100.00	130.00	0.00
261	94	254	148.81	100.00	130.00	0.00
262	254	99	102.14	100.00	130.00	0.00
263	99	255	387.72	100.00	130.00	0.00
264	255	132	289.01	100.00	130.00	0.00
265	132	133	282.41	100.00	130.00	0.00
266	79	82	232.85	100.00	130.00	0.00
267	82	81	210.57	100.00	130.00	0.00
268	81	80	49.94	100.00	130.00	0.00
269	80	83	280.35	100.00	130.00	0.00
270	83	62	331.04	100.00	130.00	0.00
271	62	86	225.62	100.00	130.00	0.00
272	86	88	187.69	125.00	130.00	0.00
273	88	233	157.87	100.00	130.00	0.00
274	233	201	243.89	100.00	130.00	0.00
275	201	100	101.29	100.00	130.00	0.00
276	132	165	356.71	100.00	130.00	0.00
277	165	164	69.68	100.00	130.00	0.00
278	164	134	155.34	100.00	130.00	0.00
279	134	126	906.52	100.00	130.00	0.00
280	126	127	315.00	100.00	130.00	0.00
281	113	169	632.68	150.00	130.00	0.00
282	169	126	184.15	100.00	130.00	0.00
283	127	244	123.24	100.00	130.00	0.00
284	244	243	67.54	100.00	130.00	0.00
285	243	128	140.38	100.00	130.00	0.00

286	128	129	382.62	100.00	130.00	0.00
287	106	237	294.04	100.00	130.00	0.00
288	237	107	406.02	100.00	130.00	0.00
289	107	108	111.83	100.00	130.00	0.00
290	109	188	457.93	350.00	130.00	0.00
291	188	51	165.68	350.00	130.00	0.00
292	51	52	38.63	350.00	130.00	0.00
293	52	256	422.28	100.00	130.00	0.00
294	256	120	243.49	100.00	130.00	0.00
295	120	118	220.11	100.00	130.00	0.00
296	120	119	204.87	100.00	130.00	0.00
297	119	117	111.09	100.00	130.00	0.00
298	119	116	205.38	100.00	130.00	0.00
299	119	118	55.48	100.00	130.00	0.00
300	35	47	110.86	200.00	130.00	0.00
301	47	187	112.89	100.00	130.00	0.00
302	187	44	77.84	100.00	130.00	0.00
303	44	43	153.46	100.00	130.00	0.00
304	43	42	464.02	100.00	130.00	0.00
305	42	41	481.27	100.00	130.00	0.00
306	49	185	214.32	200.00	130.00	0.00
307	185	186	383.55	200.00	130.00	0.00
308	186	52	96.32	200.00	130.00	0.00
309	44	45	90.52	100.00	130.00	0.00
310	45	46	184.64	100.00	130.00	0.00
311	46	50	291.38	100.00	130.00	0.00
312	50	51	260.28	100.00	130.00	0.00
313	47	48	28.45	200.00	130.00	0.00
330	272	136	100.00	200.00	130.00	0.00
331	271	1	1000.00	250.00	130.00	0.00
335	269	52	1.00	400.00	130.00	0.00
336	270	209	1.00	200.00	130.00	0.00

[ENERGY]

Global Efficiency 75

Global Price 0

Demand Charge 0

[TIMES]

Duration 4:00

Hydraulic Timestep 1:00

Report Timestep 0:01

```
Report Start	0:00
[OPTIONS]
 Units		LPS
 Headloss	H-W
 Specific Gravity	1.0
 Viscosity	1.0
 Trials		40
 Accuracy	0.001
 CHECKFREQ	2
 MAXCHECK	10
 DAMPLIMIT	0
 Unbalanced	Continue 10
 Pattern	0.1
 Demand Multiplier	1.0
 Emitter Exponent	0.5
 Quality	Chlorine mg/L
 Diffusivity	1.0
 Tolerance	0.01
[BACKDROP]
 DIMENSIONS	1649324.15	4942192.85	1656006.10	4948224.15
 UNITS		None
 FILE
 OFFSET		0.00		0.00
[END]
```

APENDIX II

1. **Table of total results from base-case scenario in total 268 nodes**
2. **Tables of results from Sensitivity Analysis**

1. Table of total results from base-case scenario in total 268 nodes

Base case scenario results

TOC =7000gr, 10.3 mg bacteria, time =30min, Initial conditions: CL2 = 0.6mg/l . S = 0.3 mg/l. Xb = 0.08 ug/l, Demand multiplier = 1

# node	Population per Node	Total times infected	Percentage of Population	Population influenced	Percentage of Population Influenced	Consumer-Minutes exposure	TOC/person (mg/L)	Bacteria/person (CFU/mL)	Consumers exposed to TOC	Consumers exposed to Bacteria	Total TOC (g)	Total Bacterial mass (mg)	Contamination duration
1	29	1	0,015%	40125	20,5%	1,58E+06	7,98	193	40125	36150	7209	24	180
2	697	3	0,357%	19480	10,0%	6,11E+05	16,75	274	19480	15692	7096	15	174
3	2463	13	1,260%	18783	9,6%	5,94E+05	19,22	281	18783	14995	7085	15	157
4	1325	14	0,678%	10784	5,5%	3,49E+05	66,41	359	10784	10784	7072	14	79
5	461	16	0,236%	4509	2,3%	1,43E+05	194,86	734	4509	4509	7029	12	64
6	375	28	0,192%	3788	1,9%	1,17E+05	309,06	845	3788	3788	7024	11	48
7	495	19	0,253%	13091	6,7%	4,28E+05	25,04	309	13091	13091	7087	14	173
8	1018	18	0,521%	14109	7,2%	4,58E+05	22,72	294	14109	14109	7092	15	177
9	557	9	0,285%	15387	7,9%	5,11E+05	18,01	310	15387	13956	7102	15	205
10	855	8	0,437%	21086	10,8%	7,42E+05	14,81	292	21086	15824	7143	16	183
11	212	7	0,108%	31497	16,1%	1,23E+06	9,64	244	31497	21866	7209	19	190
12	15	8	0,008%	20983	10,7%	6,63E+05	14,97	273	20983	16474	7108	16	181
13	274	9	0,140%	19057	9,8%	6,00E+05	16,91	281	19057	15269	7089	15	176
14	173	9	0,089%	1911	1,0%	6,07E+04	315,66	1779	1911	1911	7013	12	93
15	1584	15	0,810%	1584	0,8%	4,75E+04	1180,12	1926	1584	1584	7010	11	30
16	15	2	0,008%	22356	11,4%	6,84E+05	14,24	480	22356	7203	7122	12	179
17	1008	3	0,516%	2861	1,5%	8,93E+04	384,81	1099	2861	2861	7019	11	51
18	2242	4	1,147%	28622	14,6%	1,17E+06	11,24	236	28622	24253	7157	20	178
19	0	2	0,000%	28690	14,7%	1,18E+06	10,79	243	28690	24321	7159	21	185
20	735	3	0,376%	18821	9,6%	6,30E+05	15,15	269	18821	17390	7127	16	200

21	2213	5	1,132%	17994	9,2%	5,95E+05	16,15	273	17994	16563	7119	16	196
22	509	6	0,260%	15781	8,1%	5,29E+05	18,86	299	15781	14350	7106	15	191
23	634	9	0,324%	14743	7,5%	4,87E+05	20,82	288	14743	14743	7099	15	185
24	1316	21	0,673%	8313	4,3%	2,77E+05	42,44	453	8313	8313	7056	13	160
25	284	23	0,145%	6982	3,6%	2,35E+05	61,65	530	6982	6982	7048	13	131
26	216	33	0,111%	6693	3,4%	2,17E+05	89,58	510	6693	6693	7045	12	94
27	308	34	0,158%	6477	3,3%	2,08E+05	93,54	532	6477	6477	7043	12	93
28	3413	52	1,746%	3413	1,7%	1,02E+05	548,59	913	3413	3413	7021	11	30
29	447	28	0,229%	4700	2,4%	1,44E+05	193,00	719	4700	4700	7030	12	62
30	20	27	0,010%	4720	2,4%	1,50E+05	180,56	712	4720	4720	7031	12	66
31	10	26	0,005%	7136	3,7%	2,28E+05	71,17	488	7136	7136	7047	12	111
32	1407	11	0,720%	1513	0,8%	4,37E+04	819,63	1968	1513	1513	6821	10	44
33	1124	10	0,575%	9249	4,7%	2,99E+05	53,07	414	9249	9249	6994	13	114
34	932	9	0,477%	10181	5,2%	3,36E+05	44,78	397	10181	10181	7010	14	123
35	572	8	0,293%	30606	15,7%	9,64E+05	10,37	277	30606	15914	7140	15	180
36	677	36	0,346%	4028	2,1%	1,26E+05	202,24	795	4028	4028	7026	11	69
37	1431	42	0,732%	1431	0,7%	4,29E+04	1306,11	2103	1431	1431	7009	11	30
38	1013	10	0,518%	2444	1,3%	7,48E+04	376,46	1303	2444	2444	7016	11	61
39	3716	9	1,901%	6160	3,2%	1,89E+05	114,27	558	6160	6160	7039	12	80
40	2060	8	1,054%	8220	4,2%	2,50E+05	73,01	455	8220	8220	7052	13	94
41	3735	6	1,911%	13755	7,0%	4,35E+05	36,82	315	13755	13755	7090	15	112
42	1800	19	0,921%	1800	0,9%	5,40E+04	1038,70	1697	1800	1800	7011	11	30
43	1138	13	0,582%	2938	1,5%	8,99E+04	374,74	1093	2938	2938	7019	11	51
44	682	12	0,349%	3620	1,9%	1,13E+05	282,21	894	3620	3620	7024	11	55
45	154	5	0,079%	3774	1,9%	1,22E+05	256,76	853	3774	3774	7025	11	58
46	548	4	0,280%	4322	2,2%	1,38E+05	209,83	765	4322	4322	7028	12	62
47	591	7	0,302%	34861	17,8%	1,10E+06	9,04	238	34861	20169	7172	17	182
48	658	6	0,337%	35519	18,2%	1,12E+06	8,84	234	35519	20827	7179	17	183
49	567	4	0,290%	23641	12,1%	8,40E+05	13,04	226	23641	23641	7169	19	186
50	869	3	0,445%	5191	2,7%	1,69E+05	159,44	660	5191	5191	7035	12	68

51	466	2	0,238%	92371	47,3%	3,55E+06	2,99	137	92371	84937	7515	41	218
52	265	1	0,136%	112975	57,8%	4,25E+06	2,47	127	112975	106913	7633	48	219
53	1330	19	0,680%	8344	4,3%	2,66E+05	87,49	423	8344	8344	6935	12	76
54	312	15	0,160%	4950	2,5%	1,57E+05	247,09	667	4950	4950	7033	12	46
55	663	16	0,339%	4638	2,4%	1,43E+05	310,91	701	4638	4638	7030	11	39
56	3975	27	2,034%	3975	2,0%	1,19E+05	471,27	799	3975	3975	7025	11	30
57	586	21	0,300%	6409	3,3%	1,98E+05	131,16	521	6409	6409	6830	12	65
58	1848	32	0,945%	1848	0,9%	5,54E+04	963,62	1579	1848	1848	6678	10	30
59	1258	33	0,644%	3260	1,7%	9,98E+04	325,07	971	3260	3260	7021	11	53
60	1335	15	0,683%	4980	2,5%	1,54E+05	102,99	687	4980	4980	6988	12	109
61	749	34	0,383%	749	0,4%	2,25E+04	2493,88	3973	749	749	7005	10	30
62	557	17	0,285%	2599	1,3%	8,14E+04	222,67	1211	2599	2599	7017	11	97
63	586	12	0,300%	11969	6,1%	3,85E+05	32,62	341	11969	11969	7027	14	144
64	1407	13	0,720%	7868	4,0%	1,99E+05	50,34	627	7868	5447	6981	12	141
65	543	14	0,278%	6461	3,3%	1,63E+05	61,48	827	6461	4040	6952	12	140
66	538	15	0,275%	3190	1,6%	9,61E+04	172,09	1008	3190	3190	6931	11	101
67	231	16	0,118%	3839	2,0%	1,01E+05	152,99	838	3839	3839	6828	11	93
68	658	24	0,337%	6936	3,5%	2,27E+05	61,07	507	6936	6936	7042	12	133
69	1085	19	0,555%	8021	4,1%	2,63E+05	50,59	444	8021	8021	7050	12	139
70	629	18	0,322%	8650	4,4%	2,87E+05	44,39	420	8650	8650	7055	13	147
71	509	17	0,260%	9159	4,7%	3,05E+05	41,11	424	9159	8587	7059	13	150
72	183	16	0,094%	9342	4,8%	3,11E+05	39,77	417	9342	8770	7060	13	152
73	845	15	0,432%	10187	5,2%	3,41E+05	35,80	388	10187	9615	7067	13	155
74	269	14	0,138%	10456	5,3%	3,54E+05	33,80	385	10456	9884	7069	13	160
75	0	13	0,000%	10456	5,3%	3,59E+05	33,19	386	10456	9884	7070	13	163
76	2228	11	1,140%	13366	6,8%	4,50E+05	24,67	326	13366	12794	7089	15	172
77	495	7	0,253%	14674	7,5%	5,07E+05	21,39	316	14674	14102	7100	16	181
78	1479	25	0,757%	6278	3,2%	2,04E+05	73,49	551	6278	6278	7036	12	122
79	769	33	0,393%	4515	2,3%	1,45E+05	142,81	705	4515	4515	7012	11	87
80	2156	48	1,103%	2728	1,4%	8,24E+04	334,44	1126	2728	2728	6957	11	61

81	600	34	0,307%	3328	1,7%	1,03E+05	250,70	922	3328	3328	6988	11	67
82	418	34	0,214%	3746	1,9%	1,19E+05	191,63	839	3746	3746	6999	11	78
83	346	32	0,177%	1009	0,5%	3,09E+04	957,78	2987	1009	1009	7006	11	58
84	236	28	0,121%	2072	1,1%	6,57E+04	211,56	1543	2072	2072	7014	11	128
85	1882	26	0,963%	4766	2,4%	1,51E+05	80,29	688	4766	4766	7031	11	147
86	452	10	0,231%	3051	1,6%	9,76E+04	170,44	1046	3051	3051	7020	11	108
87	1599	15	0,818%	7955	4,1%	2,62E+05	31,06	459	7955	7955	7042	13	228
88	2002	9	1,024%	10997	5,6%	3,45E+05	43,59	349	10997	10997	7071	13	118
89	692	8	0,354%	21687	11,1%	9,07E+05	11,39	235	21687	21687	7161	18	232
90	884	7	0,452%	22571	11,5%	9,46E+05	10,86	231	22571	22571	7170	18	234
91	960	6	0,491%	56911	29,1%	2,19E+06	5,53	150	56911	48671	7393	26	188
92	1076	12	0,551%	12597	6,4%	5,39E+05	19,43	319	12597	12597	7067	14	231
93	97	25	0,050%	1149	0,6%	3,64E+04	912,25	2420	1149	1149	6682	10	51
94	1090	8	0,558%	6822	3,5%	2,18E+05	40,50	533	6822	6822	7045	13	204
95	692	7	0,354%	12591	6,4%	4,17E+05	21,53	328	12591	12591	7081	14	209
96	1282	6	0,656%	13873	7,1%	4,55E+05	19,47	304	13873	13873	7090	15	210
97	289	5	0,148%	14162	7,2%	4,71E+05	18,46	307	14162	14162	7092	15	217
98	1325	3	0,678%	15636	8,0%	5,27E+05	16,30	296	15636	14973	7103	15	223
99	25	10	0,013%	966	0,5%	2,99E+04	951,17	3555	966	966	7006	12	61
100	989	26	0,506%	7855	4,0%	2,50E+05	93,27	444	7855	7855	7052	12	77
101	1532	23	0,784%	17255	8,8%	5,86E+05	25,39	254	17255	17255	7120	15	130
102	2252	11	1,152%	21991	11,3%	7,43E+05	18,98	222	21991	21991	7150	17	137
103	817	18	0,418%	817	0,4%	2,45E+04	2286,44	3656	817	817	7005	10	30
104	10	11	0,005%	827	0,4%	2,56E+04	1110,90	4042	827	827	7005	12	61
105	49	10	0,025%	21499	11,0%	7,14E+05	13,91	246	21499	17980	7142	16	191
106	533	10	0,273%	22524	11,5%	7,68E+05	18,03	224	22524	22524	7156	18	141
107	490	6	0,251%	23658	12,1%	8,00E+05	14,85	249	23658	20139	7160	18	163
108	423	5	0,216%	40678	20,8%	1,51E+06	7,47	159	40678	34171	7251	19	191
109	1119	4	0,573%	92331	47,2%	3,44E+06	3,07	131	92331	78689	7516	36	212
110	149	5	0,076%	27810	14,2%	1,10E+06	14,15	217	27810	23079	7180	18	146

111	216	6	0,111%	22730	11,6%	8,02E+05	17,75	232	22730	20597	7163	17	142
112	1421	10	0,727%	27183	13,9%	8,61E+05	11,02	199	27183	24012	7151	17	191
113	3898	14	1,994%	13165	6,7%	4,12E+05	49,49	302	13165	13165	7085	14	87
114	845	27	0,432%	845	0,4%	2,54E+04	2073,56	3319	845	845	6571	10	30
115	2861	8	1,464%	16026	8,2%	5,04E+05	34,77	306	16026	13438	7104	14	102
116	0	7	0,000%	8410	4,3%	3,58E+05	37,80	392	8410	8410	7072	12	178
117	3044	14	1,557%	3044	1,6%	9,13E+04	614,89	1037	3044	3044	7019	11	30
118	0	11	0,000%	8405	4,3%	2,84E+05	39,52	466	8405	8405	7058	14	170
119	0	10	0,000%	8405	4,3%	3,53E+05	39,36	444	8405	8405	7071	13	171
120	1455	3	0,744%	9860	5,0%	4,11E+05	31,58	423	9860	9860	7083	15	182
121	889	12	0,455%	5361	2,7%	1,88E+05	65,64	670	5361	5361	7038	13	160
122	850	8	0,435%	6373	3,3%	2,10E+05	65,97	557	6373	6373	7042	12	134
123	711	9	0,364%	5523	2,8%	1,84E+05	82,21	620	5523	5523	7037	12	124
124	0	35	0,000%	3707	1,9%	1,25E+05	222,97	839	3707	3707	7026	11	68
125	634	38	0,324%	3702	1,9%	1,17E+05	248,84	857	3702	3702	7024	11	61
126	1076	25	0,551%	4721	2,4%	1,54E+05	212,79	688	4721	4721	7032	11	56
127	605	26	0,310%	3645	1,9%	1,18E+05	328,03	856	3645	3645	7024	11	47
128	2588	70	1,324%	2588	1,3%	7,76E+04	722,94	1182	2588	2588	7016	11	30
129	480	53	0,246%	3068	1,6%	9,46E+04	381,34	1014	3068	3068	7020	11	48
130	773	10	0,395%	4179	2,1%	1,42E+05	166,13	782	4179	4179	7029	11	81
131	2261	8	1,157%	7055	3,6%	2,27E+05	86,85	506	7055	7055	7046	12	92
132	1268	14	0,649%	2209	1,1%	6,72E+04	453,60	1403	2209	2209	7014	11	56
133	1013	11	0,518%	5269	2,7%	1,65E+05	69,03	652	5269	5269	7002	12	154
134	725	9	0,371%	11749	6,0%	4,47E+05	29,23	339	11749	11749	7083	14	165
135	404	5	0,207%	18178	9,3%	6,95E+05	18,68	267	18178	18178	7131	17	168
136	504	1	0,258%	38265	19,6%	1,37E+06	6,38	192	38265	37256	7260	25	238
137	557	4	0,285%	18735	9,6%	7,14E+05	18,13	267	18735	18735	7132	18	168
138	1177	9	0,602%	28360	14,5%	9,09E+05	10,47	215	28360	22601	7162	17	193
139	797	21	0,408%	18211	9,3%	6,23E+05	23,72	246	18211	18211	7128	16	132
140	0	2	0,000%	13052	6,7%	4,41E+05	23,39	337	13052	13052	7060	15	185

141	0	2	0,000%	19513	10,0%	7,11E+05	17,06	270	19513	19513	7074	18	170
142	0	3	0,000%	19513	10,0%	6,94E+05	17,57	264	19513	19513	7070	18	165
143	385	3	0,197%	13052	6,7%	4,37E+05	24,31	336	13052	13052	7060	15	178
144	159	4	0,081%	19513	10,0%	6,94E+05	17,67	263	19513	19513	7070	18	164
145	164	4	0,084%	12667	6,5%	4,21E+05	25,30	346	12667	12667	7052	15	176
146	490	5	0,251%	12503	6,4%	4,08E+05	30,67	329	12503	12503	7046	14	147
147	591	6	0,302%	12560	6,4%	4,03E+05	30,90	329	12560	12560	7035	14	145
148	44	6	0,023%	12013	6,1%	3,86E+05	32,28	340	12013	12013	7029	14	145
149	207	13	0,106%	5936	3,0%	1,89E+05	78,69	586	5936	5936	7007	12	120
150	749	14	0,383%	5729	2,9%	1,80E+05	83,59	603	5729	5729	7004	12	117
151	385	16	0,197%	1048	0,5%	3,21E+04	876,81	2948	1048	1048	7007	11	61
152	663	49	0,339%	663	0,3%	1,99E+04	2817,13	4477	663	663	7004	10	30
153	255	29	0,130%	1264	0,6%	3,96E+04	498,37	2464	1264	1264	7008	11	89
154	284	26	0,145%	4799	2,5%	1,56E+05	99,99	718	4799	4799	7018	12	117
155	1119	9	0,573%	5634	2,9%	1,81E+05	97,82	594	5634	5634	7027	12	102
156	15	8	0,008%	5649	2,9%	1,81E+05	96,61	593	5649	5649	7027	12	103
157	149	4	0,076%	14311	7,3%	4,81E+05	18,11	306	14311	14311	7094	15	219
158	4076	2	2,085%	19712	10,1%	6,50E+05	12,47	258	19712	19049	7129	17	232
159	154	2	0,079%	18990	9,7%	7,29E+05	17,78	274	18990	18990	7131	18	169
160	101	3	0,052%	18836	9,6%	7,25E+05	17,93	271	18836	18836	7133	18	169
161	10	7	0,005%	7065	3,6%	2,34E+05	82,27	511	7065	7065	7048	13	97
162	591	8	0,302%	12340	6,3%	4,72E+05	27,52	329	12340	12340	7088	14	167
163	476	7	0,244%	12816	6,6%	4,89E+05	26,34	326	12816	12816	7089	15	168
164	265	10	0,136%	2849	1,5%	9,03E+04	281,54	1102	2849	2849	7018	11	70
165	375	11	0,192%	2584	1,3%	8,07E+04	319,47	1200	2584	2584	7017	11	68
166	130	14	0,067%	3198	1,6%	1,02E+05	283,29	982	3198	3198	7021	11	62
167	130	13	0,067%	3328	1,7%	1,09E+05	255,78	949	3328	3328	7023	11	66
168	34	12	0,017%	3362	1,7%	1,13E+05	225,85	951	3362	3362	7023	11	74
169	4546	15	2,326%	9267	4,7%	2,89E+05	87,07	385	9267	9267	7060	13	70
170	1268	13	0,649%	9713	5,0%	3,17E+05	25,37	389	9713	9713	7054	13	229

171	490	14	0,251%	8445	4,3%	2,75E+05	29,26	443	8445	8445	7042	13	228
172	423	13	0,216%	5425	2,8%	1,76E+05	64,05	628	5425	5425	7036	12	162
173	236	14	0,121%	5002	2,6%	1,60E+05	70,30	678	5002	5002	7033	12	160
174	0	11	0,000%	4274	2,2%	1,47E+05	114,43	791	4274	4274	7030	12	115
175	538	10	0,275%	4812	2,5%	1,64E+05	97,45	711	4812	4812	7034	12	120
176	0	20	0,000%	3707	1,9%	1,33E+05	157,98	873	3707	3707	7028	11	96
177	0	18	0,000%	3804	1,9%	1,37E+05	125,25	866	3804	3804	7028	12	118
178	5	16	0,003%	3809	1,9%	1,40E+05	112,69	886	3809	3809	7028	12	131
179	0	15	0,000%	3809	1,9%	1,39E+05	104,68	899	3809	3809	7027	12	141
180	0	17	0,000%	3804	1,9%	1,38E+05	119,19	879	3804	3804	7028	12	124
181	0	9	0,000%	3044	1,6%	9,44E+04	542,60	1044	3044	3044	7020	11	34
182	5	8	0,003%	3049	1,6%	9,76E+04	449,27	1051	3049	3049	7020	11	41
183	884	5	0,452%	9299	4,8%	3,87E+05	32,91	389	9299	9299	7077	13	185
184	20	5	0,010%	13775	7,0%	4,45E+05	35,82	319	13775	13775	7092	15	115
185	807	3	0,413%	24448	12,5%	8,69E+05	12,42	225	24448	24448	7174	19	189
186	1138	2	0,582%	25586	13,1%	9,16E+05	11,58	223	25586	25586	7184	20	194
187	44	8	0,023%	3664	1,9%	1,18E+05	235,96	885	3664	3664	7025	11	65
188	591	3	0,302%	92922	47,5%	3,47E+06	2,98	138	92922	79943	7515	39	217
189	1873	9	0,958%	19959	10,2%	6,68E+05	16,56	236	19959	18595	7106	15	172
190	562	11	0,288%	20623	10,6%	6,82E+05	17,52	256	20623	17104	7135	15	158
191	817	12	0,418%	20061	10,3%	6,64E+05	18,35	263	20061	16542	7133	15	155
192	1033	13	0,529%	19244	9,8%	6,40E+05	19,25	280	19244	15725	7129	15	154
193	1920	37	0,982%	3351	1,7%	1,02E+05	274,79	947	3351	3351	7021	11	61
194	2141	35	1,095%	6169	3,2%	1,92E+05	103,74	554	6169	6169	7040	12	88
195	25	11	0,013%	6718	3,4%	2,24E+05	73,60	538	6718	6718	7046	13	114
196	5	24	0,003%	6698	3,4%	2,24E+05	76,51	523	6698	6698	7046	12	110
197	1978	24	1,012%	9609	4,9%	3,17E+05	48,62	383	9609	9609	7066	13	121
198	188	24	0,096%	8116	4,2%	2,63E+05	86,92	433	8116	8116	7054	12	80
199	73	25	0,037%	7928	4,1%	2,57E+05	90,09	440	7928	7928	7053	12	79
200	874	27	0,447%	5219	2,7%	1,64E+05	143,76	638	5219	5219	7034	12	75

201	1647	31	0,843%	1647	0,8%	4,94E+04	1135,04	1845	1647	1647	7010	11	30
202	298	27	0,152%	2300	1,2%	7,10E+04	519,13	1342	2300	2300	7015	11	47
203	2002	38	1,024%	2002	1,0%	6,01E+04	934,07	1515	2002	2002	7012	11	30
204	1085	28	0,555%	4345	2,2%	1,36E+05	187,54	753	4345	4345	7028	11	69
205	485	10	0,248%	3745	1,9%	1,18E+05	267,96	847	3745	3745	7024	11	56
206	260	17	0,133%	4048	2,1%	1,29E+05	231,45	813	4048	4048	7027	12	60
207	370	8	0,189%	15113	7,7%	5,08E+05	20,00	307	15113	13682	7103	15	188
208	159	7	0,081%	15272	7,8%	5,10E+05	19,69	306	15272	13841	7103	15	189
209	552	1	0,282%	35582	18,2%	1,44E+06	9,32	230	35582	30320	7172	24	173
210	735	2	0,376%	19556	10,0%	6,51E+05	14,44	263	19556	18125	7129	17	202
211	0	5	0,000%	31642	16,2%	1,24E+06	9,39	249	31642	22011	7209	19	194
212	145	6	0,074%	31642	16,2%	1,23E+06	9,49	245	31642	22011	7207	19	192
213	154	10	0,079%	1738	0,9%	5,37E+04	529,05	1824	1738	1738	7011	11	61
214	269	4	0,138%	1853	0,9%	5,72E+04	704,01	1643	1853	1853	7012	11	43
215	0	5	0,000%	14732	7,5%	5,20E+05	20,63	321	14732	14160	7103	16	187
216	92	9	0,047%	14073	7,2%	4,84E+05	22,79	321	14073	13501	7095	15	177
217	682	12	0,349%	11138	5,7%	3,84E+05	30,99	369	11138	10566	7075	14	164
218	284	18	0,145%	1033	0,5%	3,17E+04	968,96	2954	1033	1033	7007	11	56
219	711	12	0,364%	18922	9,7%	6,54E+05	22,34	243	18922	18922	7134	16	135
220	442	7	0,226%	6815	3,5%	2,25E+05	58,24	527	6815	6815	7046	13	142
221	159	22	0,081%	17414	8,9%	5,91E+05	24,97	254	17414	17414	7121	15	131
222	29	6	0,015%	7094	3,6%	2,35E+05	81,10	511	7094	7094	7048	13	98
223	221	12	0,113%	4274	2,2%	1,43E+05	129,00	784	4274	4274	7029	12	102
224	346	13	0,177%	4053	2,1%	1,33E+05	149,14	816	4053	4053	7027	12	93
225	0	22	0,000%	3707	1,9%	1,26E+05	207,69	864	3707	3707	7026	11	73
226	0	21	0,000%	3707	1,9%	1,30E+05	168,49	877	3707	3707	7027	11	90
227	97	19	0,050%	3804	1,9%	1,34E+05	146,31	863	3804	3804	7027	11	101
228	39	14	0,020%	3848	2,0%	1,43E+05	96,13	907	3848	3848	7029	12	152
229	624	13	0,319%	4472	2,3%	1,61E+05	80,64	797	4472	4472	7033	12	156
230	514	15	0,263%	8858	4,5%	2,80E+05	60,37	679	8858	4883	7019	12	105

231	495	20	0,253%	8808	4,5%	2,89E+05	38,61	431	8808	8808	7057	13	166
232	15	22	0,008%	6997	3,6%	2,41E+05	54,46	541	6997	6997	7049	13	148
233	552	10	0,282%	2199	1,1%	6,76E+04	418,31	1450	2199	2199	7014	11	61
234	687	5	0,351%	57598	29,5%	2,21E+06	5,35	155	57598	49358	7395	27	192
235	2333	6	1,194%	27522	14,1%	8,42E+05	13,49	305	27522	13375	7148	14	154
236	2261	7	1,157%	18287	9,4%	5,72E+05	28,82	289	18287	14623	7116	15	108
237	644	7	0,329%	23168	11,9%	7,89E+05	16,26	249	23168	19649	7159	17	152
238	898	12	0,459%	2047	1,0%	6,45E+04	335,28	1506	2047	2047	6949	11	81
239	394	10	0,202%	5663	2,9%	1,81E+05	61,51	609	5663	5663	7010	12	161
240	452	6	0,231%	13268	6,8%	5,08E+05	25,30	322	13268	13268	7091	15	169
241	44	11	0,023%	3406	1,7%	1,15E+05	219,95	927	3406	3406	7023	11	75
242	615	9	0,315%	4794	2,5%	1,60E+05	143,13	693	4794	4794	7033	12	82
243	207	28	0,106%	2795	1,4%	8,64E+04	528,61	1102	2795	2795	7018	11	38
244	245	27	0,125%	3040	1,6%	9,66E+04	439,85	1017	3040	3040	7020	11	42
245	0	36	0,000%	3707	1,9%	1,24E+05	226,30	835	3707	3707	7026	11	67
246	5	37	0,003%	3707	1,9%	1,21E+05	236,88	848	3707	3707	7025	11	64
247	5	6	0,003%	8415	4,3%	3,62E+05	37,36	396	8415	8415	7073	12	180
248	0	7	0,000%	8220	4,2%	2,59E+05	67,97	464	8220	8220	7054	13	101
249	840	29	0,430%	4253	2,2%	1,31E+05	216,69	794	4253	4253	7027	12	61
250	495	25	0,253%	7631	3,9%	2,50E+05	64,28	459	7631	7631	7052	12	115
251	605	20	0,310%	7014	3,6%	2,19E+05	113,62	486	7014	7014	6874	12	69
252	653	14	0,334%	9511	4,9%	3,01E+05	43,55	616	9511	5536	7041	12	136
253	68	3	0,035%	28690	14,7%	1,18E+06	10,85	241	28690	24321	7159	21	184
254	0	9	0,000%	966	0,5%	3,09E+04	651,94	3538	966	966	7006	12	89
255	941	24	0,481%	941	0,5%	2,82E+04	1985,37	3172	941	941	7006	10	30
256	1061	2	0,543%	10921	5,6%	4,44E+05	27,92	393	10921	10921	7090	15	186
257	298	5	0,152%	19354	9,9%	6,86E+05	19,74	285	19354	15379	7069	15	148
258	0	2	0,000%	15025	7,7%	5,31E+05	19,70	325	15025	14453	7103	16	192
259	240	3	0,123%	15025	7,7%	5,27E+05	19,90	322	15025	14453	7102	16	190
260	53	4	0,027%	14785	7,6%	5,22E+05	20,33	325	14785	14213	7102	16	189

261	58	6	0,030%	14732	7,5%	5,14E+05	20,96	317	14732	14160	7101	16	184
262	106	8	0,054%	14179	7,3%	4,89E+05	22,24	324	14179	13607	7096	15	180
263	615	10	0,315%	13981	7,2%	4,78E+05	22,94	321	13981	13409	7095	15	177
264	92	4	0,047%	18086	9,3%	6,07E+05	15,83	276	18086	16655	7122	16	199
265	106	25	0,054%	106	0,1%	3,18E+03	17611,72	27771	106	106	7001	10	30
266	572	69	0,293%	572	0,3%	1,72E+04	3265,07	5183	572	572	7004	10	30
267	812	27	0,415%	2884	1,5%	9,21E+04	139,07	1111	2884	2884	7019	11	140
268	207	26	0,106%	1052	0,5%	3,24E+04	1149,86	2666	1052	1052	6653	10	44

2. Total results from Sensitivity analysis to Node 52

	Mass Injection								
	-40,00%	-30%	-20%	-10%	0%	10%	20%	30%	40%
	4200	4900	5600	6300	7000	7700	8400	9100	9800
Total Population Exposed	110387	110387	112975	112975	112975	112975	116388	116388	117567
	-2%	-2%	0%	0%	0%	0%	3%	3%	4%
CME	3,60E+06	3,81E+06	3,94E+06	4,04E+06	4,25E+06	4,34E+06	4,42E+06	4,52E+06	4,63E+06
	-15%	-10%	-7%	-5%	0%	2%	4%	6%	9%
Average TOC Concentration (mg/L)	1,54	1,79	1,99	2,22	2,47	2,70	2,85	3,08	3,31
	-38%	-27%	-20%	-10%	0%	9%	15%	25%	34%
Average Bacterial Concentration (CFU/mL)	75,85	80,10	89,37	103,26	112,66	125,52	139,26	153,31	169,18
	-33%	-29%	-21%	-8%	0%	11%	24%	36%	50%
Population Exposed to Bact.	84794	95429	99536	99536	104030	105338	106164	106164	106913
	-18%	-8%	-4%	-4%	0%	1%	2%	2%	3%
Total bacterial mass (mg)	22,512	26,754	31,136	35,973	41,020	46,277	51,744	56,966	63,308
	-45%	-35%	-24%	-12%	0%	13%	26%	39%	54%
Total TOC mass (mg)	4652,34	5411,75	6138,21	6858,93	7633,42	8352,21	9074,02	9801,11	10538,95
	-39%	-29%	-20%	-10%	0%	9%	19%	28%	38%

	Time injection								
	-40%	-30%	-20%	-10%	0%	10%	20%	30%	40%
	18,0	21,00	24,00	27,00	30,0	33	36	39	42
Total Population Exposed	116388	116388	116388	112975	112975	112975	112975	112975	112975
	3%	3%	3%	0%	0%	0%	0%	0%	0%
CME	2,63E+06	3,02E+06	3,40E+06	4,55E+06	4,25E+06	4,42E+06	5,10E+06	5,53E+06	5,91E+06
	-38%	-29%	-20%	7%	0%	4%	20%	30%	39%
Average TOC Concentration (mg/L)	3,606	3,236	3,013	2,766	2,470	2,198	2,001	1,729	1,482
	46%	31%	22%	12%	0%	-11%	-19%	-30%	-40%
Average Bacterial Concentration (CFU/mL)	127,306	122,799	118,293	116,040	112,66	110,407	108,154	102,521	100,267
	13%	9%	5%	3%	0%	-2%	-4%	-9%	-11%
Population Exposed to Bact.	106913	106164	106164	105338	104030	99536	99536	99617	97422
	3%	2%	2%	1%	0%	-4%	-4%	-4%	-6%
Total bacterial mass (mg)	31,175	35,687	36,918	39,379	41,020	43,481	45,532	47,173	49,634
	-24%	-13%	-10%	-4%	0%	6%	11%	15%	21%
Total TOC mass (mg)	7480,75	7503,65	7557,08	7629,60	7633,42	7686,85	7709,75	7786,08	7801,35
	-2%	-1%	-1%	-0%	0%	1%	1%	2%	2%

	BDOC concentration in water						
	0,1	0,2	0,3	0,4	0,5	0,6	0,7
	-67%	-33%	0%	33%	67%	100%	133%
Total Population Exposed	110387	112975	112975	112975	112975	112975	112975
	-2%	0%	0%	0%	0%	0%	0%
CME	4,21E+06	4,23E+06	4,25E+06	4,27E+06	4,29E+06	4,32E+06	4,38E+06
	-1%	-0,50%	0%	0,40%	1%	1,60%	3%
Average TOC Concentration (mg/L)	11,931	12,053	12,17	12,235	12,296	12,357	12,418
	-2%	-1%	0%	0,50%	1%	1,50%	2%
Average Bacterial Concentration (CFU/mL)	111,533	112,097	112,660	113,787	114,913	116,040	117,166
	-1%	-0,50%	0%	1%	2%	3%	4%
Population Exposed to Bact.	101442	101442	104030	104372	104973	106270	106270
	-2%	-2%	0%	0%	1%	2%	2%
Total Bacterial Mass (mg)	39,789	40,200	41,020	41,648	42,301	43,071	43,481
	-3%	-2%	0%	2%	3%	5%	6%
Total TOC Mass (mg)	7480,747	7557,081	7633	7672,651	7719,826	7812,190	7878,677
	-2%	-1%	0%	1%	1%	2%	3%
Average Biofilm in Pipes (cells/cm^2) (x10^6)	5,45	5,94	6,37	6,79	7,28	7,57	7,87
	-14%	-7%	0%	7%	13%	19%	24%